



Trends in biomedical analysis of red blood cells – Raman spectroscopy against other spectroscopic, microscopic and classical techniques



Jakub Dybas^{a,1}, Fatih Celal Alcicek^{a,1}, Aleksandra Wajda^b, Magdalena Kaczmarek^a, Anna Zimna^{a,c}, Katarzyna Bulat^a, Aneta Blat^{a,b}, Tetiana Stepanenko^{a,b}, Tasnim Mohaissen^{a,c}, Ewa Szczesny-Malysiak^a, David Perez-Guaita^{d,e}, Bayden R. Wood^f, Katarzyna Maria Marzec^{a,g,*}

^a Jagiellonian Center for Experimental Therapeutics, Jagiellonian University, 14 Bobrzyńskiego St., 30–348, Krakow, Poland

^b Faculty of Chemistry, Jagiellonian University, 2 Gronostajowa St., 30–387, Krakow, Poland

^c Faculty of Pharmacy, Jagiellonian University Medical College, 9 Medyczna St., 30–688, Krakow, Poland

^d FOCAS Research Institute, Technological University Dublin, City Campus, Dublin 8, Ireland

^e Department of Analytical Chemistry, University of Valencia, 50 Dr Moliner St., 46–100, Burjassot, Spain

^f Centre for Biospectroscopy, School of Chemistry, Monash University, Clayton, Victoria, 3800, Australia

^g Łukasiewicz Research Network – Krakow Institute of Technology, 73 Zakopiańska St., 30–418 Krakow, Poland

ARTICLE INFO

Article history:

Received 24 June 2021

Received in revised form

30 October 2021

Accepted 9 November 2021

Available online 15 November 2021

Keywords:

Red blood cells

Erythrocytes

Erythropathies

Biomedical analysis

Analytical techniques

Raman spectroscopy

Molecular spectroscopy

Microscopic techniques

ABSTRACT

Application of modern and innovative spectroscopic and microscopic approaches to biomedical analysis opens new horizons and sheds new light on many unexplored scientific territories. In this review, we critically summarize up-to-date Raman-based methodologies for red blood cells (RBCs) analysis used in biology and medicine, and compare them with both classical, as well as other spectroscopic and microscopic approaches. The main emphasis is placed on the advantages, disadvantages and capabilities of each technique for detection of RBC deteriorations and RBC-related diseases. Although currently used classical techniques of medical analysts serve as a gold standard for clinicians in diagnosis of erythropathies, they provide insufficient insight into RBC alterations at the molecular level. In addition, there is a demand for non-destructive and label-free analytical techniques for rapid detection and diagnosis of erythropathies. Their recognition often requires multimodal methodology comprising application of methods including sophisticated spectroscopy-based techniques, where Raman-based approaches play an important role.

© 2021 The Author(s). Published by Elsevier B.V. This is an open access article under the CC BY license (<http://creativecommons.org/licenses/by/4.0/>).

* Corresponding author. Jagiellonian Center for Experimental Therapeutics, Jagiellonian University, 14 Bobrzyńskiego St., 30–348, Krakow, Poland; Łukasiewicz Research Network – Krakow Institute of Technology, 73 Zakopiańska St., 30–418 Krakow, Poland.

E-mail addresses: jakub.dybas@jcet.eu (J. Dybas), fatih.alcicek@doctoral.uj.edu.pl (F.C. Alcicek), aleksandra.wajda@uj.edu.pl (A. Wajda), magdalena.kaczmarek@jcet.eu (M. Kaczmarek), azimna@student.uj.edu.pl (A. Zimna), katarzyna.bulat@jcet.eu (K. Bulat), aneta.blata@doctoral.uj.edu.pl (A. Blat), tetiana.stepanenko@student.uj.edu.pl (T. Stepanenko), tasnim.mohaissen@jcet.eu (T. Mohaissen), ewa.szczesny@jcet.eu (E. Szczesny-Malysiak), david.perez-guaita@uv.es (D. Perez-Guaita), bayden.wood@monash.edu (B.R. Wood), katarzyna.marzec@kit.lukasiewicz.gov.pl (K.M. Marzec).

¹ These authors contributed equally.

1. Introduction

Recently, perception and understanding of the role of red blood cells (RBCs) have changed – from being passive and dedicated only to transport of gases, to having an active function in the progression of many pathologies and constituting an attractive target for detection of diseases related with cardiovascular system. Therefore, there is a field for the application of innovative and label-free analytical techniques for rapid detection of RBC alterations, which may serve as biomarkers of specific diseases and, consequently, help in their diagnosis. Although, most of the biomedical techniques currently used to analyze RBCs have various advantages for diagnosis and/or monitoring of peculiar diseases, they are often time-consuming, require the use of labels or special sample preparation and cannot be performed *in vivo*. In turn, Raman Spectroscopy (RS) is an alternative, sensitive, non-destructive and non-

invasive technique, that provides molecular information based on chemical composition of a measured sample. Additionally, RS enables rapid label-free implementation for both *in vivo* and *in vitro* studies, due to suitability for aqueous samples, which is especially important in the analysis of biological material, e.g., tissues, cells, blood or urine. Among the Raman Spectroscopic-based techniques, which have been already applied in blood-related studies, we may distinguish normal RS, resonance RS (RRS), surface-enhanced RS (SERS), tip-enhanced RS (TERS) and non-linear RS techniques. All of these techniques can be combined with confocal microscopy and various imaging methods, such as atomic force microscopy (AFM), to obtain higher resolution images for a more accurate analysis. In the context of RBC studies, RS enables investigation and characterization of RBC membrane [1], analysis of Hb structure [2], determination and property assessment of various ligands bounded to Hb [3–7], evaluation of the quality of stored blood in transfusion medicine [8,9] and allows to diagnose/screen diseases such as thalassemia [10], sickle-cell disease (SCD) [11], malaria [12] and diabetes [13,14].

In this review, we aim to critically summarize recent RS-based methodologies for RBC analysis used in biology and medicine, and compare them with classical, as well as other spectroscopic and microscopic methods (Fig. 1), with special regard to their advantages and disadvantages. First, we briefly describe classical methods of medical analysis used for obtaining information about RBCs. Subsequently, the novel methods based on microscopy and spectroscopy are outlined with an extensive summary of recent applications of RS (and related techniques). Finally, we compare the techniques in terms of different analytical features, including obtained information, analysis time and cost.

2. RBCs and the methodologies of sample preparation

Red Blood Cells (RBCs), i.e., erythrocytes, are the most abundant cells in the blood. The first observation of RBCs was performed with

use of a microscope by Jan Swammerdam in 1658. Antoni van Leeuwenhoek described their shape and size and defined them as “red corpuscles” in 1674 and their first illustration was presented in 1695 [15].

The major function of RBCs is to transport oxygen (O_2) from the respiratory epithelium to the tissues and cells, and carbon dioxide (CO_2) in the reverse direction. Additionally, RBCs possess antioxidant activity for protection against oxidizing agents [16]. The regular shape of an RBC is a “biconcave disc” which provides a larger surface area to facilitate the diffusion of gases. In order to ensure oxygen delivery to each part of the body, RBCs must pass through the tiny capillaries, what is possible due to RBC membrane properties provided by the phospholipid bilayer and cytoskeleton backed up by a sophisticated spectrin network [17]. Such composition ensures extreme flexibility and deformability that allows reversible shape change. Moreover, during maturation mammalian RBCs lose nuclei, mitochondria and other organelles in order to provide maximum capacity for hemoglobin (Hb), a specialized protein directly responsible for the transport of gases (i.e., O_2 and CO_2).

Hb belongs to the group of heme proteins (or hemoproteins) where the globin motif contains a unique prosthetic group – the heme. The globin part is a tetrameric protein containing two pairs of subunits (out of α , β , γ , δ , and ϵ) stabilized by ionic interactions and hydrogen bonds [18]. The most common globin type in human adult RBCs (up to 98%) is composed of two α and two β subunits ($\alpha_2\beta_2$) and is called HbA [19]. Each subunit in Hb is covalently bound with heme, composed of protoporphyrin and an iron ion, with a high affinity to O_2 molecule. The most common, heme B (called also ferroprotoporphyrin IX) possesses additional substituents: four methyl, two propanoic and two vinyl groups, bounded to the pyrrole rings. Bounded iron ion has six coordination sites; four of them are occupied by nitrogen of the porphyrin ring, one by a proximal histidine and the sixth remains free [20,21]. The presence of a distal histidine in the proximity of this last

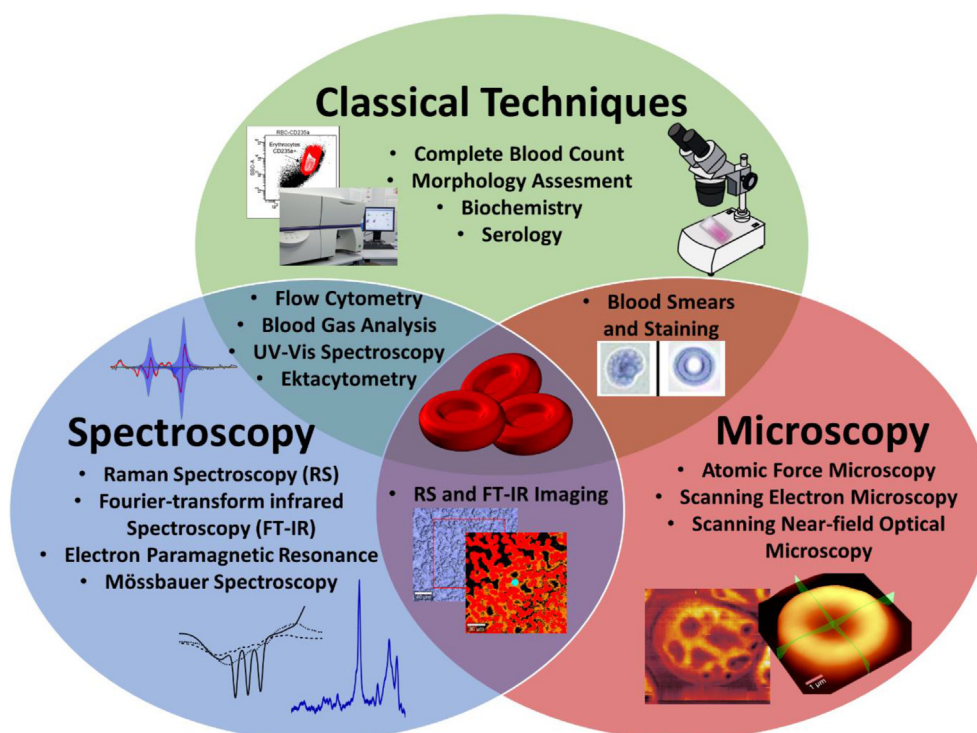


Fig. 1. Scheme of the most important techniques used in RBC studies.

coordination site decreases Hb affinity to CO₂ and protects the iron ion from oxidation of ferrous (Fe²⁺) to ferric (Fe³⁺) state, unable to bind oxygen [22].

Circulation through the blood vessels and transport of high amounts of O₂ exposes RBCs to oxidative stress caused by different chemicals, especially reactive oxygen species (ROS). Therefore, RBCs have a potent antioxidant system, including both enzymatic (e.g., superoxide dismutase (SOD), catalase, glutathione peroxidase, and peroxiredoxin-2 (PRDX-2)) and non-enzymatic (e.g., glutathione, ascorbic acid, etc.) pathways [23]. Due to the lack of mitochondria, the main energy source of RBCs is glucose, metabolized during an anaerobic process – the Embden-Meyerhof pathway [24,25].

2.1. RBCs isolation

RBCs comprise up to 98% of all cells present in the blood. Nevertheless, white blood cells and platelets can obscure and interfere with the results of analysis, therefore RBCs isolation procedures are often inevitable. Moreover, RBCs isolation, especially using density-based separation, can be successfully applied to diagnose iron deficiency or identify sickle cell disease [26,27].

Human whole blood samples are usually acquired from freshly withdrawn venous blood or aspirated from plastic bags containing packed RBCs (pRBCs) used in transfusion medicine. Blood samples from small animals are obtained by cardiac puncture, preferably from the ventricle, after anesthesia with either isoflurane inhalation or xylazine and ketamine injection [28,29]. Samples must be collected into syringes containing appropriate anticoagulant, e.g., heparin, citrate or EDTA. The choice of a specific anticoagulant is experiment-dependent and must be compliant with further isolation protocols, e.g. Ringer-Tris buffer solution, commonly used as a medium when heparin is the chosen anticoagulant, will evoke blood coagulation if citrate or EDTA are applied, due to the presence of calcium ions. Therefore, 0.9% NaCl (saline solution) or Tyrode's buffer would be a preferred choice [30–32].

RBCs are isolated from the whole blood by gradient centrifugation. Parameters must be evaluated carefully and chosen depending on the RBCs origin, in order to isolate them gently but neat. Human blood samples can be centrifuged with 500×g, while smaller RBCs require higher accelerations, e.g., murine blood should be centrifuged with at least 800×g [1,3,6]. Higher accelerations can alter RBCs membrane and cause hemolysis, and therefore should be avoided [33]. Centrifugation is repeated at least three times; after each spinning the supernatant together with the buffy coat containing WBCs and platelets is aspirated, while sedimented RBCs are washed with a proper buffer or saline solution [1,3,6,31]. The purity of RBC fraction can be evaluated using a complete blood count and the number of WBCs cannot exceed 200/mm³. In terms of short-term storage, isolated RBCs can be stored at 4 °C in a buffer or saline solution supplemented with glucose and bovine serum albumin [3,31]. After a slight acidification, storage time can be prolonged to 3–7 weeks. For a long-term storage, cryopreservation where RBCs are suspended in a cryoprotectant, e.g., glycerol, and placed in –80 °C, is preferred. It extends the shelf-life to over 10 years [29,34].

2.2. RBCs fixation

Long-term storage of RBCs outside the organism can cause morphological changes and biochemical alterations through autolytic processes. Otherwise, RBCs fixation can be applied to keep their morphology, structure and biochemistry close to physiological [35–37]. Various chemical fixatives such as formaldehyde, glutaraldehyde, acetaldehyde, acrolein, acetone, methanol or acetic acid

are commonly applied in RBCs studies [35,37,38]. Their effect on morphology and biochemical structure of RBCs has been broadly described elsewhere [35,37–39].

Glutaraldehyde is probably the most commonly used fixative intended for RBCs, due to low price and broad commercial availability. It's characterized by high reactivity, relatively low toxicity and rapid cell penetration. Furthermore, glutaraldehyde exhibits the capability to effectively react and crosslink several functional groups of RBC membrane proteins [39,40]. However, the choice of proper glutaraldehyde concentration is of highest importance, as it may impact RBC properties and lead to deformation of the RBC structure (e.g., shrinkage or swelling) [37]. Previous research revealed that low percentage of glutaraldehyde concentration (ca. 1%) does not affect the structure of RBCs skeletal matrix in a significant manner [38]. On the other hand, high percentage concentration of glutaraldehyde (ca. 8%) had negative impact on cellular osmosis [39]. The use of 0.01–1% glutaraldehyde concentration was shown to eliminate the problem of RBCs hemolysis [41,42]. Squier et al. also stated that the optimal glutaraldehyde concentration for human RBCs is contained between 1 and 1.5% [43]. Most studies suggest that in case of human RBCs, fixation with 1% glutaraldehyde is the most suitable [34,38–40]. It has been confirmed that 1% glutaraldehyde protects mechanical properties of RBCs (e.g., lateral forces, roughness) against changes caused by increasing temperature [44]. Nonetheless, recent studies have reported that 1% glutaraldehyde, if used inappropriately, may cause formation of advanced Heinz body-like aggregates and result in RBCs cytoskeleton deformations [45]. Asghari-Khiavi et al. proved that the erythrocytes fixed with 2% glutaraldehyde showed high-level autofluorescence during Raman spectra measurements (at excitation of 532 nm) [37]. On the other hand, formaldehyde dramatically reduced autofluorescence, but its use resulted in Hb loss. The researchers suggested the application of formaldehyde (3%) in conjunction with glutaraldehyde (0.1%) for spectroscopic investigations [37,46]. Thus, the process of sample preparation should employ a verified protocol depending on the chosen method for RBC evaluation. For murine RBCs 0.5% glutaraldehyde is sufficient, as the higher concentrations (1% or 2% glutaraldehyde solution) induce partial degradation of RBC membranes [1].

2.3. RBC membrane isolation

The first step of RBC membrane isolation is their lysis, i.e., breakdown of the cell membrane. Ideally, if sample consists only from washed RBCs, as anticoagulant remnants can interact with membrane proteins (heparin) or modulate Hb oxygen binding properties (citrate and EDTA) [29]. Lysis can be performed by overnight freezing in either 10-fold volume excess of 0.9% saline solution, where formation of ice crystals produces slow mechanical damage [1], or 1-fold volume excess of cold distilled water, where the hypotonic environment and cell swelling [29] lead to vast and immediate rupture of membranes but leaving a sample without presence of any other reagents. Then, samples are centrifuged with at least 3000×g acceleration, and RBC membranes are aspirated from the layer just above the surface of dissolved Hb [1]. Alternatively, after the first centrifugation the pellet containing RBC membranes can be re-suspended in lysis solution (e.g., cold distilled water) and subjected to another centrifugation to obtain a neater sample [31].

2.4. RBCs sample preparation for Raman-based studies

RBC samples for RS measurements do not require any special preparation. However, for non-single cell measurements samples may require dilution to at least 1:1000 (v/v) [3,6]. This is related to

the strong optical absorption of highly concentrated RBCs suspensions when the wavelength of the applied excitation is overlapping or close to the absorption band of Hb [33,47]. It is known, that the incident light can be absorbed by the sample, and the higher sample concentration, the greater absorption of the light, and therefore the greater energy of excitation light diminishing before it reaches the voxel (focal plane). Moreover, scattered photons can also be absorbed by the sample, what is known as reabsorption of Raman scattering and remains especially prominent when concentration of the sample is too high [48–50]. Preferably, the RBC sample should be put on a substrate suitable for RS [51]. RBCs or RBC membrane samples can be measured in the whole volume of a solution in special cuvettes suitable for RS [52], placed as a drop and measured with an immersive objective [21] or they can be smeared, air-dried and measured with an air objective [2]. Samples can also be placed in a special microscope equipped with a cooling/heating chamber and a device providing the appropriate physiological environment to maintain cell viability [3,33].

3. Techniques of RBCs analysis in biology and medicine

Assessment of RBCs' parameters, such as their number, morphology, structure alterations, enzyme activity, etc., is crucial for the diagnosis of various pathological states. Depending on the expected information, different techniques/methods of investigation are applied. The complete blood count (CBC) is the most frequently used test that gives important information regarding the cellular components of peripheral blood, such as the number of RBCs (RBC), total amount of hemoglobin (HGB), average size of an RBC (MCV), etc. [53,54]. Values of a CBC test may allow both to diagnose and monitor numerous diseases, such as anemia, infections, malignancies, and inflammatory diseases [53,55,56]. To confirm CBC findings and/or to assess the morphology of RBCs by reviewing its main aspects such as size, shape, color, inclusions and arrangement, a blood smear examination (BSE) can be performed [57]. Briefly, a drop of blood is placed on a slide and smeared to obtain a specimen to be examined under an optical microscope [58]. BSE helps to make a definitive diagnosis in some cases of malignancy, infection and especially anemia, because it enables to assess the morphology of RBCs (e.g., acanthocyte (spur cell), bite cell/blister cell, basophilic stippling, echinocyte (burr cell), elliptocyte, Heinz body, schistocyte, sickle cell, target cell, teardrop cell, etc. [59]), although it mostly provides prominent information regarding differential diagnoses and serves as a guide for further tests, if necessary [60].

To assess RBC morphology in a more specialized way, serology, measurements of biochemical markers, flow cytometry and ektacytometry are routinely used. Serology is a blood test based on antigen-antibody reaction, and is mostly used before transfusions to indicate blood groups (ABO and D typing [61]) along with other antigens and antibodies. Moreover, it can be applied to monitor immune response during bacterial and viral infections, such as HBV, HCV, HIV, *Treponema pallidum* (syphilis), etc., and to diagnose some of infectious pathologies such as Lyme disease [62]. Biochemical measurements can be performed to determine pH [63], enzyme activities (e.g., lactate dehydrogenase (LDH) [64], alanine aminotransferase (ALT) [64], glucose 6-phosphate dehydrogenase (G6PD) [65], glutathione reductase (GDH) [65], etc.), individual molecules (e.g., glucose [63], adenosine triphosphate (ATP) [65], 2,3-diphosphoglycerate (2,3-DPG) [65], cell membrane stomatin [66], etc.), anions (Cl^- , HCO_3^- , etc.) [67], cations (Na^+ , K^+ , Ca^{2+} , etc.) [63], etc. Such analysis may facilitate diagnosis and indicate the stage of a disease or deficiency. Flow cytometry enables the analysis of RBC surface antigens, such as CD235a present

on the mature RBCs [68], CD71 characteristic for reticulocytes [69], CD47 whose change is related to obesity [70] and myelodysplastic syndrome [71], CD35, CD55 and CD59 observed in chronic kidney disease [72]. Measurements of the fluorescence emission of antibodies, along with the analysis of RBCs shape, can be used to diagnose and/or screen RBCs membrane disorders. For instance, mean RBC fluorescence emission of the dye eosin-5' maleimide (EMA) is used in the assessment of hereditary spherocytosis (HS) [73]. Ektacytometry allows to measure the deformability of RBCs by monitoring changes in shear stress or an osmotic gradient. This is a useful method to diagnose RBC membrane-related disorders such as HS, hereditary elliptocytosis (HE), hereditary pyropoikilocytosis (HPP), hereditary stomatocytoses, etc. [74–76]. Blood gas analysis provides information about respiratory, hemodynamic and metabolic conditions of the body in a rapid way by measuring acid-base balance and oxygenation ratio in blood, to diagnose and monitor the patients mostly in emergency services and intensive care units [77].

Recently, “omics” technologies gained attention in RBCs studies. Proteomics, metabolomics, genomics and lipidomics, vigorously broadened analytical possibilities of erythrocyte analysis. However, due to vast amount of information they incorporate, they require a separate review and were discussed in detail elsewhere [34,78,79], what allowed to focus herein on spectroscopic and microscopic techniques alone.

3.1. Chosen classical techniques of RBCs analysis

3.1.1. Complete blood count (CBC)

Complete blood count (CBC) provides significant information regarding the cellular components of peripheral blood, and due to its relative inexpensiveness and accessibility is the most frequently used blood test. CBC includes the number/values of RBCs, white blood cells (WBC), platelets, Hb (marked also as HGB), hematocrit (HCT), mean corpuscular volume (MCV), mean corpuscular hemoglobin (MCH), mean corpuscular hemoglobin concentration (MCHC) and red cell distribution width (RDW), also called red cell indices [53,57].

Assessment and evaluation of CBC parameters allows both to diagnose and monitor variable pathologies, including anemia [55], infections [80], malignancies [56] and inflammatory diseases [53]. One of the most important parameters is Hb concentration. Its value below the reference range may indicate anemia and could help in diagnosis of iron or vitamin B12 deficiency, thalassemia, etc. [53]. Attainment of definitive diagnosis could be reached by interpretation of MCV value, i.e., the average size of an RBC [53,57]. Changes in HCT value (the volume percentage of RBCs in the blood) could be caused either by physiological conditions such as pregnancy, or multiple diseases such as viral infections, bone marrow disease (e.g., by toxin exposure, malignancies, etc.), chronic bleeding, erythropoietin hormone level changes, polycythemia rubra vera, etc. [53]. Importantly, CBC can be performed with differential values allowing determination of the exact numbers of different WBC types and their percentages in the blood, what can be an indicator of WBCs-related diseases, such as infections, leukemia etc. [81].

3.1.2. Morphology assessment – blood smears and staining

The blood smear (BS) examination (BSE) is still a very useful and important tool for the morphology assessment of RBCs [82]. In general, BSE can be performed to confirm and/or clarify the CBC test results, which may sometimes provide [83] false-negatives or false-positives. Additionally, BSE delivers relevant information concerning WBCs, platelets, and RBCs morphology, which cannot be

obtained with CBC alone. The main aspects of the RBCs morphology assessment are count, shape, size, color, inclusions and arrangement [57].

To obtain comprehensive and valuable information from BSE, there are a few crucial requirements to be fulfilled, regarding sample collection, pre-analytic variables (transport time, temperature, amount, instrument, patient's conditions, etc.), slide preparation, staining artifacts, as well as skilled and experienced staff [60,82,84].

To prepare a wedge smear, which is the most commonly used smear type, after emplacing a small drop of blood on a short edge of a clean glass slide with a proper pipette, a spreader slide should be used (Fig. 2A). The spreader slide is put adjacently in front of the blood drop and has to touch the glass slide at approximately 30–45° angle. After smearing, the blood needs to be left to air-dry, therewith, the smear slide is obtained. There are different methods of blood smear preparation, depending on the purpose of analysis, such as malaria detection or reticulocyte counting [58].

It is recommended to perform fixation before staining, however, staining can also be performed without fixation, shortly after air-drying of the slide, to obtain ultimate quality for examination. Moreover, glass slides are commonly coated with poly-L-lysine or Cell-Tak for cell immobilization. Manual or automated staining techniques can be applied to dye the slides. It is recommended to immerse the slides in reagent solutions to prevent any precipitation due to evaporation while performing the staining manually. To determine the quality of the staining procedure, distinguishing all cell types in the blood smear under a light microscope is a very useful and powerful criterion. There are several methods for

staining blood smear slides, including Romanowsky, Giemsa, Wright or May-Grünwald [58].

BSE may enable definitive diagnosis, although it is mostly an auxiliary test that provides significant information regarding differential diagnoses and serves as a guide for further tests, if necessary. BSE is useful to identify most of the inherited leukocyte and platelet disorders (e.g., the Chediak-Higashi [85] and the Pelger-Huet [86] anomalies, the gray platelet, i.e., α -storage pool disease [87] or Paris-Trousseau syndrome [88]), some of the hematologic malignancies (e.g., chronic lymphocytic leukemia (CLL) [89], plasma cell leukemia (PCL) [90], hairy cell leukemia [91] and prolymphocytic leukemia (PLL) [92]), and parasitemias (e.g., *Babesia* species [93], trypanosomiasis [94], filariasis [95], dengue fever [96,97]). All these pathologies have distinct morphological features that allow making conclusions towards a definitive diagnosis. Similarly, RBCs may display morphological changes (e.g., acanthocyte – spur cell, anisochromia, bite cell/blister cell, basophilic stippling, echinocyte – burr cell, elliptocyte, Heinz body, hypochromia, polychromasia, schistocyte, sickle cell, target cell, teardrop cell, etc. [59]), that also allow to make a direct, definitive diagnosis (e.g., homozygous hemoglobin C disease [98], hemoglobin SC disease [99], lead poisoning [100], arsenic poisoning [101], iron deficiency [102]). Scanning electron microscopy (SEM) is extremely useful in the analysis of such RBC-related alterations, since it allows the three-dimensional visualization of RBCs [103]. This microscopy approach is commonly used in RBC studies and has greatly expanded the knowledge, as well as understanding of the RBC surface alterations [104]. Examples of RBC morphological alterations are presented in Fig. 2B.

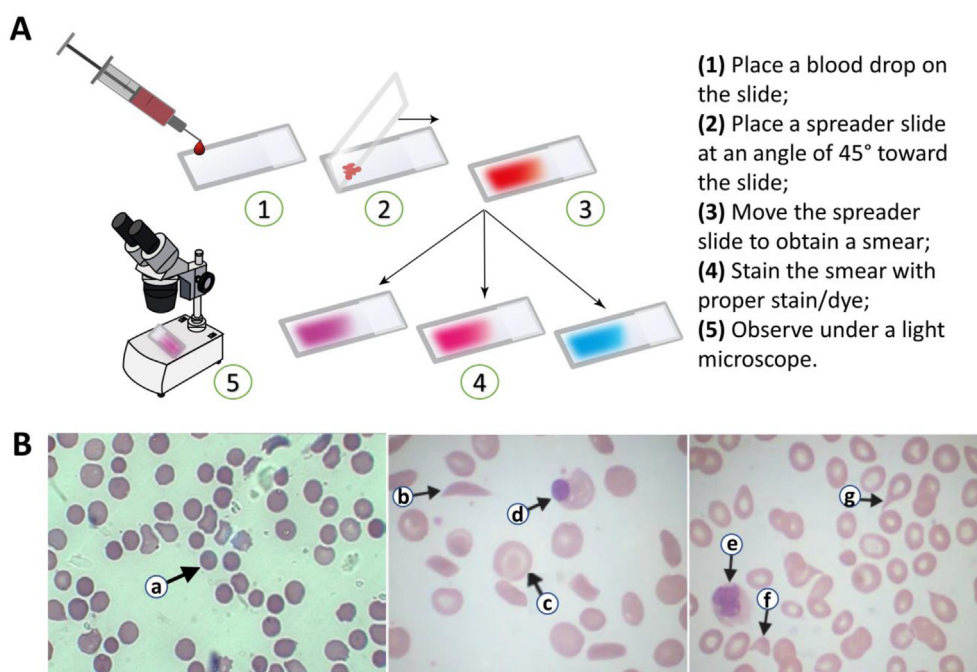


Fig. 2. (A) Scheme of the morphology assessment: (1) placement of a blood drop on the glass slide, (2) putting a spreader slide at an angle of 45° towards the slide, (3) movement of the spreader slide to obtain a blood smear, (4) staining the smear, (5) observation of a sample under the light microscope; (B) Examples of the RBC morphological alterations: (a) hereditary spherocytosis characterized by numerous spherocytes (hyperchromatic cells with a regular outline); (b) irreversibly sickled red cells (drepanocytes) observed in sickle cell syndromes (SS, SC, S- β -thalassemia); (c) target cells observed in sickle cell disease, hemoglobin C trait, hemoglobin CC disease, thalassemias, iron deficiency, asplenia; (d) nucleated RBCs present in peripheral blood smear suggesting severe stress of the bone marrow; (e) neutrophil precursors seen with circulating nucleated RBCs during onset of marrow fibrosis; (f) fragmented RBCs observed in disseminated intravascular coagulopathy (DIC), thrombotic thrombocytopenic purpura (TTP), hemolytic uraemic syndrome (HUS); (g) tear drop cells (dacryocytes) observed in myelofibrosis, myelophthisia (marrow infiltrations), extramedullary hemopoiesis, hereditary elliptocytosis, hereditary pyropoikilocytosis, severe iron deficiency, megaloblastic anaemia, thalassemias and myelodysplastic syndrome. Figure (a) was adapted from [105] under the terms of the Creative Commons Attribution License, Figures (b–g) were adapted from [106] under the terms of the Creative Commons Attribution License.

3.1.3. Serology

Serology is a branch of medicine that addresses immunological reactions between antibodies and antigens in the blood. Typically, it is implied in transfusions, in order to assess blood groups and the presence of certain antibodies. The analysis is performed right after blood donation, when the blood sample is being tested for common viruses/bacteria and the donor's blood group is typed. Standard laboratory procedures include direct (forward) ABO and D typing with the use of anti-A, anti-B and anti-D (VI-) reagents and indirect (reverse) typing with A1 and B antigens. Forward typing is based on the reaction between patient's ABO and D antigens on RBCs with anti-A, anti-B and anti-D (VI-) reagents, while reverse typing covers the reaction of patient's antibodies in serum with standard RBCs. Agglutination is an indicator of a positive test result and is assessed visually [61]. Donated blood is also checked for bacterial and viral infections, which usually include hepatitis viruses B and C (HBV, HCV), human immunodeficiency virus (HIV) and *Treponema pallidum* (syphilis). The blood is tested for specific antigens (HBV) and antibodies (HCV, HIV, syphilis) with use of ELISA (enzyme-linked immunosorbent assay) [107,108]. Finally, right before the transfusion, the recipient's serum is tested towards alloantibodies against RBC's antigens. RBC's antigens comprise an enormous group of non-ABO antigens with different immunogenicity, that are not usually typed (for example Lewis, Lutheran, MNS). After a donor-recipient mismatch, the alloantibodies are produced, what can lead to delayed hemolytic transfusion reactions. Therefore, the indirect antiglobulin (indirect Coombs) test is performed towards clinically significant alloantibodies. The recipient's plasma is combined with standard RBCs with known antigens [109]. As previously, agglutination is a positive result and based on that the alloantibodies are identified. The final step in serological typing is a cross-match – donor's RBC are mixed with recipient's plasma; no agglutination is an indication for transfusion [110].

3.1.4. Biochemical parameters measurements

Biochemical measurements are a complex system of basic parameters that reflect the condition of erythrocytes. They comprise different analytical methods that are relatively fast and simple, so they can be used in every laboratory provided with accurate equipment. Primarily, biochemical parameters are used in order to assess the level of hemolysis. It can be done by a spectrophotometric measurement of a supernatant at 540 nm (reflecting Hb concentration) and a subsequent comparison with control [111]. Moreover, concentration of intracellular enzymes, such as lactate dehydrogenase (LDH) and alanine aminotransferase (ALT) is analyzed. These two strictly correlate with cell damage [64] and can also indicate ongoing hemolysis. However, based on previous studies, the best marker for hemolysis is total (or indirect) bilirubin, the product of heme degradation [112].

Biochemical analysis can be performed in order to control functioning of the stored RBCs. Storage lesions, the effect of prolonged storage of erythrocytes, include decrease in antioxidant enzymes: glucose 6-phosphate dehydrogenase (G6PD) and glutathione reductase (GDH); loss of RBC membrane; reduced levels of adenosine triphosphate (ATP) and 2,3-diphosphoglycerate (2,3-DPG). These are accompanied by increased LDH enzyme activity, higher lactate level and decreased pH. The measurement of G6PD and LDH activity is performed by colorimetric quantification of enzymatic reaction and can indicate RBC physiology state [113]. Commonly used colorimetric and fluorescent analyses comprise quantification of various enzymes' activity and concentration of certain molecules or a group of compounds, e.g., total proteins using BCA protein assay [114] or phospholipid level [115].

Another important biochemical marker is ATP level, which can be measured in a solution, in the presence or absence of cells,

mainly via luciferin-luciferase bioluminescence technique, suitable for both intracellular ATP, as well as released from the RBCs [116]. ATP can be released by low-O₂ exposure, mechanical deformation, acidosis, etc. [117]. Deformation-induced ATP release from RBCs may activate the purinergic receptors on the endothelium and result in vasodilation that causes increased perfusion of the tissue/organ [118]. RBCs from diabetic patients showed reduced ATP release in response to deformation [119]. It is also reported that ATP released from RBCs stimulates synthesis of NO in rabbit lungs [120]. Even though many other studies claim that RBCs-derived ATP is an important mediator in the vascular environment, this matter still needs to be explored.

To add up, biochemical analysis is widely used in diagnosis of RBCs diseases, such as sickle cell anaemia [121], thalassemia [122], malaria [123] or dehydrated hereditary stomatocytosis [124].

3.1.5. Flow cytometry

Among techniques employed for cell studies, flow cytometry plays a prominent role in the analysis of RBC surface antigen expression. The use of antibodies carrying fluorophores gives multiple opportunities to efficiently explore the erythrocyte population, since flow cytometry allows for a concomitant detection of several signals in one sample, limited only by the number of available laser lines and filters.

Specific antigens are either present or absent on RBCs and enable positive/negative cell identification. CD45, the common leukocyte antigen, is present in almost all cells of hemopoietic lineage, excluding the RBCs [125]. Thus, when assessing fraction purity after RBC isolation, labelling the cells with anti-CD45 antibody gives the idea about the number of different types of WBCs in the population [126–128]. On the other hand, CD235a, also known as Glycophorin A, is a sialoglycoprotein present on the membrane of mature erythrocytes [129]. It may come in handy when a need to distinguish RBCs from other components of the whole blood occurs [126,128,130].

RBCs live up to 120 days and are constantly produced in the bone marrow [131] and thus, RBCs of different ages can be found in the blood stream. Early-stage RBCs called 'reticulocytes' can be differentiated from the mature ones by the assessment of CD71, also known as the transferrin receptor, as this protein is lost during maturation process [69,130,132]. The same applies for CD34, specifically expressed in human hematopoietic progenitors [129,133].

Erythrocytes exist in the complex world of blood circulation where they take part in the regulation of many processes. Thus, not only erythrocyte-specific antigens are investigated, because some of these proteins are subjected to changes in various conditions. CD47, a glycoprotein associated with the Rh macro complex and integrin signal transduction complex, also plays an important role as a marker of self (a "don't eat me" signal) [134]. Its binding to signal regulatory protein- α inhibits the activation of macrophages and phagocytosis [135]. Changes in CD47 were observed with use of flow cytometry in many conditions, namely in obesity [70], myelodysplastic syndrome [71], systemic sclerosis [136] and during red blood cell storage [134,137]. The latter also influences the expression of CD35, CD55 and CD59 [137], proteins that are a part of the complement system regulation. Moreover, changes in CD35, CD55 and CD59 were observed in the erythrocytes in chronic kidney disease [72].

Another aspect of the RBC physiology that can be easily studied by means of flow cytometry is phosphatidylserine exhibition on the surface of the cell membrane. The loss of phospholipid asymmetry is an apoptotic 'eat me' signal [138], that carries information about the RBC condition [139,140]. It was extensively studied, due to its link to the pathophysiology of β -thalassemia [141,142].

Finally, cell-specific markers described above are frequently used to identify microvesicles shed by the erythrocytes in various conditions, both *ex vivo* [143–146] and during RBC storage [147–150].

3.1.6. Ektacytometry

To ensure proper exchange of gases (O_2 and CO_2) in body organs through microcirculation, RBCs must be adapted to be repeatedly deformed to pass through capillaries narrower than their own diameter. RBCs deformability is defined as the ability to modify their shape in response to interactions imposed not only by fluid forces, but also by the vessel walls [151]. RBC deformability is an important hemorheological parameter frequently evaluated in experimental and clinical studies [152–154].

The decrease in erythrocyte deformability is a common risk factor for microvascular diseases, such as hypertension [155–157], heart failure [158], diabetes mellitus [159,160] and sickle cell anemia [161,162], as well as atherosclerosis and aging [115]. A disease can alter the deformability of RBCs, however, RBC deformability affects pathophysiology of the disease itself, creating a vicious circle. Erythrocyte deformability can be measured with use of techniques such as rheoscopy [163,164], filtration [159] and ektacytometry [152].

Ektacytometer is a device that measures optical deformability of RBCs and their aggregation. More precisely, it measures the diffraction pattern created when a highly diluted red cell suspension is exposed to a laser light [165]. The diffraction pattern reflects RBCs deformation (RBCs suspended in a high-viscosity liquid and exposed to a flow-generated shear stress). To characterize deformability, ektacytometry applies increasing shear stress to the cells kept in a constant osmolality [166]. Evaluation of the diffraction elongation pattern is performed in two ways: by photodiodes that measure light intensity in a defined location, and by cameras using image analysis. Results are expressed as elongation index (EI) or deformation index, both indexes increase with the increase in cell deformability and reflect the aspect ratio of the elliptical diffraction pattern [167]. EI is based on the image patterns and calculated by an image processing algorithm, using the formula $EI = (A - B)/(A + B)$ where A is the length of the major axis of the ellipse and B is the length of the minor axis of the ellipse [151].

Ektacytometry is a fast and simple laboratory technique which allows to perform an automated, rapid experiment to assess the deformability of RBCs within several minutes [151,168,169]. There are commercially available ektacytometers, which differ depending on their shearing geometries: Couette cylinders (Lorca), a flow channel (RheoScan-D) and rotating parallel plates (Rheodyn SSD) [151].

3.1.7. UV–Vis absorption spectroscopy

UV–Vis absorption spectroscopy (UV–Vis), also called spectrophotometry or electronic absorption spectroscopy, allows to study interaction of the matter with light from 190 to 780 nm wavelength range. Absorption spectrum of RBCs is dominated by Hb' porphyrin ring electronic transitions, with the most abundant located around 390–450 nm and called the Soret (or B) band [21,170,171] originating from the configuration of $\pi-\pi^*$ electronic transitions, i.e., $a_{2u} \rightarrow e_g$ and $a_{1u} \rightarrow e_g$. Due to additive individual transition moments of these electronic transitions, the Soret band is far more intense than any other porphyrin electronic transition [172]. In the 480–650 nm wavelength range, up to four Q bands are present and their exact number, position and integral intensity ratio are indispensable for differentiation, characterization and definition of various Hb types and adducts [173]. Usually, there are two Q bands: (1) Q_0 (or α) band, located further from the Soret band, also arising from $\pi-\pi^*$ transition but in contrary to the Soret band both individual transition moments here are nearly cancelled resulting in its

far lower intensity; (2) the remaining intensity is borrowed back from the Q_v (or β) band, which is located at lower wavelengths and results from vibronic mixing between the Soret and Q_0 band [33,172]. In the absorption spectra of Hb species containing ferrous (Fe^{2+}) ion, usually only one broad Q band occurs, whereas Hb species with ferric (Fe^{3+}) ion are characterized by the presence of both, Q_0 and Q_v [3,6,171]. Additionally, their relative integral intensity ratio is an indicator of the sixth ligand stability – the lower Q_0 band compared to Q_v band, the more stable adduct is formed [173]. In exceptional cases, e.g., in Hb species with high-spin ferric ion as in case of metHb, an additional band around 620–640 nm arising from porphyrin to metal charge transfer transition is observed [172]. Examples of the UV–Vis spectra of various Hb species are presented in Fig. 3.

3.1.8. Blood gas analysis

Blood Gas Analysis (BGA) is a reference technique commonly used to characterize the concentration of arterial/venous blood gases, i.e., O_2 and CO_2 . However, it may also be used to determine pH of the blood, as well as concentration of chosen ions and main RBC metabolites, e.g., lactates. It requires small sample volume (ca. 10 μ l), usually taken from the radial artery, and provides results

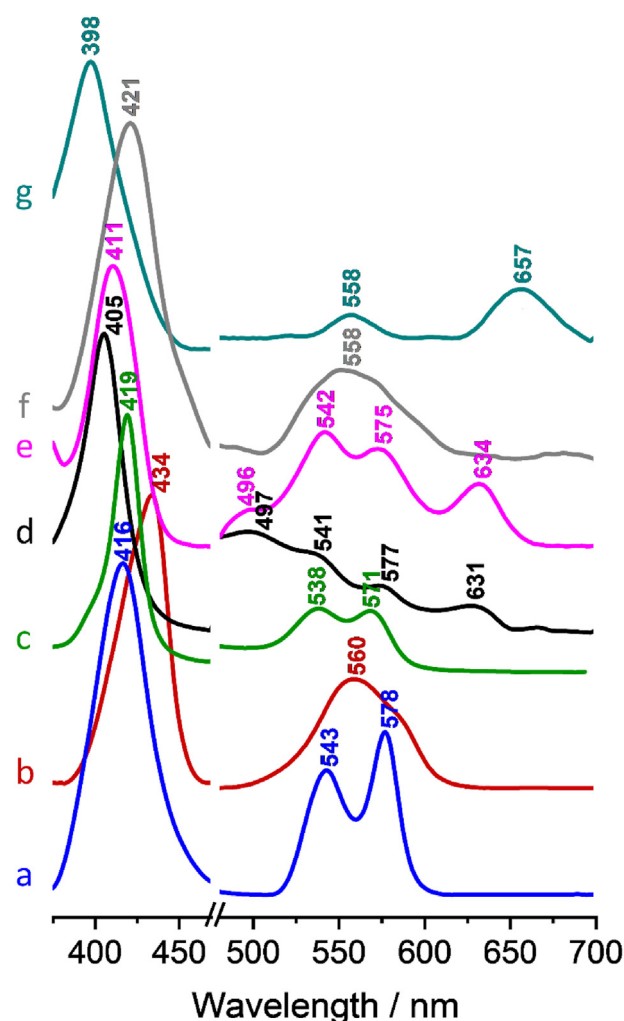


Fig. 3. Examples of the UV–Vis spectra of various Hb species inside functional RBCs: (a) oxyHb, (b) deoxyHb, (c) HbCO, (d) metHb, (e) metHbNO₂, (f) metHbCN, (g) hematin. The UV–Vis spectra are presented in the 375–700 nm wavelength region, Q-bands region (475–700 nm) was twice enlarged.

within minutes. BGA measures blood gas tension, arterial partial pressure of oxygen (PaO_2) and carbon dioxide (PaCO_2), pH and oxygen saturation (SaO_2). Results are often an essential part of diagnosis, used for managing the oxygenation status and acid-base balance of critically ill patients in the Intensive Care Units [174]. They are also crucial for diagnosis and differentiation between different causes of metabolic acidosis and detection of the anion gap [174]. Some of the newer BGA systems can additionally detect various species of Hb adducts, including deoxyHb, oxyHb, methHb and HbCO, and therefore are extremely useful in rapid diagnosis of methemoglobinemia and carbon monoxide poisoning [6]. The principle of these measurements lies in the incorporation of proper oximeters and is based on spectrophotometry [175].

Moreover, to monitor anaerobic glycolysis in pRBCs, measurements of basic ions can be performed with use of BGA, i.e., Na^+ , K^+ , Cl^- and HCO_3^- . Anaerobic metabolism in RBCs is indicated by elevated K^+ concentration and decreased Na^+ levels, due to the blockage of Na^+/K^+ ATPase in the state of ATP deficiency [63]. Anaerobic metabolism also contributes to pH lowering, due to increased lactic acid concentration [65]. Changes in Cl^- and HCO_3^- concentrations indicate structural deformations, mainly due to the modification of Band 3, the main transporter of the afore mentioned ions [67,176]. It was proven that metabolic changes are ahead of hemolysis and therefore ion and LDH measurements are crucial for monitoring RBCs physiology and viability [113,176].

3.2. Raman Spectroscopy (RS) in RBCs studies

Raman Spectroscopy (RS) is one of the molecular spectroscopy techniques, which allows for label-free and nondestructive detection and identification of molecules, based on characteristic spectra unique for each molecular system [97,177]. This technique uses inelastic light scattering phenomenon, named Raman scattering, discovered by Chandrasekhara Venkata Raman (C. V. Raman) in 1928 [178], where detected energy change corresponds to vibrational energy levels of the molecule [97]. More specifically, it measures intensity of inelastically scattered photons as a function of the energy shift given in wavenumber values (Raman shift) from the elastically scattered photons (Rayleigh scattering), i.e., those with unchanged energy [179]. From the quantum-mechanical point of view, Raman scattering corresponds to a two-photon process where a molecule is excited from the ground state into a virtual excited state by incident light photon, which is subsequently annihilated, followed by a return of the molecule into a lower (anti-Stokes) or higher (Stokes) vibrational state accompanied by an emission of the created photon.

Since Raman scattering is a relatively weak effect because only one photon per 10^5 – 10^7 is inelastically scattered [21], the development of more sensitive Raman-based techniques was needed. Among them, one of the most powerful, especially in the context of heme protein studies, is Resonance Raman Spectroscopy (RRS), where the signal obtained is greatly enhanced if the incident light energy is close to or on the energy of electronic absorption band [179]. Furthermore, interaction of a molecule with nano-structural metal substrate (e.g., gold, silver) leads to plasmon-assisted scattering, which was used to design Surface Enhanced Raman Scattering (SERS) and its variation – Tip-enhanced Raman Scattering (TERS), where the contact between a molecule and metal is ensured by a metallized tip controlled by Atomic Force Microscopy (AFM) [97]. On the other hand, combination of Raman spectrometer with confocal microscope gave rise to confocal Raman microscopy (CRS) and allowed to study not only chemical composition of the samples through identification of their characteristic functional groups, but also to study their distribution in 2D and even 3D images [97,177]. Moreover, CRS development brought other advantages, like

reduced fluorescence and background spectra from unwanted matrix components or contaminations, collection of the spectra only from the exact spot or a chosen focal plane. Therefore, it also enabled measurements of samples hidden beneath other materials, e.g., RBCs in the plastic bag or bone under the skin, however, due to light absorption of the covering material, it was impossible until Spatially Offset Raman Spectroscopy (SORS) was introduced [97,177]. In SORS, collection of scattered light is shifted (about few millimeters – offset) from incident light, allowing to obtain reflected signal from the depth of the sample instead of its surface.

All the above-mentioned RS techniques, i.e., RRS, SERS, TERS, CRS and SORS are based on spontaneous Raman scattering. A need for a further increase in Raman signal intensity for a faster and more accurate measurements led to the development of non-linear Raman variants, where Raman scattering is forced by use of two spatially coincident laser pulses (pump and probe). In Stimulated Raman Spectroscopy (SRS) two photons are involved – one from the pumping and one from probing (or Stokes) laser. If the difference in energy between their frequencies matches the energy of vibrational energy level, stimulated Raman loss (or gain) can be observed, what greatly reduces the time of spectra collection and allows to perform ultrafast imaging [180,181]. An alternative is the Coherent anti-Stokes Raman Spectroscopy (CARS), which employs three photons – two from pumping and one from probing laser, for a greater enhancement of the obtained Raman signal [180,181].

3.2.1. Spontaneous Raman scattering

In contrast to Fourier-transform absorption infrared (FT-IR) spectroscopy (see chapter 3.3.1), where the vibration is active only if at least one component of the dipole moment changes, in RS the change of at least one component of the polarizability tensor is required [177]. Therefore, the more intense (more active) the band is in IR spectroscopy, the weaker (more forbidden) it is in RS and vice versa, what makes these techniques complementary. Classical example is water molecule, with FTIR spectrum dominated by fundamental O–H stretching (ca. 3600 cm^{-1}) and H–O–H bending (ca. 1600 cm^{-1}) vibrations, what efficiently precludes measurements of aqueous samples [21,177]. Since water is a weak Raman scatterer, this leads to one of the main superiorities of RS over FT-IR – RS makes it possible to examine body fluids and cells within water environment [181]. Accordingly, strong Raman scatterers are non-polar compounds, like lipids [4,182], and those with conjugated double-bonds and high symmetry, such as heme [4,97,182], which additionally possesses a chromophore, providing even further enhancement of Raman intensity if a proper excitation wavelength is used (due to resonance Raman effect – please see 3.2.1.2).

The simplest way to obtain a Raman spectrum is the single point measurement, where the spot size varies, depending on the excitation wavelength and the optics, especially numerical aperture of the objective in case of Raman microscopy [97,183]. In many biological applications, where the exact position where the information is collected can be neglected or the sample is homogenous, this approach is sufficient and commonly preferred, because it provides chemical characterization of the studied object within seconds [183]. However, in more sophisticated analysis of heterogeneous samples, line scan, 2D- and even 3D-Raman imaging can be applied, increasing time of analysis but also combining chemical information with its spatial localization and distribution [97,182,183].

Spatial (lateral, Δx -y) and depth (Δz) resolutions are defined by excitation wavelength (λ) and the size of numerical aperture (NA) [97,181]. Their theoretical values can be calculated from the Rayleigh criterion (Δx -y $\approx 0.61\lambda/\text{NA}$ and $\Delta z \approx \lambda/\text{NA}^2$) [97,177]. The spatial resolution can go as low as the diffraction limit (ca.

250–300 nm) which is rarely achieved in practice except when operating in confocal mode [97].

3.2.1.1. Non-resonance Raman spectroscopy (RS). Even though RS can be successfully applied to biological samples to extract information about their chemical composition [182], the Raman signal from fresh RBCs is dominated by Hb, which is related to the highly polarisable nature of the heme prosthetic group because of its high symmetry. The heme structure provides strong resonance Raman enhancement for all types of hemoporphyrins, including hemoglobin, myoglobin, cytochromes, etc. [1,47]. Due to this phenomenon, it remains impossible to acquire reliable insight into other RBC components, e.g., membrane proteins, even with application of non-resonant excitation wavelengths like 1064 nm [1,47]. It was previously reported that fresh RBCs, which contain the majority of oxyHb, do not exhibit fluorescence [184,185], contrary to aged blood cells [186,187] or tissues/cells contaminated with the Hb [188]. In the case of dried RBCs or tissues/cells contaminated with Hb, an increase in background counts is commonly observed. The origin of such background is the result of the intrinsic fluorescence of degradation products [189,190], excitonic interactions throughout the network of heme aggregates and profound photothermal effects resulting from the increased absorption of photons [188]. However, RS can shed some light on the RBC-derived samples not containing Hb, e.g., RBC membranes (so called “ghosts” RBCs) where Hb is lost during isolation process

(please see example in Fig. 4A) [1,191], as well as RBCs with completely degraded Hb, e.g., in advanced Heinz body-like aggregates (AHBA) as presented in Fig. 4B–C [45]. Recently, RS-based approach was successfully used to prove adverse effect of mobile phone signal on RBCs leading to reduced hemoglobin oxygen affinity connected with increased intracellular Ca^{2+} level and thus increased activation of voltage gated membrane channels depended on calcium ions [192].

Careful RBC membrane isolation leading to cleansing of the sample from Hb (see chapter 2.3) allows to reveal the Raman signature of other, non-resonant biochemical components. Inclusion of such procedure into Raman spectroscopy studies was reported for the first time in 1975 by Lippert et al., who managed to estimate the configuration of membrane proteins (mainly α -helices), as well as configuration of hydrophobic side chains of phospholipids (all-trans) [191]. More recently, such procedure was applied to investigate RBC membrane alterations connected with aging, hypercholesterolemia and atherosclerosis reflected by variations in lipid-related fractions, i.e., the amount of phospholipids, cholesterol esters, esterified lipids, total lipid content and lipid unsaturation level [1,115,193,194]. Another approach to obtain information about RBC membrane and membrane-bounded Hb remains optical trapping, e.g., using vortex beam [195]. Such RS-based approach provided additional diagnostic information in detection of erythropathies which extended information obtained from classical techniques.

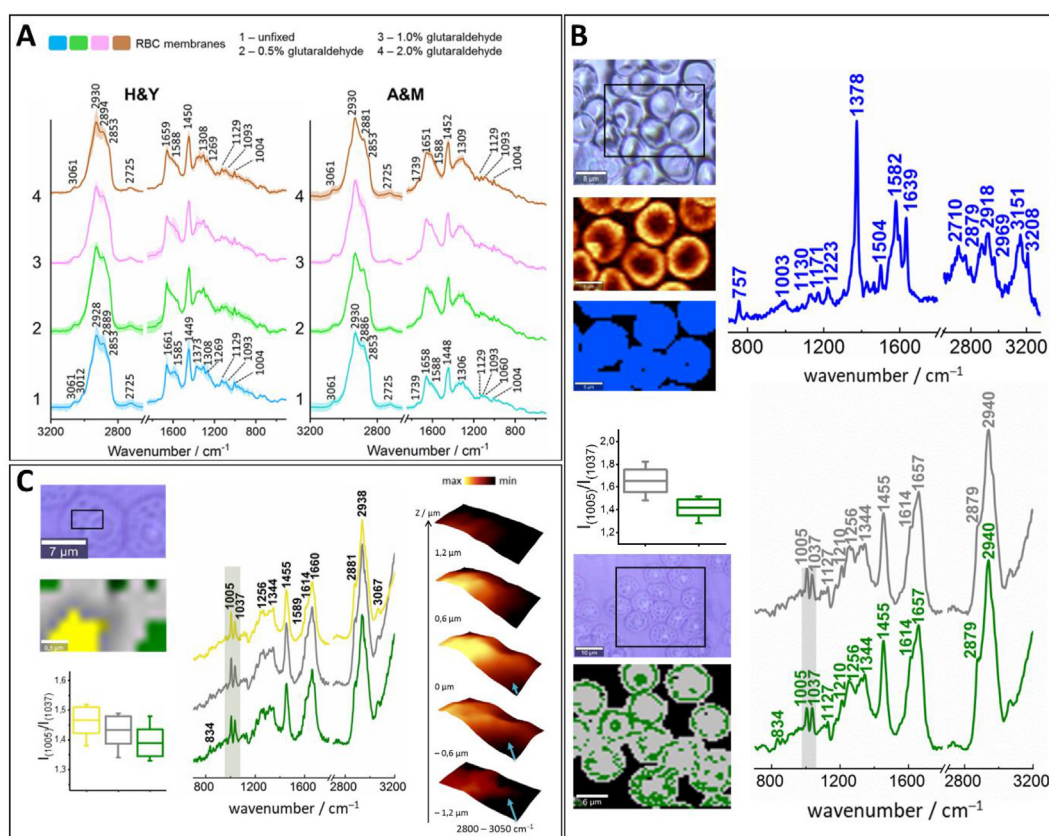


Fig. 4. (A) Averaged Raman spectra acquired from isolated RBC membranes and presented with their SD, collected with use of the 488 nm excitations. Raman spectra lack resonant components from Hb, since it was removed during isolation of RBC membranes, what enables insight into protein-lipid composition of the membranes. (B) Upper panel presents an example of Raman imaging performed on untreated RBCs with majority of oxyHb, with resonance Raman spectrum typical for heme-related compounds. Lower panel includes Raman imaging of the sample treated with high concentration of oxidative agent, what lead to complete Hb degradation and formation of AHBA – advanced Heinz-bodies like aggregates, characterized by normal Raman spectrum without any resonant features. (C) High-magnification Raman imaging of a single AHBA presented with corresponding Raman spectra and 3D Z-stack images. Again, the spectra lack resonant components and enable, e.g., insight into changes in phenylalanine conformation caused by oxidative damage. Figure in panel A was adapted with permission from [1], copyright (2019) American Chemical Society while figures in panel B and C were adapted from [45] with permission from the Royal Society of Chemistry.

All kinds of samples containing products of Hb degradation and/or heme metabolism can be probed with RS. Raman imaging was successfully applied to study Hb metabolites and waste products, such as biliverdin, bilirubin, hematin and hemichrome in macrophages and Kupffer cells [4]. If oxidative damage is sufficiently high, Hb can be degraded even further, leading to formation of AHBA bodies – aggregates of denatured Hb remnants [196]. Although their presence can be detected with histological methods, RS can enhance obtained information, delivering a new insight into this known phenomenon, as in the work of Bulat et al., where AHBA were formed under high, local concentration of oxidative agents [45]. Due to complete lack of Hb-related resonant components, it was possible to detect and characterize sophisticated changes in phenylalanine conformation caused by interaction with glutaraldehyde, providing additional proof for the RBC cytoskeleton alteration.

3.2.1.2. Resonance Raman Spectroscopy (RRS). Resonance Raman (RR) effect greatly enhances Raman intensities providing up to a 10^6 -fold increase above off-resonance values, allowing extremely sensitive detection and characterization of studied samples [21,179]. RR spectra are obtained when excitation light source energy is close to that of dipole-allowed electronic absorption band (electronic transition) and the more allowed the transition, the more intense electronic band and thus the bigger resonance enhancement [179,197]. Based on the vibronic theory, Andreas C. Albrecht distinguished two major mechanisms of RR intensity enhancement: Franck-Condon scattering mechanism involving the displacement of the ground and excited states along a vibrational normal coordinate, and Herzberg-Teller vibronic coupling when the energy transfer induced by a vibrational excitation occurs [33,172,179,198,199]. The first, so-called A-term, dominates when the excitation wavelength is close to the energy of strongly allowed electronic transitions (e.g., Soret band) and results in an enhancement of totally symmetric modes; the latter (so-called B-term) dominates when excitation energy matches weakly allowed electronic transitions (e.g., Q bands) and results mostly in an enhancement of non-totally symmetric modes [172,179]. The A-term, being the leading RR scattering mechanism and providing the biggest enhancement, involves a single electronic excited state and easily vanishes off resonance. Totally symmetric modes do not lead to a distortion of the molecule, are ineffective in mixing two excited states and therefore are not enhanced via B-term mechanism, contrary to non-totally symmetric modes. Interestingly, B-term does not vanish as quickly even far-off resonance [179]. If the electronic transition is strongly forbidden, enhancement cannot occur via neither A- nor B-terms, yet excitation with such energy leads to RR effect, what was explained by a C-term mechanism [199]. This unique enhancement arises due to the coupling of the forbidden electronic transition with another one, strongly allowed, and dominates, especially when the energy is matched to the vibronic side band of such forbidden transition (e.g., 514.5 nm, which is close to Q_v band) [172,179]. Special features of C-term enhancement led to the appearance of overtones and combination tones of vibrational modes, which are involved in coupling of these two electronic states [171,179]. Examples of the Raman spectra recorded with different excitation wavelengths, together with their correlation to the UV-Vis absorption spectrum and enhancement of given molecule part, are presented in Fig. 5.

High molecular symmetry and unique electronic structure of heme makes it an excellent Raman scatterer, and Hb became a metalloprotein most thoroughly investigated by means of RRS [197]. Application of RS and RRS to RBCs analysis was developed in 1970s and 1980s by Spiro, Rousseau, Asher, Kitagawa, Champion and many others who gave it a strong foundation [197,199–204].

They defined all the most important modes and assigned them to marker bands of oxidation and spin states [200,203] thorough isotopic labelling and investigated various Hb derivatives [201,203] and adducts [205–207]. One of the most important modes, symmetrical pyrrole half-ring stretching vibration is marked as ν_4 and regarded as the oxidation state marker band [33,197,200]. In case of the ferric ion it is located around $1375\text{--}1380\text{ cm}^{-1}$, while for ferrous ion is redshifted to ca 1360 cm^{-1} . On the contrary, the ν_3 , ν_2 and ν_{10} modes are sensitive to porphyrin ring deformation and reflect iron ion spin state, being located at higher wavenumbers for low-spin (LS, at around 1510 , 1590 and 1640 cm^{-1} , respectively) and redshifted in case of high-spin (HS, at around 1480 , 1560 and 1610 cm^{-1} , respectively) iron ion [33,197,200]. However, all these works were done mainly on isolated Hb proteins or Hb standard compounds, therefore in the XXI century, with the development of Raman microscopes, studies on Hb encapsulated within RBCs and functional RBCs themselves became more and more common, providing information on Hb conformational and structural changes, Hb ordering, formation of aggregates, oxidation and spin state alterations, formation of Hb adducts, pathology-related changes in RBCs and even RBC membranes deterioration [1–3,6,45,97,171,208,209]. An example of Hb structural study is presented on Fig. 6A, where differences between an isolated oxyHb adduct (isolated protein) and oxyHb adduct formed inside functional RBCs are highlighted [5].

All the above-mentioned features make RRS powerful and versatile method to study vibrational and electronic structures of samples containing at least one chromophore [179]. It enables selective enhancement of modes connected with an individual chromophore (or given modes within one chromophore), due to different resonance mechanism depending on used excitation energy (please see Fig. 5). Due to high sensitivity, it allows rapid measurements and monitoring of kinetics with time-resolved techniques [197]. However, autofluorescence can overwhelm RR spectra and therefore this is the main disadvantage of this technique. Moreover, due to high complicity, meaningful analysis requires isotope substitution or quantum calculations, and since factors controlling the extent of enhancement are not well understood, this technique cannot be applied for absolute quantitation [179].

RBCs rich in Hb make a perfect study subject, because all Raman-related techniques allow monitoring of oxygen saturation [210], metHb level [211], various Hb adducts [2,3,6,7], malaria detection [97], elucidation of disorders such as thalassemia or sickle-cell disease [10,96], Celiac disease [212] and many more [47,171,209,213]. An example of Raman spectra of RBCs is presented in Fig. 6B (Hb adducts formed after sodium nitrite treatment).

RRS is a useful method to investigate the structure of hemozoin, the insoluble pigment composed of numerous heme dimers stabilized by hydrogen bonds and $\pi\text{--}\pi$ interactions [214]. Therefore, RRS can detect and visualize changes (RR imaging) associated with loss of hemoglobin and increase in hemozoin – biochemical changes caused by *Plasmodium* infection on a single cell level (Fig. 7) [97,215]. It was previously reported that in the RBCs, the heme environment is highly concentrated and induces the series of hyper-enhanced overtone and combination modes, which are more intense than the fundamentals, especially when using 514 nm excitation and collecting the parallel polarized light component (see Fig. 5A) [171]. In case of malaria-infected cells the fundamental region of the spectrum is dominated by hemozoin bands which obscure oxyHb bands, whereas oxyHb bands dominate the non-fundamental region of the spectrum. Consequently, it is possible to obtain information about the relative contribution of hemozoin and oxyHb in individual RBCs infected with *Plasmodium falciparum*. This confirms a potential diagnostic application of the non-fundamental region of the Raman spectrum to distinguish

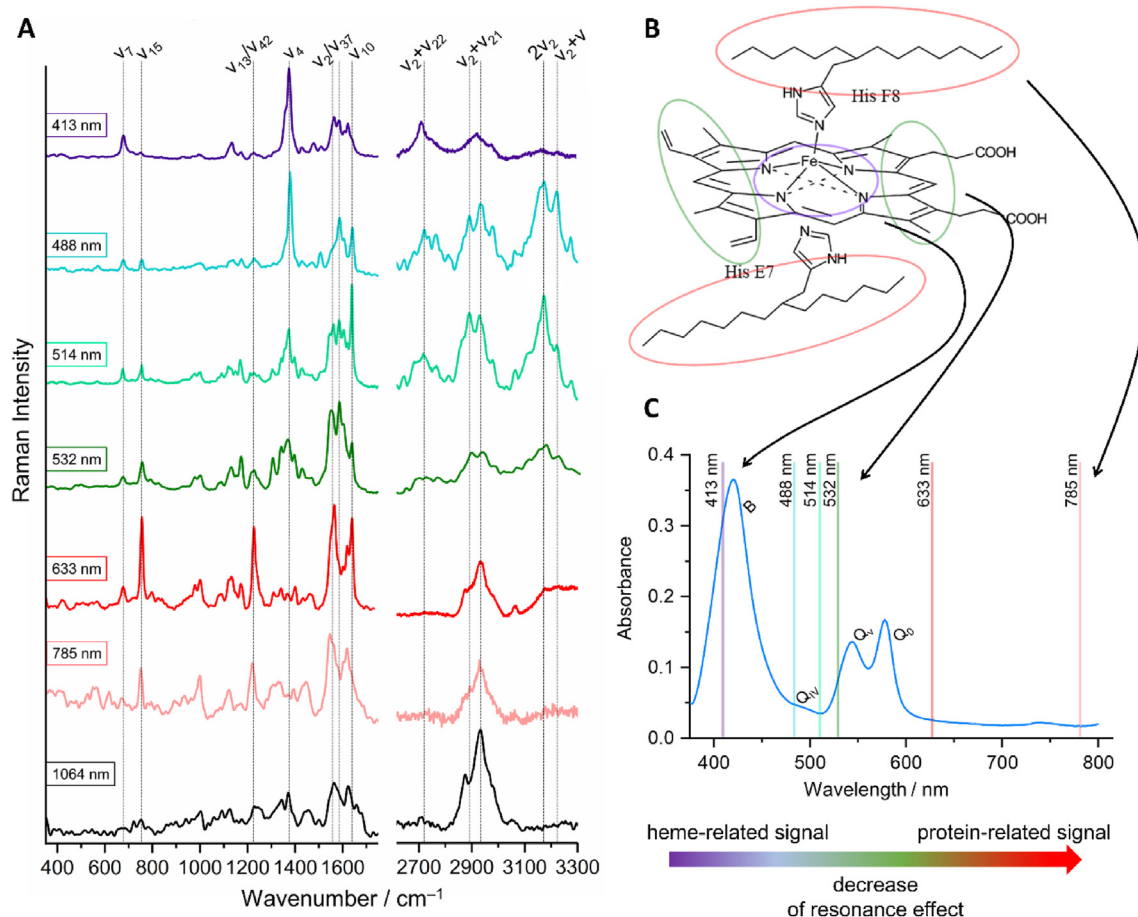


Fig. 5. (A) A set of Raman spectra recorded from isolated RBCs with various excitation wavelengths (413, 488, 514, 532, 633, 785 and 1064 nm). The most important heme modes were assigned and marked with lines. (B) Structure of the heme with marked areas of oscillations involved in resonance mechanism depending on the used excitation wavelength and (C) UV–Vis absorption spectrum of isolated RBCs with assignments of the bands and marked wavelengths. The colours used to mark excitation wavelengths correspond with each other on all panels (A–C). The Figure adapted from [33] under the terms of the Creative Commons Attribution License.

different forms of Hb in RBCs, especially oxyHb and dysfunctional hemozoin. It can be concluded that such non-fundamental region improves the potential diagnostic capability of the Raman technique for various hemopathies, providing a more detailed molecular fingerprint of the heme structure [97,171].

RR was also applied for a quick and accurate diagnosis of sickle cell disease [216], by detection of spectral changes induced in the polypeptide chain in the β -globin, what made it possible to distinguish between HbS and HbA [217]. Another erythropathy that can be detected by RR is thalassemia, a disease caused by a genetic defect, leading to a reduction of the synthesis rate of one of the globin chains that makes up Hb [218]. It is possible to distinguish between normal and thalassemic RBCs by analyzing Raman spectrum of a single, optically trapped erythrocyte (using Raman tweezers), based on the characteristic changes in Hb-related modes positions [219]. Raman spectroscopy imaging was also used in arterial clot analysis to define thrombi origin, what in turn enabled differentiation of clinically valid parameters of an acute ischemic stroke [220].

3.2.1.3. Surface-enhanced Raman Spectroscopy (SERS) and tip-enhanced Raman spectroscopy (TERS). Surface-Enhanced Raman Scattering (SERS) is a modern label-free analytical technique allowing molecule-specific and fast detection of the studied material. The adsorption of the measured molecules onto a nanoscale roughened metal surface can provide a 10^6 – 10^8 increase in Raman

scattering intensity, enabling single molecule detection with quenched fluorescence. SERS typically uses metal surfaces containing gold or silver metallic coatings, placed on the nanostructured substrates or prepared in the form of nanoparticles with different morphologies [221]. SERS is reported to be a highly promising and sensitive method for characterization of the whole human blood, blood plasma, single RBC, erythrocyte ghosts and Hb variants enclosed within functional RBCs (see: Fig. 8A) [52,222–228]. SERS and corresponding normal Raman spectrum reveals significant differences, and their direct comparison is often misleading. The SERS signal originates from the interaction of molecules with the metallic substrate surface, which could affect the symmetry of molecules and lead to variations in the band positions and changes in their relative intensities. Additionally, some of the bands can be attributed purely to the substrate or substrate-sample interaction. The SERS effect is also highly localized, so it is possible to acquire the signal solely from the part of the molecule located closely to the substrate [221]. In consequence, only selected vibrations affected by the SERS effect would produce bands with enhanced intensities. However, combination of both, SERS and RS spectra, can provide alternative and complementary information about hemeprotein-based samples and other analytes, even when embedded in complex biological matrix. Due to much higher Raman intensities, especially in the low-frequency range, SERS allows to obtain much more detailed spectral data compared with normal RS, and therefore enables detection and identification of the blood components present in low

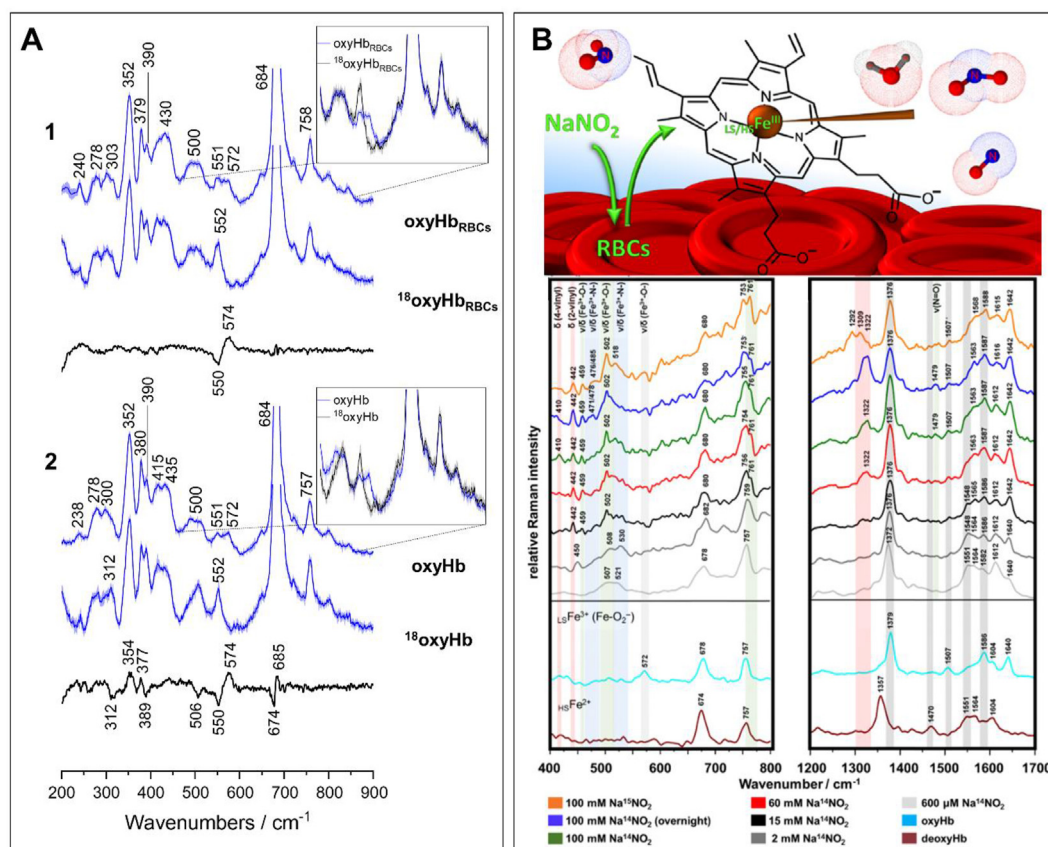


Fig. 6. (A) Resonance Raman spectra of oxyHb and ¹⁸O-substituted oxyHb (1) enclosed within RBCs and (2) isolated from RBCs recorded with 413 nm excitation wavelength. The RRS spectra are presented with their standard deviation (blue shadows), differential spectra (black lines) and insets corresponding to the expanded area in the 450–850 cm⁻¹ spectral range. The Figure was adapted with permission from [5] provided by Elsevier and Copyright Clearance Center. (B) Raman spectra recorded from isolated RBCs with 488 nm excitation wavelength. The bottom panel comprises basic Hb adducts – deoxy- and oxyHb, while the upper panel comprises Hb adducts formed after exposure to increasing sodium nitrite doses (please see the legend for details). The most important heme modes were assigned and marked with the coloured lines. The Figure was adapted with permission from [3]. Copyright (2016) American Chemical Society.

concentrations [52,224]. The excellent signal-to-noise SERS spectra of RBCs can be acquired using nanoparticle SERS substrates covered with gold or silver, with 785 and 514 nm laser excitations [52]. However, slight shifts in bands' position can result from the variation of SERS enhancement mechanisms, related to metal-surface interactions, surface orientation and distance dependency, what can complicate vibrational band assignments [52,229].

Brazhe et al. demonstrated that SERS signal of living RBCs originating from submembrane Hb is associated with cytosolic domain of an anion exchanger AE1 (band 3). Additionally, SERS spectra of RBCs were different when compared to SERS spectra of free isolated cytosolic Hb, what indicated their different conformations and molecular properties. The study revealed that submembrane Hb population was different from the cytoplasmic population dominated the spectrum of Hb [227]. SERS technique has been extensively used as a valuable tool for selective detection of Hb variants, e.g., oxy- and met-RBCs [52]. It was shown to be useful in diagnosis of diabetes, because of the spectral distinction between glycated hemoglobin (*HbA1c*) and HbA (adult hemoglobin) [223]. There is also a possibility to quantify a total hematin concentration in human RBC cytosol without the necessity of separating it from Hb due to the stronger SERS signal from hematin compared to the other biological components [230]. SERS was also previously used for rapid malaria detection using silver nanorod array substrates [12]. An interesting application of SERS technique

comprises investigation of the role of RBC membrane in the nanoparticle uptake. Specific interaction between nanoparticles with Hb, RBCs and the RBC membrane is crucial in nanotoxicity research. It was reported that SERS spectral information about RBCs and their components strongly depended on the type of SERS substrates and the size of the nanoparticles, as well as external conditions. The research indicated hemolytic activity of silver nanoparticles in contrast to gold nanoparticles, which left the cells intact (Fig. 8B) [225].

The other powerful Raman technique is Tip-enhanced Raman spectroscopy (TERS). TERS is a variant of SERS that allows studying cell surfaces with sub-nanometer spatial resolution. TERS spectra show oxidation changes on the surfaces of hemoglobin crystals [222] and drugs binding to the surface of hemozoin (iron–porphyrin–proteinoid blood complex) in nanoscale, within a single sectioned erythrocyte [231]. Reports about the application of TERS to RBCs analysis are scant, but the above-mentioned study of heme-based samples may prove the potential use of this method for future RBCs analyses.

3.2.2. Non-linear Raman scattering: coherent anti-Stokes Raman Spectroscopy (CARS) and stimulated Raman spectroscopy (SRS)

As a method of RBCs analysis in biology and medicine, CARS is an attractive alternative to other traditional techniques. The capability of CARS microscopy for tight focusing, non-linear excitation

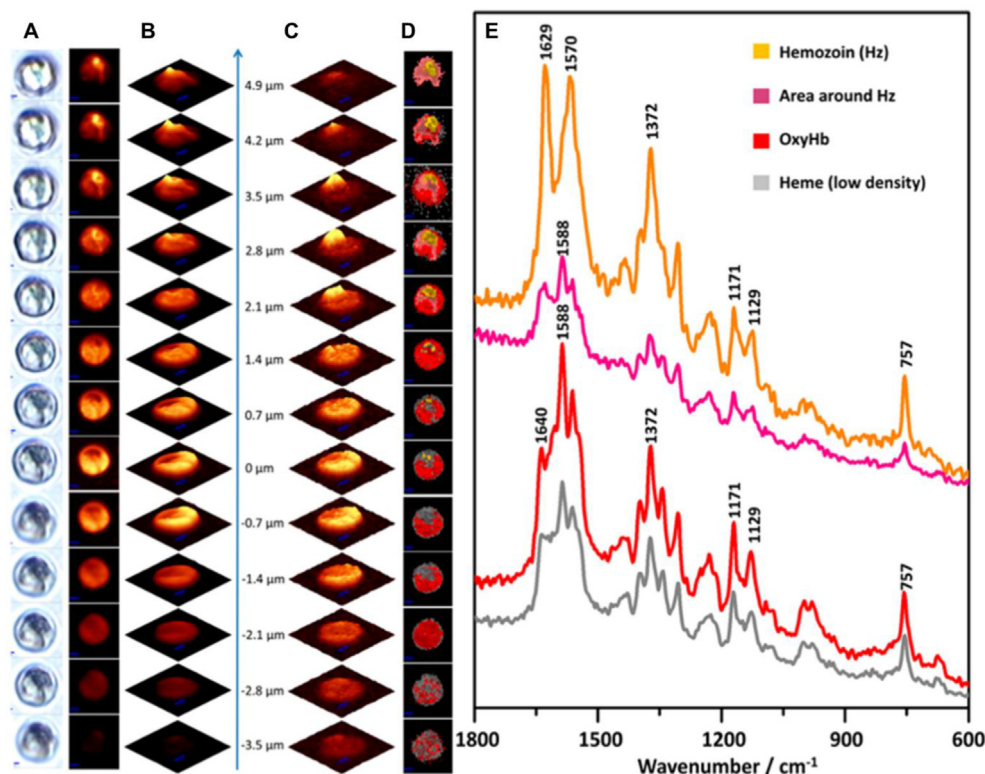


Fig. 7. Raman images and spectra of malaria infected RBC. (A) visual images on the level of Raman stack measurement; (B) autofluorescence of RBC; (C) Raman integration images based on the heme modes observed in 1500 – 1700 cm^{-1} spectral range; (D) KMC images with four distinct classes color-coded as follows: hemozoin (yellow), oxyHb (red), low density heme (gray) and altered area around hemozoin (pink). Figure was adapted with permission from [97]. Copyright (2018) American Chemical Society.

and acquisition of chemically selective signal allows obtaining cellular images with high 3D spatial resolution. This method is noninvasive and does not require the use of any staining, fixation procedure or metal surfaces. CARS microscopy signal intensities are much stronger compared with RS microscopy, and thus can be collected with much higher speed. Therefore, CARS imaging is more useful to monitor dynamic processes, e.g., in RBCs, to track changes in blood in real-time [232].

The possibility to follow Hb oxygenation state [233] or visualize lipid bilayers from different organelle membranes was demonstrated, as the aliphatic CH_2 bonds in lipid chains give very strong CARS signal, allowing rapid cell imaging under physiological conditions [177]. High sensitivity of this technique to detect even a single monolayer of lipids allowed observation of phospholipids in erythrocyte ghosts (Fig. 9) and unilamellar vesicles without fluorescence labeling and fixation procedures [234]. CARS was found useful in the examination of RBCs aggregation, as the interaction between these cells in dynamic environment can help to develop novel tools for diagnosis and treatment of various pathologies, such as diabetes or hypertension [235].

Stimulated Raman spectroscopy (SRS) is another variant of Raman spectroscopy characterized by much higher signal intensity, compared to normal RS or even CARS, and allowing high-speed and high-throughput single cell analysis [183]. Similar to CARS, SRS is a label-free vibrational imaging tool that finds application in rapid imaging of sample discrete frequencies. Even so SRS imaging is possible in the fingerprint region, and like CARS, it has been being mainly applied in the high wavenumber region in the vicinity of CH modes for analysis of lipid, protein and nucleic acid analysis within

a living cell (ca. 2800–3800 cm^{-1}) [236]. Suzuki et al. used the combination of flow cytometry and SRS to perform marker-free detection of cancer cells in the blood. They carried out SRS imaging and flow cytometry measurements to obtain large amounts of human whole blood cells images (mostly RBCs) [237]. Moreover, there is a possibility to use simultaneous multicolor SRS imaging, by adding a fiber amplifier to conventional SRS setup, in order to image WBCs and RBCs simultaneously in the bloodstream of living animal [238]. Improvement of SRS photodetectors allowed the researchers to capture individual RBCs moving through a capillary in real-time, what gives new opportunities for future biological imaging and medical diagnostics [239].

3.3. Correlative molecular spectroscopies and microscopic techniques in RBCs analysis

3.3.1. FT–IR spectroscopy

FT–IR spectroscopy is widely used for *in situ* studies of biological samples, delivering information about various biochemical components, such as proteins, lipids, nucleic acids, carbohydrates, heme proteins and inorganic crystals, without a need for any labels and without any impact on the measured sample. The differentiation of biological samples is based mostly on the relative amounts of compounds present in the cell, e.g., proteins (Amide I/II modes), carbohydrates (C–O stretching mode), lipids (C=O ester carbonyl stretching) and phospholipids/nucleic acids (phosphodiester stretching modes). The FT–IR imaging of the distribution of the main components of biological samples is challenging in both transmission and transfection microscopic modes because of the

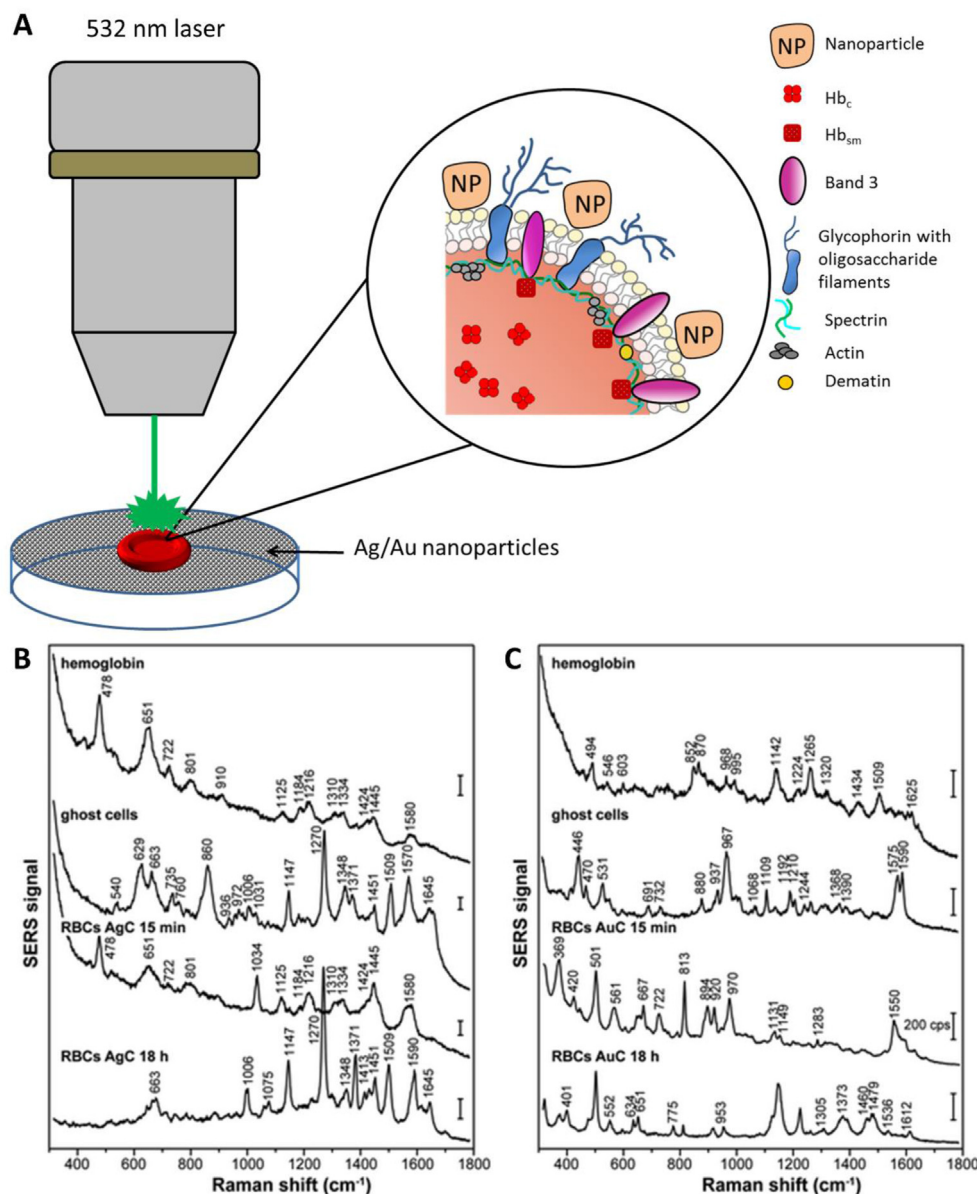


Fig. 8. (A) Schematic diagram of a SERS experiment with nanoparticle (NP) attached to the RBC membrane to enhance Raman signal acquired from RBC membrane components. (B–C) Set of SERS spectra of Hb, ghost cells (RBC membranes) and intact RBCs on (B) Ag or (C) AuC nanoparticles recorded with 785 nm excitation wavelength. Spectra presented on (B–C) were adapted from [225] with permission from the Royal Society of Chemistry.

diffraction limited resolution. Attenuated Total Reflection (ATR) microscopy can improve the spatial resolution (2–4 μm), but only probes the outer parts of the biological material as the penetration depth is limited to 2 μm [240–242]. Apart from a very fast collection time (over 16 000 spectra in 5 min) IR imaging also provides high quality spectra, which can be analyzed using chemometric methods. FT–IR was also reported to be an excellent tool for studying biochemical profile of the membrane and the inside of RBCs [1,243].

The state of cell membrane is mainly determined by lipid spectral region and is intimately connected with the structure and chemical nature of lipids [244]. The intensity ratio of the 2960 cm^{-1} (CH_3 antisymmetric stretching) to 2930 cm^{-1} (CH_2 antisymmetric stretching) provides information about the lengths of acyl chains. Their changes may denominate chemical signs of oxidative stress and aging process, as was reported by previous studies [1,245].

FT–IR enables identification of peroxidative damage of RBC membranes resulting from the loss of unsaturation of the fatty acyl chains and formation of the C–O groups. It can be semi-quantitatively monitored via the 3012 cm^{-1} band assigned to the olefinic = C–H stretching modes and generation of the 1260 cm^{-1} band corresponding to C–O stretching vibrations [1,246]. Changes in the CH stretching region (3100–2800 cm^{-1}) in RBCs turned out to be characteristic for different stages of the malaria parasite development [97,214], atherosclerosis disease [1] and exercise-related oxidative stress [247]. Additional advantage of FT–IR lays in the possibility of recognizing kinds of lipids occurring in the RBC sample, and identification of alterations in phospholipids, cholesterol esters and cholesterol content in the erythrocytes. This is possible due to observation of different changes, e.g., in the intensities and shifts of bands at: 1236 cm^{-1} (assigned to antisymmetric stretching vibrations of the PO_2 groups), 1167 cm^{-1}

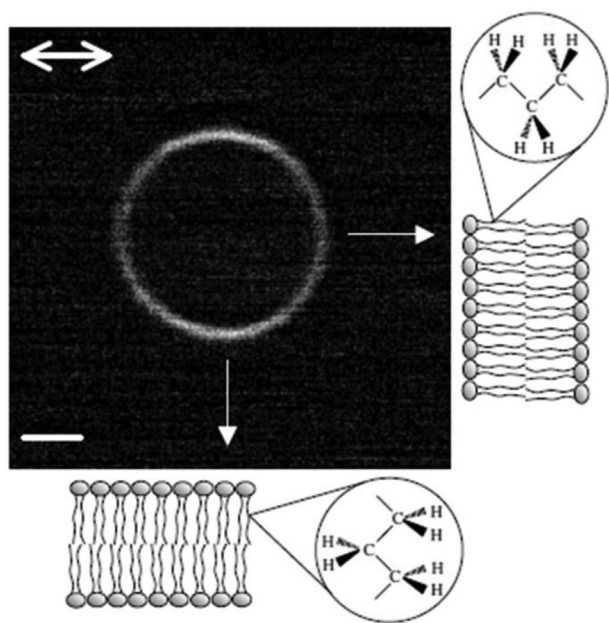


Fig. 9. F-CARS image of the RBC ghost (membrane) taken in the equatorial xy plane at a 2845 cm^{-1} wavenumber; the intensity corresponds to the orientation of the bilayer giving higher intensity (top and bottom of the RBC ghost) when averaged C–H bond orientation is in parallel with the incident beams. Figure adapted with permission from [234] provided by John Wiley and Sons, and Copyright Clearance Center.

(corresponding to the $-\text{CO}-\text{O}-\text{C}$ asymmetric stretching modes) and 1055 cm^{-1} (the C–O bending vibrations) [1]. It is worth noting that chemical change of the lipid profile of the membrane can be observed on FT–IR spectra when intact RBCs are measured (without having to isolate ghosts) [1]. Petibois et al. also showed the analytic potential of FT–IR to determine exercise-induced metabolic alterations seen as changes in glucose and lactate content, by the analysis of the bands that correspond to the vibrations of C–O bonds in molecules (at 1033 cm^{-1} and 1127 cm^{-1} , respectively) [248]. FT–IR enables detailed studies of the protein secondary structure in RBCs by the determination of amide I bands positions at $1680, 1660, 1652, 1638, 1629$, and 1619 cm^{-1} , indicating the presence of different kinds of structures: intramolecular aggregates, turns, α -helices, unordered structure, β -sheets and intermolecular aggregates, respectively [249]. This feature was described in some previous reports, describing storage time-dependent changes in RBCs and modifications resulting from diseases such as gastric cancer or atherosclerosis [1,250,251]. However, in the case of standard FT–IR methods, such as ATR–FT–IR, observed changes are related rather to hemoglobin structure, than to membrane and cytoskeleton protein alterations. Oxygenated form of hemoglobin can be detected in RBCs using FT–IR by the analysis of the band at 1104 cm^{-1} assigned to the $\text{O}=\text{O}$ stretching vibration [250]. A huge potential of FT–IR for RBCs studies is also associated with the possibility of disease detection in wet pRBC samples, e.g., identification and quantification of malaria parasite infection [252,253]. Moreover, it enables to eliminate significant contribution of anticoagulants, such as EDTA or heparin to the spectral profile of RBCs [252]. FT–IR with the submicron and nanoscale resolution gives the possibility to check the local chemical variability within single cell, investigate chemical differences between the central and border region of individual RBC, determine the secondary structure of membrane proteins, as well as to image parasites within the RBCs [1,154,245,254]. Various examples of FTR applications in RBCs studies are presented in Fig. 10.

3.3.2. Electron paramagnetic resonance spectroscopy (EPR)

Electron paramagnetic resonance (EPR) spectroscopy, also known as electron spin resonance (ESR) or electron magnetic resonance (EMR) is based on the absorption of electromagnetic radiation by a paramagnetic sample placed in a strong magnetic field. EPR is a standard method used for characterization of samples with unpaired electrons, i.e., containing paramagnetic centers. Such centers either occur naturally within samples or can be induced by exposition to some physical factors, e.g., ionizing radiation [255]. Due to high sensitivity, this technique can provide valuable data on the presence, identity, concentration, structure, mobility and intermolecular interactions of radicals in a studied sample [256].

In human blood natural paramagnetic centers are present, such as molecular complexes containing ferric (Fe^{3+}) iron ion (transferrin, metHb) or copper (Cu^{2+}) ions (ceruloplasmin), as well as free radicals, e.g., H_2O_2 , NO , OH^\cdot , O_2^\cdot [257,258]. RBCs are commonly studied with use of EPR, not only because they contain metHb, but especially because of their function as oxygen carriers, what includes them in the group of reactive oxygen species (ROS) generators. Since some ROS are short-lived, the spin-trapping technique is commonly employed. In this approach, special compounds named Spin Traps are added to react covalently with free radicals to form more stable spin adducts with a relatively longer half-life, what enables more accurate EPR detection and identification [259].

Currently EPR spectroscopy is used in studies investigating the influence of both ionizing radiation [260] and free radicals on the blood and RBCs properties, where not only the oxidation state of the iron ion is monitored, but also lipid peroxidation in the RBC membrane [261,262]. EPR is suitable for investigation of the RBC membrane components and its resistance in response to environmental conditions [263–265] or pathologies [266,267]. Moreover, EPR is used in pre-transfusion assessment of RBCs quality, e.g., monitoring of oxygenation level [268,269]. Hb adducts, especially nitrite-related intermediates such as HbNO^+ , is currently broadly run with EPR spectroscopy [6,270,271], as it seems that NO released by RBCs may play an important role in regulating vascular function under hypoxic conditions [270]. The detection limit of Hb adducts, which are paramagnetically active, reaches sub-nanomolar concentrations [272].

3.3.3. Mössbauer spectroscopy

Mössbauer spectroscopy is based on the recoilless resonant absorption and emission of the gamma radiation, and allows to study the hyperfine nuclear interactions [273]. This highly sensitive method can be used to monitor the valence and spin states of a probing atom, types of its neighbors and associated chemical bonds.

The majority of Mössbauer measurements involve the 2% ^{57}Fe isotope of iron, and for this reason this technique is extremely suitable for heme protein studies including biological samples like RBCs [274–276]. However, only ^{57}Fe is active in Mössbauer spectroscopy and thus requires high concentrations of the Hb in the sample, preferably millimolar or higher. Usually, whole blood or isolated RBCs are measured without further dilutions [6,277]. This method allows the detection and monitoring of oxidation and spin states of various Hb forms in isolated proteins [278] and proteins encapsulated inside RBCs [279]. Taking into consideration that oxidation and spin states of Hb are sensitive to homeostatic imbalance in RBCs exposed to pathological conditions or storage, Mössbauer spectroscopy is a powerful tool for monitoring RBCs functionality. Depending on the Hb form, the iron ion would bond with different atoms or groups of atoms, such as O_2 (in oxyHb), CO , H_2O (in metHb), CN^- , F , N_2 , NO , OH^- , etc. [275]. All these ligands are present in the sixth coordination site, that significantly modifies nuclear and electron properties of an iron ion, and therefore, Mössbauer spectroscopy can be used for differentiation of Hb adducts [276].

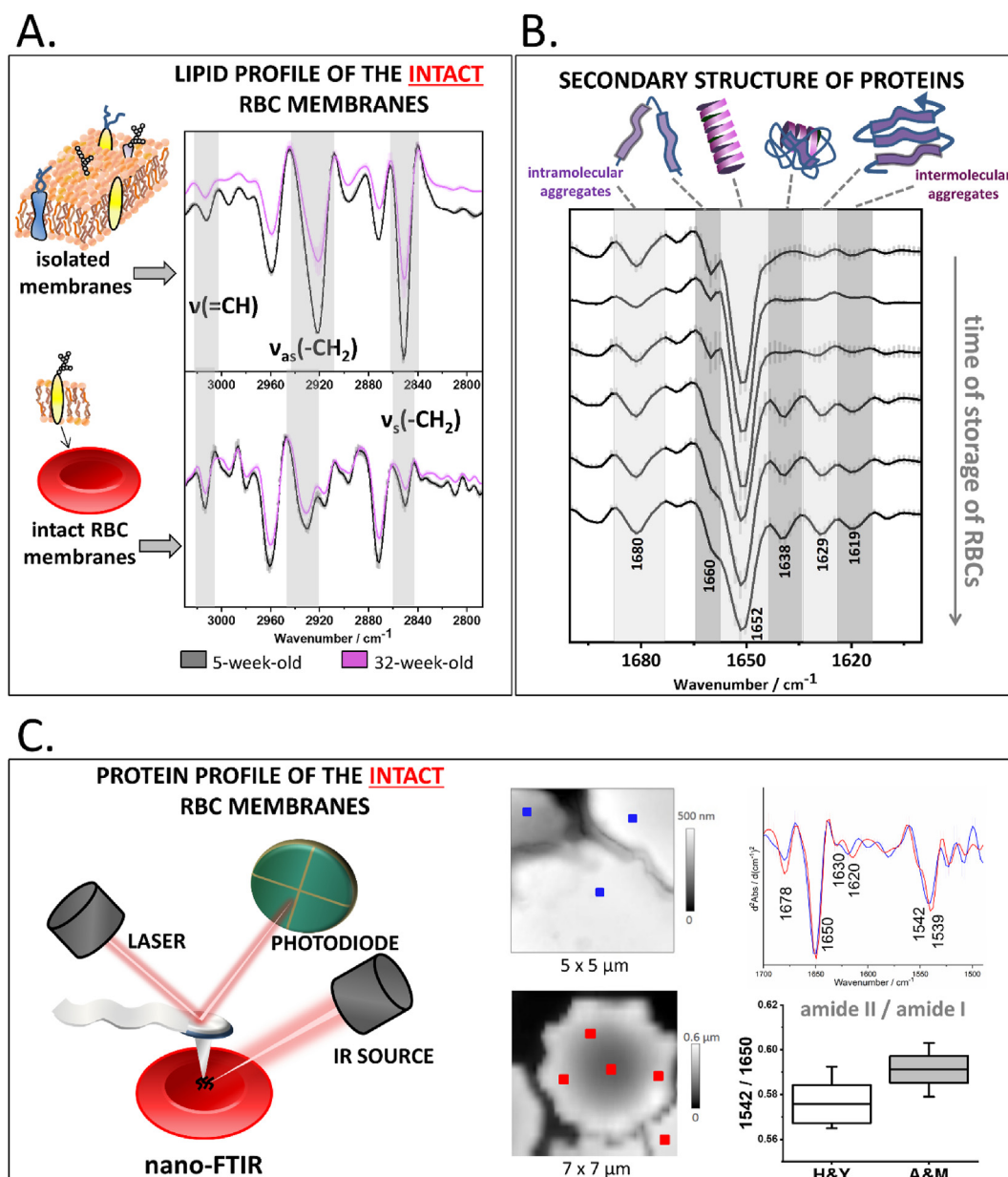


Fig. 10. (A) The comparison of second derivative ATR-FT-IR spectra in the range of 3050 – 2800 cm^{-1} of intact RBCs and isolated membranes derived from 5-weeks-old and 32-weeks old mice. (B) Second derivative ATR-FT-IR spectra in the range of 1700 – 1600 cm^{-1} of the pure RBC fraction of pRBCs collected after 1 – 6 weeks of storage for exemplary blood donor, showing the alterations in the secondary structure of Hb during storage of pRBCs. (C) A scheme of nano-FT-IR measurement, topography images of healthy and young (H&Y) RBCs and atherosclerosis and mature (A&M) RBCs (dots in the topography image mark positions from where the nano-FT-IR spectra were recorded), and a comparison of averaged second derivative nano-FT-IR spectra for H&Y and A&M in the region of 1700 – 1500 cm^{-1} , the ratios of amide II to amide I bands for the corresponding spectra. Figures in panel D were partially adapted with permission from [1]. Copyright (2019) American Chemical Society.

Interestingly, on the base of the Mössbauer spectra of RBCs that were exposed to low doses of ionizing radiation, it was previously reported that such radiation not only affects normal Hb adducts, but causes formation of a new type of Hb adducts with new hyperfine parameters of isomeric shift and quadrupole splitting [280,281]. Mössbauer spectroscopy can also be used to monitor oxygen rebinding in healthy and pathological RBCs [282,282,283] during aging or storage processes [277].

3.3.4. Atomic force microscope (AFM)

Atomic force microscope (AFM) enables live cell imaging and membrane surface characterization at nanometer resolution [284,285]. AFM provides resolution up to 1000 times greater than

optical microscopy, reaching values in the range of 1–2 nm (lateral, X–Y) and 10 nm (height, Z) which are limited by the radius of the AFM tip [286,287]. AFM works mainly in three different modes: contact, non-contact and tipping mode. Contact mode is associated with repulsive forces, where the AFM cantilever is in physical contact with sample surface. It is well suited for dried and fixed samples and is commonly used for force and friction measurements. Non-contact mode is associated with attractive forces. Gentle above-surface scanning with the cantilever prevents penetration and rupture of highly sensitive samples. Tipping mode, an intermediate between contact and non-contact modes, is associated with repulsive forces, and is used for liquid measurements and especially preferred for non-fixed samples [288].

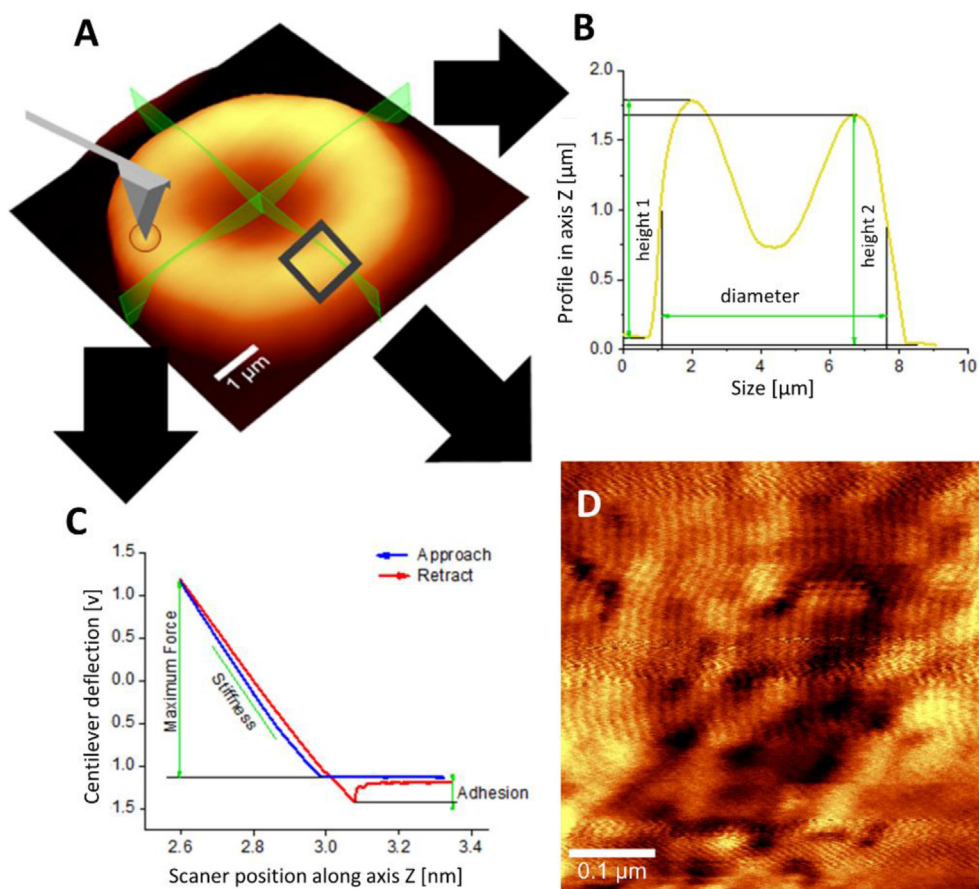


Fig. 11. An example of AFM application in RBCs studies: (A) Topography of a single RBC in microscale; (B) cross-section profile of a scanned RBC; (C) force-curve of the AFM cantilever indentation into RBC membrane; (D) topography of RBC's membrane skeleton in nanoscale.

This powerful tool is commonly used in RBCs measurements, even on a single cell level, to assess their morphology and surface alterations, including quantitative analysis (Fig. 11). AFM imaging gives opportunity to study topographical alterations of the RBCs during aging and storage processes, as well as in response to altered or pathological conditions [158,282,289,290]. Application of AFM was previously reported to give insight into biconcave disc shape of healthy RBCs, as well as enabled the analysis of altered RBC shapes, like oval cells, stomatocytes, echinocytes with characteristic spicules, and spherical RBC which are unable to preserve functionality [282,291,292]. This technique was also used to show the influence of fixation on the shape and appearance of the erythrocytes [37,38,115] related to aging and atherosclerosis [115].

As the AFM is a perfect tool for nanoscale measurements, changes in the RBCs membrane, e.g., in their cytoskeleton, can be studied as well. Mathematical models such as multifractals [293,294] or simple cross sections of each RBC image can deliver additional information about structural changes in the RBC membrane skeleton [282,292]. It was confirmed that RBCs diameter, height and volume, is changing during their life span, what can be a consequence of normal RBCs development and vesiculation process [292,295] or is associated with pathological conditions [279,283] and infection [296]. Structural organization of the membrane skeleton, crucial for proper RBC functionality, can be disrupted and changed from its typical hexagonal spectrin grid into other unordered forms [282,297]. Some diseases cause not only size, shape and morphology alterations, but also protein aggregates formation on RBCs surface [298].

AFM technique also allows for determination of the force curves of the measured membrane surface, what delivers direct information about RBC's adhesion, elasticity and stiffness [299,300]. It is commonly known that any change in the elasticity of the RBC membrane, including a decrease/increase in stiffness and roughness, indirectly influences RBCs deformability, and therefore alters their functionality and gas exchange properties [158,301].

AFM is often combined with other spectroscopic devices, such as Raman imaging, what provides better insight into RBC structure and allows for the measurement of the same cell with both techniques [45,302]. On the other hand, AFM combined with infrared spectroscopy (AFM-IR) can be important and irreplaceable tool which gives deeper insight into mechanical and chemical properties with spatial resolution better than any other methods [154].

3.3.5. Scanning near-field optical microscopy (SNOM)

Scanning near-field optical microscopy (SNOM) combines the advantages of classic optical microscopy with the benefits of a near-field scanning technique. Therefore, it can simultaneously provide high-resolution optical images and topographic information in nanoscale [303–306]. Typical SNOM resolution is between 50 and 100 nm and is mainly determined by the size of tip aperture (in the aperture-SNOM, a-SNOM) or probe dimension (in the scattering-SNOM, s-SNOM) [303,306,307]. Various set-ups of SNOM allow to investigate the reflection or transmission properties of the sample [303–305,308]. Moreover, if materials contain fluorophores, fluorescence can also be measured [309–311]. Recently, SNOM technique has been successfully used in materials' science and

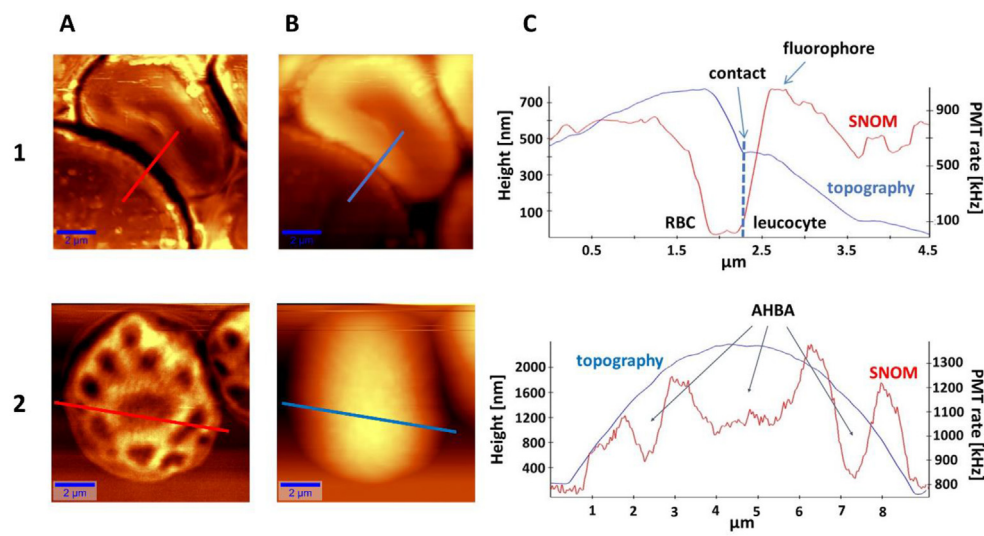


Fig. 12. (A) SNOM results, (B) topography images and (C) comparison of the SNOM and topography images cross-sections prepared according to red/blue marking lines for: (1) normal RBC in contact with leucocyte (adapted with permission from [2] provided by John Wiley and Sons, and Copyright Clearance Center) and (2) RBC with Heinz body-like aggregates (AHBA) after glutaraldehyde treatment (adapted from [45] with permission from the Royal Society of Chemistry).

Table 1

Comparison of benefits, limitations and drawbacks of classic, spectroscopic and microscopic approaches to biomedical analysis of RBCs presented within manuscript.

Technique	Non-destructive	Label-free	Level of expertise	Cost of analysis	Time of analysis
Complete blood count (CBC)	X	X	+	+	+
Morphology assessment	X	X	++	++	+++
Serology	X	X	++	++	+++
Biochemical parameters	X	X	+	+++	++
Flow cytometry	X	X	+++	+++	++
Ektacytometry	X	X	+	++	+
UV–Vis Absorption spectroscopy	V	V	++	+	++
Blood gas analysis (BGA)	X	V	+	+++	+
Raman spectroscopy (RS)	V	V	++	+	++
Resonance RS (RRS)	V	V	++	+	++
Enhanced RS (SERS, TERS)	V	V	+++	++	++
Non-linear RS (CARS, SRS)	V	V	+++	+	++
FT–IR spectroscopy	V	V	++	+	++
EPR	X	V/X	++	++	++
Mössbauer spectroscopy	X	V	+++	+++	+++
AFM	V	V	+++	+++	+++
SNOM	V	V	+++	+++	+++

Legend: V – confirmation, X – negation, +, ++, +++ – scaling, where + means low required expertise, low cost of analysis and low time of analysis, respectively, whereas +++ high required expertise, high cost of analysis and high time of analysis, respectively.

biomedical research [303,312]. However, its application to biological objects (especially living cells), may cause many technical problems, due to their complicated nature [307,313]. Thus, very often SNOM is only a support and complement to other techniques. Usually, it is coupled with spectroscopic methods [2,45,314–317].

Up to date, SNOM has not been widely applied in RBCs studies. Nonetheless, Enderle et al. proved that fluorescence SNOM is a powerful tool for investigation of RBC membranes. They imaged colocalization of parasite proteins in human erythrocytes infected by malaria [309,318]. Other researchers used SNOM to detect distribution of the protein complement receptor 1 (CR1/CD35) and quantitatively measure its clusters in RBC membrane [319]. Furthermore, previous studies have shown application possibilities of the s-SNOM to create high-resolution refractive index (RI) map of the erythrocyte, what can serve as a potential disease biomarker [320]. On the other hand, cytochalasin penetration into the RBC plasma membrane has been demonstrated by the a-SNOM

measurements in tapping mode [307]. Some interesting results considering the RBCs have also been revealed using transmission SNOM. The erythrocytes are partially transparent to the blue laser light (488 nm) [2], however, in spots with advanced Heinz body-like aggregates (AHBA) formed during glutaraldehyde treatment, the excitation light signal was found to be less detectable (Fig. 12) [45]. In addition, complementary methods (Raman spectroscopy, staining) supported SNOM results and allowed to confirm the presence of Fe^{3+} ions in the AHBA.

4. Conclusions and outlook

Innovative spectroscopic and microscopic approaches, especially those based on Raman spectroscopy, have a potential to become valuable methods in medical diagnostics. Commonly used biochemical techniques increasingly occur to be insufficient to determine alterations or deteriorations of RBCs at the molecular

level. Explanation of the etiology of some complex RBC alterations often requires multimodal methodology with out-of-the-box approach, comprising application of methods including sophisticated spectroscopy-based (Raman, FT-IR, EPR, etc.) and microscopic (AFM, SNOM) techniques, that until now have not even been considered to be used in medical diagnostics.

Depending on the research direction and expected results, the choice of a proper experimental technique is essential. Up to date, none of the available methodologies provides full insight into RBCs morphology and functionality at the same time. Each of the currently available techniques used in RBCs studies is characterized by pros and cons that must be considered in the design of the experiment (see Table 1 for details).

Most of the classical approaches in RBCs studies, including medical analytics, are destructive and require the use of labels or dyes. They are often time-consuming, demand high level of expertise and long-time data analysis, while their cost remains relatively high. Although they are commonly used in biomedical facilities and serve as a gold standard for clinicians, in order to fully understand molecular and mechanistic aspects of erythropathies, they need to be supported by innovative spectroscopic and microscopic approaches.

Deformability, one of the most studied parameters of red blood cell functionality, can be assessed by means of ektacytometry. However, despite giving an insight into mechanical properties, along with its suitability for clinical analysis, simplicity and high reproducibility, this technique cannot provide explanation of changes in RBC elasticity and shape alterations. On the contrary, AFM delivers more complex information about RBC membrane skeleton [282,292] including spectrin grid [282,297] or vesiculation process [292], supporting and expanding the knowledge obtained from ektacytometry. AFM microimages not only provide the same information as SEM, but additionally are able to deliver information about exact parameter of the sample size in nano-scale [176,292]. Due to the use of interactions between measured sample and scanning cantilever, AFM can be used in RBCs studies for direct measurements of single red cell morphology, providing insight into alterations and quantitative data about RBC surface properties, supporting and expanding knowledge obtained from SEM, ektacytometry and morphological assessment. Changes in morphology can be precisely tracked with use of visual microscope and proper dyes, however, changes at the molecular level can be tracked only with application of more advanced techniques, as presented in case of advanced Heinz body-like aggregates (AHBA) [45]. This work showed that only by supporting classical approaches with innovative AFM-SNOM-RS-based approach, AHBA identification and characterization on the molecular level was possible [45].

The biggest advantages of vibrational spectroscopy-based techniques include their non-destructiveness and lack of requirements of any labels or dyes. Preparation of samples is mostly restricted to its dilution or placement on a special type of substrate. The combination of RS and IR-based approaches allow for a complementary analysis of RBCs and RBC membranes. Recent studies clearly proved that their application allowed for explanation of hemoglobin-oxygen binding efficiency through comprehension of irreversible changes of the secondary and quaternary structure of Hb during human RBC storage [115,321]. Although affinity to oxygen or oxygen carrying capacity can be easily assessed by BGA or UV-Vis, an insight into molecular changes in protein conformation is exclusive to this vibrational spectroscopy techniques. Classic methods assess levels of lactic acid, hemolysis (and thus increased cell-free Hb) and alterations in ionic balance, however, they require labels and/or chemical reagents, whereas vibrational spectroscopy techniques can deliver the same information in an easier and faster way, without any sample

preparation [96,248,322,323]. Application of both, Raman and IR for analysis of isolated RBC membranes allowed to obtain rapid information about their biochemistry and could become a future standard complementary to biomedical analysis approach in diagnostics of various erythropathies [1,115,158,193]. The biggest advantage of the Raman-based approaches in RBC studies is related to the richness of information provided by Raman spectra regarding heme and Hb-related changes. General quantification of main Hb adducts can be assessed by UV-Vis and BGA analysis [266–269]. However, more sophisticated analysis of various nitrosyl-, nitroxyl-, carboxy- or sulf-Hb adducts, which is of importance in cardiovascular medicine [324–327], can be provided only by RR and other Raman-related techniques [3,5,6,33]. Unique properties of heme and its ability to scatter light so strongly allowed to develop methodology used in malaria diagnosis through detection of hemozoin inside RBCs [97,231,244,328]. Interestingly, application of TERS allowed for detection of hemozoin crystals of a size of less than 20 nm, far beyond the diffraction-limited spatial resolution [231]. Moreover, these studies have now moved towards *in vivo* application [97]. The use of Raman-based methodologies is not restricted only to malaria diagnostics, but reaches much further, including diagnosis of sickle cell disease, thalassemia, arterial clot analysis, alterations in RBC membranes, formation of Hb agglomerates, etc. [1,45,97,115,217,219,328].

Another considerable factor is the interpretability of information obtained with each technique. While each method of classical analysis provides a single or a few values of given and known parameters, which could be directly interpreted by a researcher or clinician (e.g., RBC count, deformability, etc.), spectroscopic methods such as RS provide label-free information as a set of overlapped bands representing the composition of the RBCs. This, on the one hand, can be considered as a disadvantage, as it requires the use of sophisticated data mining or machine learning methods to extract the information needed [97,171,213,253,254]. The need of complex treatment of data delays interpretation of the results and makes the technique less appealing to non-specialist spectroscopists, such as biologists and clinicians. On the other hand, the use of sophisticated data analysis ensures that a large amount of molecular information is extracted from spectroscopic data, exploiting the true label-free nature of this technique and providing a snapshot of the phenotype of the RBCs.

In summary, currently used classic and reference methods, such as CBC, morphology, serology, biochemistry, flow cytometry, ektacytometry, etc., cannot be replaced, however, as we evidenced in this review, the insight they provide can be enhanced and improved by increasing the technique palette used in RBCs studies with innovative spectroscopic and microscopic approaches.

Declaration of competing interest

The authors declare that they have no known competing financial interests or personal relationships that could have appeared to influence the work reported in this paper.

Acknowledgements

This work was supported by the National Science Centre, Poland (UMO 2016/23/B/ST4/00795).

References

- [1] A. Blat, J. Dybas, M. Kaczmarek, K. Chrabaszcz, K. Bulat, R.B. Kostogryś, A. Cernescu, K. Malek, K.M. Marzec, An analysis of isolated and intact RBC membranes—a comparison of a semiquantitative approach by means of FTIR, nano-FTIR, and Raman spectroscopies, *Anal. Chem.* 91 (2019) 9867–9874. <https://doi.org/10.1021/acs.analchem.9b01536>.

- [2] K.M. Marzec, A. Rygula, B.R. Wood, S. Chlopicki, M. Baranska, High-Resolution Raman imaging reveals spatial location of heme oxidation sites in single red blood cells of dried smears, *J. Raman Spectrosc.* 46 (2014) 76–83. <https://doi.org/10.1002/jrs.4600>.
- [3] K.M. Marzec, J. Dybas, S. Chlopicki, M. Baranska, Resonance Raman in vitro detection and differentiation of the nitrite-induced hemoglobin adducts in functional human red blood cells, *J. Phys. Chem. B* 120 (2016) 12249–12260. <https://doi.org/10.1021/acs.jpcc.6b08359>.
- [4] J. Dybas, M. Grosicki, M. Baranska, K.M. Marzec, Raman imaging of heme metabolism: in situ in macrophages and Kupffer cells, *Analyst* 143 (2018) 3489–3498. <https://doi.org/10.1039/c8an00282g>.
- [5] J. Dybas, M.J. Bokamper, K.M. Marzec, P.J. Mak, Probing the structure-function relationship of hemoglobin in living human red blood cells, *Spectrochim. Acta Part A Mol. Biomol. Spectrosc.* 239 (2020) 118530. <https://doi.org/10.1016/j.saa.2020.118530>.
- [6] J. Dybas, P. Berkowicz, B. Proniewski, K. Dziedzic-Kocurek, J. Stanek, M. Baranska, S. Chlopicki, K.M. Marzec, Spectroscopy-based characterization of Hb-NO adducts in human red blood cells exposed to NO-donor and endothelium-derived NO, *Analyst* 143 (2018) 4335–4346. <https://doi.org/10.1039/c8an00302e>.
- [7] J. Dybas, T. Chiura, K.M. Marzec, P.J. Mak, Probing heme active sites of hemoglobin in functional red blood cells using resonance Raman spectroscopy, *J. Phys. Chem. B* 125 (2021) 3556–3565. <https://doi.org/10.1021/acs.jpcc.1c01199>.
- [8] R. Gautam, J.Y. Oh, R.P. Patel, R.A. Dluhy, Non-invasive analysis of stored red blood cells using diffuse resonance Raman spectroscopy, *Analyst* 143 (2018) 5950–5958. <https://doi.org/10.1039/c8an01135d>.
- [9] M.Z. Vardaki, H.G. Schulze, K. Serrano, M.W. Blades, D.V. Devine, R.F.B. Turner, Non-invasive monitoring of red blood cells during cold storage using handheld Raman spectroscopy, *Transfusion* 61 (2021) 2159–2168. <https://doi.org/10.1111/trf.16417>.
- [10] W. Jia, P. Chen, W. Chen, Y. Li, Raman characterizations of red blood cells with β -thalassemia using laser tweezers Raman spectroscopy, *Med. (United States)* 97 (2018). <https://doi.org/10.1097/MD.00000000000012611>.
- [11] W.R. da Silva, L. Silveira, A.B. Fernandes, Diagnosing sickle cell disease and iron deficiency anemia in human blood by Raman spectroscopy, *Laser Med. Sci.* 35 (2019) 1065–1074. <https://doi.org/10.1007/s10103-019-02887-1>.
- [12] F. Chen, B.R. Flaherty, C.E. Cohen, D.S. Peterson, Y. Zhao, Direct detection of malaria infected red blood cells by surface enhanced Raman spectroscopy, *Nanomed. Nanotechnol. Biol. Med.* 12 (2016) 1445–1451. <https://doi.org/10.1016/j.nano.2016.03.001>.
- [13] E. Guevara, J.C. Torres-Galván, M.G. Ramírez-Eliás, C. Luevano-Contreras, F.J. González, Use of Raman spectroscopy to screen diabetes mellitus with machine learning tools, *Biomed. Opt. Express* 9 (2018) 4998. <https://doi.org/10.1364/boe.9.004998>.
- [14] J. Lin, L. Shao, S. Qiu, X. Huang, M. Liu, Z. Zheng, D. Lin, Y. Xu, Z. Li, Y. Lin, R. Chen, S. Feng, Application of a near-infrared laser tweezers Raman spectroscopy system for label-free analysis and differentiation of diabetic red blood cells, *Biomed. Opt. Express* 9 (2018) 984. <https://doi.org/10.1364/boe.9.000984>.
- [15] A. van Leeuwenhoek, *Arcana Naturae Detecta Ab*, 1695.
- [16] R. Franco, G. Navarro, E. Martínez-Pinilla, Antioxidant defense mechanisms in erythrocytes and in the central nervous system, *Antioxidants* 8 (2019) 46. <https://doi.org/10.3390/antiox8020046>.
- [17] H.Y. Chang, X. Li, H. Li, G.E. Karniadakis, MD/DPD multiscale framework for predicting morphology and stresses of red blood cells in health and disease, *PLoS Comput. Biol.* 12 (2016), e1005173. <https://doi.org/10.1371/journal.pcbi.1005173>.
- [18] R.A. Harvey, *Lippincott's Illustrated Reviews, Lippincott Williams & Wilkins*, 2011.
- [19] A.J. Marengo-Rowe, Structure-function relations of human hemoglobins, *Baylor Univ. Med. Cent. Proc.* 19 (2006) 239–245. <https://doi.org/10.1080/0898280.2006.11928171>.
- [20] J.M. Jeremy M. Berg, J.L. Tymoczko, L. Stryer, *Biochemistry*, W. H. Freeman, 2007.
- [21] K. Malek, *Vibrational Spectroscopy. From Theory to Practise*, PWN, Warszawa, 2016.
- [22] M.L. Kenneth Kaushansky, M.M.L. Josef Prchal, L.B. Oliver Press, M. Caligiuri, *Williams Hematology*, ninth ed., McGraw-Hill Education, New York, 2015.
- [23] J.G. Mohanty, E. Nagababu, J.M. Rifkind, Red blood cell oxidative stress impairs oxygen delivery and induces red blood cell aging, *Front. Physiol.* 5 (FEB) (2014) 1–6. <https://doi.org/10.3389/fphys.2014.00084>.
- [24] K.A. Brown, Erythrocyte metabolism and enzyme defects, *Lab. Med.* 27 (1996) 329–333. <https://doi.org/10.1093/labmed/27.5.329>.
- [25] J.R. Hess, B.G. Solheim, Red blood cell metabolism, preservation, and oxygen delivery, in: *Ross. Princ. Transfus. Med.*, John Wiley & Sons, Chichester, West Sussex, 2016, pp. 97–109. <https://doi.org/10.1002/9781119013020.ch09>.
- [26] A.A. Kumar, M.R. Patton, J.W. Hennek, S.Y.R. Lee, G. D'Alesio-Spina, X. Yang, J. Kanter, S.S. Shevkopyas, C. Brugnara, G.M. Whitesides, Density-based separation in multiphase systems provides a simple method to identify sickle cell disease, *Proc. Natl. Acad. Sci. Unit. States Am.* 111 (2014) 14864–14869. <https://doi.org/10.1073/pnas.1414739111>.
- [27] J.W. Hennek, A.A. Kumar, A.B. Wiltchko, M.R. Patton, S.Y.R. Lee, C. Brugnara, R.P. Adams, G.M. Whitesides, Diagnosis of iron deficiency anemia using density-based fractionation of red blood cells, *Lab. Chip* 16 (2016) 3929–3939. <https://doi.org/10.1039/C6LC00875E>.
- [28] S. Parasuraman, R. Raveendran, R. Kesavan, Blood sample collection in small laboratory animals, *J. Pharmacol. Pharmacother.* 1 (2010) 87–93. <https://doi.org/10.4103/0976-500X.72350>.
- [29] L. Antonini, L. Rossi-Bernardi, E. Chiancone (Editors), *Methods in Enzymology*, ume 76, Academic Press, 1981.
- [30] P.K. Dagur, J.P. McCoy, Collection, Storage, and preparation of human blood cells, *Curr. Protoc. Cytom.* 73 (2015). <https://doi.org/10.1002/0471142956.cy0501s73>.
- [31] J.J. Olearczyk, A.H. Stephenson, A.J. Lonigro, R.S. Sprague, Heterotrimeric G protein G_i is involved in a signal transduction pathway for ATP release from erythrocytes, *Am. J. Physiol. Cell Physiol.* 286 (2004) H940–H945. <https://doi.org/10.1152/ajpheart.00677.2003>.
- [32] R.S. Sprague, M.L. Ellsworth, A.H. Stephenson, M.E. Kleinhenz, A.J. Lonigro, Deformation-induced ATP release from red blood cells requires CFTR activity, *Am. J. Physiol. Heart Circ. Physiol.* 275 (1998) H1726–H1732. <https://doi.org/10.1152/ajpheart.1998.275.5.h1726>.
- [33] J. Dybas, *Molecular Spectroscopy Studies on Chosen Hemoprotein Adducts and Their Changes in Biological Systems*, Jagiellonian University, 2019.
- [34] T. Yoshida, M. Prudent, A. D'Alessandro, Red blood cell storage lesion: causes and potential clinical consequences, *Blood Transfus* 17 (2019) 27–52. <https://doi.org/10.2450/2019.0217-18>.
- [35] P.S. Vassar, J.M. Tiards, D.E. Brooks, B. Itagenberger, G.V.F. Seaman, Physicochemical effects of aldehydes on the human erythrocyte, *J. Cell Biol.* 53 (1972) 809–818. <https://doi.org/10.1083/jcb.53.3.809>.
- [36] E. Gazi, J. Dwyer, N.P. Lockyer, J. Miyan, P. Gardner, C. Hart, M. Brown, N.W. Clarke, Fixation protocols for subcellular imaging by synchrotron-based Fourier transform infrared microspectroscopy, *Biopolymers* 77 (2005) 18–30. <https://doi.org/10.1002/bip.20167>.
- [37] M. Asghari-Khiavi, B.R. Wood, A. Mechler, K.R. Bamberg, D.W. Buckingham, B.M. Cooke, D. McNaughton, Correlation of atomic force microscopy and Raman micro-spectroscopy to study the effects of ex vivo treatment procedures on human red blood cells, *Analyst* 135 (2010) 525. <https://doi.org/10.1039/b919245j>.
- [38] V.V. Moroz, A.M. Chernysh, E.K. Kozlova, P.Y. Borshegovskaya, U.A. Bliznjuk, R.M. Rysaeva, O.Y. Gudkova, Comparison of red blood cell membrane microstructure after different physicochemical influences: atomic force microscope research, *J. Crit. Care* 25 (2010) 539.e1–539.e12. <https://doi.org/10.1016/j.jccr.2010.02.007>.
- [39] F.M.M. Morel, R.F. Baker, H. Wayland, Quantitation of human red blood cell fixation by glutaraldehyde, *J. Cell Biol.* 48 (1971) 91–100. <https://doi.org/10.1083/jcb.48.1.91>.
- [40] I. Migneault, C. Dartiguenave, M.J. Bertrand, K.C. Waldron, Glutaraldehyde: behavior in aqueous solution, reaction with proteins, and application to enzyme crosslinking, *Biotechniques* 37 (2004) 790–802. <https://doi.org/10.2144/04375rv01>.
- [41] T.J. Greenwalt, U.J. Dumaswala, M.M. Domino, The quantification of fetal-maternal hemorrhage by an enzyme-linked antibody test with glutaraldehyde fixation, *Vox Sang.* 63 (1992) 268–271. <https://doi.org/10.1111/j.1423-0410.1992.tb01233.x>.
- [42] A. Abay, G. Simionato, R. Chachanidze, A. Bogdanova, L. Hertz, P. Bianchi, E. van den Akker, M. von Lindern, M. Leonetti, G. Minetti, C. Wagner, L. Kaestner, Glutaraldehyde – a subtle tool in the investigation of healthy and pathologic red blood cells, *Front. Physiol.* 10 (2019) 514. <https://doi.org/10.3389/fphys.2019.00514>.
- [43] C.A. Squier, J.S. Hart, A. Churchland, Changes in red blood cell volume on fixation in glutaraldehyde solutions, *Histochemistry* 48 (1976) 7–16. <https://doi.org/10.1007/BF00489711>.
- [44] M.N. Starodubtseva, N.I. Yegorenkov, I.A. Nikitina, Thermo-mechanical properties of the cell surface assessed by atomic force microscopy, *Micron* 43 (2012) 1232–1238. <https://doi.org/10.1016/j.micron.2012.04.001>.
- [45] K. Bulat, J. Dybas, M. Kaczmarek, A. Rygula, A. Jasztal, E. Szczesny-Malysiak, M. Baranska, B.R. Wood, K.M. Marzec, Multimodal detection and analysis of a new type of advanced Heinz body-like aggregate (AHBA) and cytoskeleton deformation in human RBCs, *Analyst* 145 (2020) 1749–1758. <https://doi.org/10.1039/c9an01707k>.
- [46] M. Asghari-Khiavi, A. Mechler, K.R. Bamberg, D. McNaughton, B.R. Wood, A resonance Raman spectroscopic investigation into the effects of fixation and dehydration on heme environment of hemoglobin, *J. Raman Spectrosc.* 40 (2009) 1668–1674. <https://doi.org/10.1002/jrs.2317>.
- [47] B.R. Wood, S.J. Langford, B.M. Cooke, J. Lim, F.K. Glenister, M. Duriska, J.K. Unthank, D. McNaughton, Resonance Raman spectroscopy reveals new insight into the electronic structure of β -hematin and malaria pigment, *J. Am. Chem. Soc.* 126 (2004) 9233–9239. <https://doi.org/10.1021/ja038691x>.
- [48] S. Li, X. Wei, L. Li, J. Cui, D. Yang, Y. Wang, W. Zhou, S. Xie, A. Hirano, T. Tanaka, H. Kataura, H. Liu, Quantitative analysis of the effect of reabsorption on the Raman spectroscopy of distinct (n,m) carbon nanotubes, *Anal. Methods* 12 (2020) 2376–2384. <https://doi.org/10.1039/D0AY00356E>.
- [49] L.M. Uriarte, L.J. Bonales, J. Dubessy, A. Lobato, V.G. Baonza, M. Cáceres, The self-absorption phenomenon in quantitative Raman spectroscopy and how to correct its effects, *Microchem. J.* 139 (2018) 134–138. <https://doi.org/10.1016/j.microc.2018.02.013>.
- [50] E. Machalska, G. Zajac, A.J. Wierzbka, J. Kapitán, T. Andrzejów, M. Spiegel, D. Gryko, P. Bouř, M. Baranska, Recognition of the true and false resonance

- Raman optical activity, *Angew. Chem. Int. Ed.* 60 (2021) 21205–21210. <https://doi.org/10.1002/anie.202107600>.
- [51] L.T. Kerr, H.J. Byrne, B.M. Hennelly, Optimal choice of sample substrate and laser wavelength for Raman spectroscopic analysis of biological specimen, *Anal. Methods* 7 (2015) 5041–5052. <https://doi.org/10.1039/C5AY00327J>.
 - [52] W.R. Premasiri, J.C. Lee, L.D. Ziegler, Surface-enhanced Raman scattering of whole human blood, blood plasma, and red blood cells: cellular processes and bioanalytical sensing, *J. Phys. Chem. B* 116 (2012) 9376–9386. <https://doi.org/10.1021/jp304932g>.
 - [53] I. Tirado, J. Mateo, J. Soria, A. Oliver, E. Martínez-Sánchez, C. Vallvé, M. Borrell, T. Urrutia, J. Fontcuberta, The ABO blood group genotype and factor VIII levels as independent risk factors for venous thromboembolism, *Thromb. Haemostasis* 93 (2005) 468–474. <https://doi.org/10.1160/TH04-04-0251>.
 - [54] E.-H. Nah, S. Kim, S. Cho, H.-I. Cho, Complete blood count reference intervals and patterns of changes across pediatric, adult, and geriatric ages in Korea, *Ann. Lab. Med.* 38 (2018) 503–511. <https://doi.org/10.3343/alm.2018.38.6.503>.
 - [55] M.M. Wintrobe, Anemia: classification and treatment on the basis of differences in the average volume and hemoglobin content of the red corpuscles, *Arch. Intern. Med.* 54 (1934) 256–280. <https://doi.org/10.1001/archinte.1934.00160140099006>.
 - [56] PDQ Adult Treatment Editorial Board, *Adult Acute Myeloid Leukemia Treatment (PDQ®): Patient Version*, National Cancer Institute (US), 2002.
 - [57] J. Ford, Red blood cell morphology, *Int. J. Lab. Hematol.* 35 (2013) 351–357. <https://doi.org/10.1111/ijlh.12082>.
 - [58] B. Houwen, Blood film preparation and staining procedures, *Clin. Lab. Med.* 22 (2002) 1–14. [https://doi.org/10.1016/S0272-2712\(03\)00064-7](https://doi.org/10.1016/S0272-2712(03)00064-7).
 - [59] J.C. Ford, Approach to disorders of red blood cells, in: *Non-Neoplastic Hematol. Infect.*, John Wiley & Sons, 2012, pp. 45–64. <https://doi.org/10.1002/9781118118158562.ch3>.
 - [60] P. Peterson, S. McNeill, G. Gulati, Cellular morphologic analysis of peripheral blood, *Lab. Hematol. Pract.* (2012) 10–25. <https://doi.org/10.1002/9781444398595.ch2>.
 - [61] S. Karimi, P. Mehrdel, J. Farré-Lladós, J. Casals-Terré, A passive portable microfluidic blood-plasma separator for simultaneous determination of direct and indirect ABO/Rh blood typing, *Lab Chip* 19 (2019) 3249–3260. <https://doi.org/10.1039/c9lc00690g>.
 - [62] M.L. Delforge, [On the usefulness of serology testing in infectious diseases: selected topics], *Rev. Med. Brux.* 32 (2011) 285–288.
 - [63] R. Uvizi, B. Klementa, M. Adamus, J. Neiser, Biochemical changes in the patient's plasma after red blood cell transfusion, *Signa Vitae* 6 (2011) 64–71. <https://doi.org/10.22514/SV62.102011.9>.
 - [64] G. Lippi, G.L. Salvagno, M. Montagnana, G. Brocco, G.C. Guidi, Influence of hemolysis on routine clinical chemistry testing, *Clin. Chem. Lab. Med.* 44 (2006) 311–316. <https://doi.org/10.1515/CCLM.2006.054>.
 - [65] B. Ghezelbash, A. Azarkeivan, A.A. Pourfathollah, M. Deyhim, E. Hajati, A. Goodarzi, Comparative evaluation of biochemical and hematological parameters of pre-storage leukoreduction during RBC storage, *Int. J. Hematol. Stem Cell Res.* 12 (2018) 35–42.
 - [66] A.G. Kriebardis, M.H. Antonelou, K.E. Stamoulis, E. Economou-Petersen, L.H. Margaritis, I.S. Papassideri, Storage-dependent remodeling of the red blood cell membrane is associated with increased immunoglobulin G binding, lipid raft rearrangement, and caspase activation, *Transfusion* 47 (2007) 1212–1220. <https://doi.org/10.1111/j.1537-2995.2007.01254.x>.
 - [67] V.L. Tzoumakas, H.T. Georgatzakou, A.G. Kriebardis, A.L. Voulgaridou, K.E. Stamoulis, L.E. Foudoulaki-Papazis, M.H. Antonelou, I.S. Papassideri, Donor variation effect on red blood cell storage lesion: a multivariable, yet consistent, story, *Transfusion* 56 (2016) 1274–1286. <https://doi.org/10.1111/trf.13582>.
 - [68] N.G. De Isla, B.D. Riquelme, R.J. Rasia, J.R. Valverde, J.F. Stoltz, Quantification of glycophorin A and glycophorin B on normal human RBCs by flow cytometry, *Transfusion* 43 (2003) 1145–1152. <https://doi.org/10.1046/j.1537-2995.2003.00471.x>.
 - [69] M. Kono, T. Kondo, Y. Takagi, A. Wada, K. Fujimoto, Morphological definition of CD71 positive reticulocytes by various staining techniques and electron microscopy compared to reticulocytes detected by an automated hematology analyzer, *Clin. Chim. Acta* 404 (2009) 105–110. <https://doi.org/10.1016/j.cca.2009.03.017>.
 - [70] M. Wiewiora, J. Piecuch, L. Sedek, B. Mazur, K. Sosada, The effects of obesity on CD47 expression in erythrocytes, *Cytometry B Clin. Cytometry* 92 (2017) 485–491. <https://doi.org/10.1002/cyto.b.21232>.
 - [71] H. Jiang, R. Fu, H. Wang, L. Li, H. Liu, Z. Shao, CD47 is expressed abnormally on hematopoietic cells in myelodysplastic syndrome, *Leuk. Res.* 37 (2013) 907–910. <https://doi.org/10.1016/j.leukres.2013.04.008>.
 - [72] D.M. Eldewi, A.M. Alhabibi, H.M.E. El Sayed, S.A.K. Mahmoud, S.M. El Sadek, R.M. Gouda, M.A.E.M. Hassan, A.H. Ibrahim, N.F.A. El Haliem, Expression levels of complement regulatory proteins (CD35, CD55 and CD59) on peripheral blood cells of patients with chronic kidney disease, *Int. J. Gen. Med.* 12 (2019) 343–351. <https://doi.org/10.2147/IJGM.S216989>.
 - [73] R. Kar, P. Mishra, H.P. Pati, Evaluation of eosin-5-maleimide flow cytometric test in diagnosis of hereditary spherocytosis, *Int. J. Lab. Hematol.* 32 (2010) 8–16. <https://doi.org/10.1111/j.1751-553X.2008.01098.x>.
 - [74] L. Da Costa, J. Galimand, O. Fenneteau, N. Mohandas, Hereditary spherocytosis, elliptocytosis, and other red cell membrane disorders, *Blood Rev.* 27 (2013) 167–178. <https://doi.org/10.1016/j.blre.2013.04.003>.
 - [75] L. Da Costa, L. Suner, J. Galimand, A. Bonnel, T. Pascreau, N. Couque, O. Fenneteau, N. Mohandas, Diagnostic tool for red blood cell membrane disorders: assessment of a new generation ektacytometer, *Blood Cells, Mol. Dis.* 56 (2016) 9–22. <https://doi.org/10.1016/j.bcmd.2015.09.001>.
 - [76] N.L. Parrow, P.C. Violet, H. Tu, J. Nichols, C.A. Pittman, C. Fitzhugh, R.E. Fleming, N. Mohandas, J.F. Tisdale, M. Levine, Measuring deformability and red cell heterogeneity in blood by ektacytometry, *JoVE* 2018 (2018). <https://doi.org/10.3791/56910>.
 - [77] L. Gattinoni, A. Pesenti, M. Matthay, Understanding blood gas analysis, *Intensive Care Med.* 44 (2018) 91–93. <https://doi.org/10.1007/s00134-017-4824-y>.
 - [78] G. Paglia, A. D'Alessandro, O. Rolfsson, O.E. Sigurjonsson, A. Bordbar, S. Palsson, T. Nemkov, K.C. Hansen, S. Gudmundsson, B.O. Palsson, Biomarkers defining the metabolic age of red blood cells during cold storage, *Blood* 128 (2016) e43–e50. <https://doi.org/10.1182/blood-2016-06-721688>.
 - [79] A. D'Alessandro, L. Zolla, Biochemistry of red cell aging in vivo and storage lesions, *Haematologica* 7 (2013) 389–396. https://www.researchgate.net/publication/259901076_Biochemistry_of_red_cell_aging_in_vivo_and_storage_lesions. (Accessed 1 May 2019).
 - [80] W.A. Bonadio, D. Smith, J. Carmody, Correlating CBC profile and infectious outcome, *Clin. Pediatr. (Phila)* 31 (1992) 578–582. <https://doi.org/10.1177/000992289203101001>.
 - [81] D. Agrawal, R. Sarode, Complete blood count or complete blood count with differential: what's the difference? *Am. J. Med.* 130 (2017) 915–916. <https://doi.org/10.1016/j.amjmed.2017.03.049>.
 - [82] B.J. Bain, Diagnosis from the blood smear, *N. Engl. J. Med.* 353 (2005) 498–507. <https://doi.org/10.1056/NEJMr043442>.
 - [83] M. Zandecki, F. Genevieve, J. Gerard, A. Godon, Spurious counts and spurious results on haematology analysers: a review. Part II: white blood cells, red blood cells, haemoglobin, red cell indices and reticulocytes, *Int. J. Lab. Hematol.* 29 (2007) 21–41. <https://doi.org/10.1111/j.1365-2257.2006.00871.x>.
 - [84] B.I. Dalal, M.L. Brigden, Artifacts that may be present on a blood film, *Clin. Lab. Med.* 22 (2002) 81–100. [https://doi.org/10.1016/S0272-2712\(03\)00068-4](https://doi.org/10.1016/S0272-2712(03)00068-4).
 - [85] Y.A. Rodina, V.E. Matveev, D.N. Balashov, M.E. Dubrovina, A.Y. Shcherbina, Chediak-Higashi syndrome, *Pediatr. Hematol. Immunopathol.* 15 (2016) 27–33. <https://doi.org/10.20953/1726-1708-2016-1-27-33>.
 - [86] R. Colella, S.C. Hollensead, Understanding and recognizing the Pelger-Huët anomaly, *Am. J. Clin. Pathol.* 137 (2012) 358–366. <https://doi.org/10.1309/AJCP3G8MDUXYSCID>.
 - [87] A.T. Nurden, P. Nurden, The gray platelet syndrome: clinical spectrum of the disease, *Blood Rev.* 21 (2007) 21–36. <https://doi.org/10.1016/j.blre.2005.12.003>.
 - [88] R. Favier, K. Jondeau, P. Boutard, P. Grossfeld, P. Reinert, C. Jones, F. Bertoni, E.M. Cramer, Paris-Trousseau syndrome: clinical, hematological, molecular data of ten new cases, *Thromb. Haemostasis* 90 (2003) 893–897. <https://doi.org/10.1160/th03-02-0120>.
 - [89] V. Goede, M. Hallek, Chronic lymphocytic leukemia (CLL), in: *Manag. Hematol. Cancer Older People*, Springer-Verlag London Ltd, 2015, pp. 113–128. https://doi.org/10.1007/978-1-4471-2837-3_7.
 - [90] M.T. Gundersen, T. Lund, H.E.H. Moeller, N. Abildgaard, Plasma cell leukemia: definition, presentation, and treatment, *Curr. Oncol. Rep.* 21 (2019). <https://doi.org/10.1007/s11912-019-0754-x>.
 - [91] X. Troussard, E. Cornet, Hairy cell leukemia 2018: update on diagnosis, risk-stratification, and treatment, *Am. J. Hematol.* 92 (2017) 1382–1390. <https://doi.org/10.1002/ajh.24936>.
 - [92] A. Collignon, A. Wanquet, E. Maitre, E. Cornet, X. Troussard, T. Aurran-Schleinitz, Prolymphocytic leukemia: new insights in diagnosis and in treatment, *Curr. Oncol. Rep.* 19 (2017) 1–11. <https://doi.org/10.1007/s11912-017-0581-x>.
 - [93] M.J. Homer, I. Aguilar-Delfin, S.R. Telford, P.J. Krause, D.H. Persing, Babesiosis, *Clin. Microbiol. Rev.* 13 (2000) 451–469. <https://doi.org/10.1128/CMR.13.3.451-469.2000>.
 - [94] P. Büscher, G. Cecchi, V. Jamonneau, G. Priotto, Human african trypanosomiasis, *Lancet* 390 (2017) 2397–2409. [https://doi.org/10.1016/S0140-6736\(17\)31510-6](https://doi.org/10.1016/S0140-6736(17)31510-6).
 - [95] N. Mendoza, A. Li, A. Gill, S. Tying, Filariasis: diagnosis and treatment, *Dermatol. Ther.* 22 (2009) 475–490. <https://doi.org/10.1111/j.1529-8019.2009.01271.x>.
 - [96] C.G. Atkins, K. Buckley, M.W. Blades, R.F.B. Turner, Raman spectroscopy of blood and blood components, *Appl. Spectrosc.* 71 (2017) 767–793. <https://doi.org/10.1177/0003702816686593>.
 - [97] D. Perez-Guaita, K.M. Marzec, A. Hudson, C. Evans, T. Chernenko, C. Matthäus, M. Miljkovic, M. Diem, P. Heraud, J.S. Richards, D. Andrew, D.A. Anderson, C. Doerig, J. Garcia-Bustos, D. McNaughton, B.R. Wood, Parasites under the spotlight: applications of vibrational spectroscopy to malaria research, *Chem. Rev.* 118 (2018) 5330–5358. <https://doi.org/10.1021/acs.chemrev.7b00661>.
 - [98] S. Dalia, L. Zhang, Homozygous hemoglobin C disease, *Blood* 122 (2013) 1694. <https://doi.org/10.1182/blood-2013-04-498188>.

- [99] L.H. Pecker, B.A. Schaefer, L. Luchtman-Jones, Knowledge insufficient: the management of haemoglobin SC disease, *Br. J. Haematol.* 176 (2017) 515–526. <https://doi.org/10.1111/bjh.14444>.
- [100] A.L. Wani, A. Ara, J.A. Usmani, Lead toxicity: a review, *Interdiscipl. Toxicol.* 8 (2015) 55–64. <https://doi.org/10.1515/intox-2015-0009>.
- [101] M. Kuivenhoven, K. Mason, *Arsenic (Arsine) Toxicity*, StatPearls Publishing, 2019.
- [102] T.D. Johnson Wimbley, D.Y. Graham, Diagnosis and management of iron deficiency anemia in the 21st century, *Therap. Adv. Gastroenterol.* 4 (2011) 177–184. <https://doi.org/10.1177/1756283X11398736>.
- [103] L.C. Soares Medeiros, W. De Souza, C. Jiao, H. Barrabin, K. Miranda, Visualizing the 3D architecture of multiple erythrocytes infected with *Plasmodium* at nanoscale by focused ion beam-scanning electron microscopy, *PLoS One* 7 (2012), e33445. <https://doi.org/10.1371/journal.pone.0033445>.
- [104] A. Polliack, The contribution of scanning electron microscopy in haematology: its role in defining leucocyte and erythrocyte disorders, *J. Microsc.* 123 (1981) 177–187. <https://doi.org/10.1111/j.1365-2818.1981.tb01293.x>.
- [105] S. Huq, M.A. Pietroni, H. Rahman, M.T. Alam, Hereditary Spherocytosis, *J. Health Popul. Nutr.* 28 (2010). <https://doi.org/10.3329/jhpn.v28i1.4529>.
- [106] A.S. Adewoyin, B. Nwogoh, Peripheral blood film - a review, *Ann. Ib. Postgrad. Med.* 12 (2014) 71–79. <http://www.ncbi.nlm.nih.gov/pubmed/25960697>.
- [107] P. Bhattacharya, P.K. Chandra, S. Datta, A. Banerjee, S. Chakraborty, K. Rajendran, S.K. Basu, S.K. Bhattacharya, R. Chakravarty, Significant increase in HBV, HCV, HIV and syphilis infections among blood donors in West Bengal, Eastern India 2004–2005: exploratory screening reveals high frequency of occult HBV infection, *World J. Gastroenterol.* 13 (2007) 3730–3733. <https://doi.org/10.3748/wjg.v13.i27.3730>.
- [108] National Healthcare Safety Network Biovigilance Component Hemovigilance Module Surveillance Protocol, 2018.
- [109] C.A. Tormey, J.E. Hendrickson, Transfusion-related red blood cell alloantibodies: induction and consequences, *Blood* 133 (2019) 1821–1830. <https://doi.org/10.1182/blood-2018-08-833962>.
- [110] S. Maral, S. Bakanay, S. Akinci, A. Yikilmaz, P. Comert, I. Dilek, The least incompatible crossmatch red blood cell transfusion by biological compatibility test, *Glob. J. Transfus. Med.* 4 (2019) 154. https://doi.org/10.4103/gjtm.gjtm_37_19.
- [111] A. Orbach, O. Zelig, S. Yedgar, G. Barshtein, Biophysical and biochemical markers of red blood cell fragility, *Transfus. Med. Hemotherapy* 44 (2017) 183–187. <https://doi.org/10.1159/000452106>.
- [112] C.T. Quinn, E.P. Smith, S. Arbabi, P.K. Khera, C.J. Lindsell, O. Niss, C.H. Joiner, R.S. Franco, R.M. Cohen, Biochemical surrogate markers of hemolysis do not correlate with directly measured erythrocyte survival in sickle cell anemia, *Am. J. Hematol.* 91 (2016) 1195–1201. <https://doi.org/10.1002/ajh.24562>.
- [113] S. Shastri, A. Shivhare, M. Murugesan, P.B. Baliga, Red cell storage lesion and the effect of buffy-coat reduction on the biochemical parameters, *Transfus. Apher. Sci.* 58 (2019) 179–182. <https://doi.org/10.1016/j.transci.2019.01.003>.
- [114] R.E. Brown, K.L. Jarvis, K.J. Hyland, Protein measurement using bicinchoninic acid: elimination of interfering substances, *Anal. Biochem.* 180 (1989) 136–139. [https://doi.org/10.1016/0003-2697\(89\)90101-2](https://doi.org/10.1016/0003-2697(89)90101-2).
- [115] J. Dybas, K. Bulat, A. Blat, T. Mohaissen, A. Wajda, M. Mardyla, M. Kaczmarek, M. Franczyk-Zarow, K. Malek, S. Chlopicki, K.M. Marzec, Age-related and atherosclerosis-related erythropathy in ApoE/LDLR-/- mice, *Biochim. Biophys. Acta (BBA) - Mol. Basis Dis.* 1866 (2020) 165972. <https://doi.org/10.1016/j.bbadis.2020.165972>.
- [116] K.V. Wood, Y.A. Lam, W.D. McElroy, Introduction to beetle luciferases and their applications, *J. Biolumin. Chemilumin.* 4 (1989) 289–301. <https://doi.org/10.1002/bio.1170040141>.
- [117] R.S. Sprague, A.H. Stephenson, M.L. Ellsworth, Red not dead: signaling in and from erythrocytes, *Trends Endocrinol. Metabol.* 18 (2007) 350–355. <https://doi.org/10.1016/j.tem.2007.08.008>.
- [118] D. Communi, E. Raspe, S. Pirotton, J.-M. Boeynaems, Coexpression of P2Y and P2U receptors on aortic endothelial cells, *Circ. Res.* 76 (1995) 191–198. <https://doi.org/10.1161/01.RES.76.2.191>.
- [119] W. Subasinghe, D.M. Spence, Simultaneous determination of cell aging and ATP release from erythrocytes and its implications in type 2 diabetes, *Anal. Chim. Acta* 618 (2008) 227–233. <https://doi.org/10.1016/j.aca.2008.04.061>.
- [120] R.S. Sprague, M.L. Ellsworth, A.H. Stephenson, A.J. Lonigro, ATP: the red blood cell link to NO and local control of the pulmonary circulation, *Am. J. Physiol. Cell Physiol.* 271 (1996) H2717–H2722. <https://doi.org/10.1152/ajpheart.1996.271.6.H2717>.
- [121] R.P. Heibel, Reconstructing sickle cell disease: a data-based analysis of the “hyperhemolysis paradigm” for pulmonary hypertension from the perspective of evidence-based medicine, *Am. J. Hematol.* 86 (2011) 123–154. <https://doi.org/10.1002/ajh.21952>.
- [122] V. Brancaloni, E. Di Piero, I. Motta, M.D. Cappellini, Laboratory diagnosis of thalassemia, *Int. J. Lab. Hematol.* 38 (2016) 32–40. <https://doi.org/10.1111/ijlh.12527>.
- [123] P. Kishore, K.K. Dayanand, V. Chandrashekar, B. Mukhi, S.K. Ghosh, S. Kumari, D.C. Gowda, R.N. Achur, C-reactive Protein Levels as a Potential Diagnostic Marker during Malarial Infections, n.d. www.ejpmr.com.
- [124] R. Rapetti-Maass, V. Picard, C. Guitton, K. Ghazal, V. Proulle, C. Badens, O. Soriani, L. Garçon, H. Guizouarn, Red blood cell Gardos channel (KCNK4): the essential determinant of erythrocyte dehydration in hereditary xerocytosis, *Haematologica* 102 (2017) e415–e418. <https://doi.org/10.3324/haematol.2017.171389>.
- [125] M.H. Dahlke, S.R. Larsen, J.E.J. Rasko, H.J. Schlitt, The biology of CD45 and its use as a therapeutic target, *Leuk. Lymphoma* 45 (2004) 229–236. <https://doi.org/10.1080/1042819031000151932>.
- [126] R. Keawvichit, L. Khawwisetsut, P. Chaichompoo, K. Polsrila, S. Sukklad, K. Sukapirom, A. Khuapinant, S. Fuchareon, K. Pattanapanyasat, Platelet activation and platelet-leukocyte interaction in β -thalassemia/hemoglobin E patients with marked nucleated erythrocytosis, *Ann. Hematol.* 91 (2012) 1685–1694. <https://doi.org/10.1007/s00277-012-1522-2>.
- [127] W. Gorczyca, Z.Y. Sun, W. Cronin, X. Li, S. Mau, S. Tugulea, Immunophenotypic Pattern of Myeloid Populations by Flow Cytometry Analysis, Academic Press, 2011. <https://doi.org/10.1016/B978-0-12-385493-3.00010-3>.
- [128] F. Dei Zotti, R. Verdoy, D. Brusa, I.I. Lobysheva, J.L. Balligand, Redox regulation of nitrosyl-hemoglobin in human erythrocytes, *Redox Biol.* 34 (2020) 101399. <https://doi.org/10.1016/j.redox.2019.101399>.
- [129] N. Okumura, K. Tsuji, T. Nakahata, Changes in Cell Surface Antigen Expressions during Proliferation and Differentiation of Human Erythroid Progenitors, n.d.
- [130] A. Gaikwad, R. Nussenzweig, E. Liu, S. Gottschalk, K.T. Chang, J.T. Prchal, In vitro expansion of erythroid progenitors from polycythemia vera patients leads to decrease in JAK2V617F allele, *Exp. Hematol.* 35 (2007) 587–595. <https://doi.org/10.1016/j.exphem.2006.12.007>.
- [131] S.T. Callender, E.O. Powell, L.J. Witts, The life-span of the red cell in man, *J. Pathol. Bacteriol.* 57 (1945) 129–139. <https://doi.org/10.1002/path.1700570116>.
- [132] B. Malleret, F. Xu, N. Mohandas, R. Suwanarusk, C. Chu, J.A. Leite, K. Low, C. Turner, K. Sriprawat, R. Zhang, O. Bertrand, Y. Colin, F.T.M. Costa, C.N. Ong, M.L. Ng, C.T. Lim, F. Nosten, L. Rénia, B. Russell, Significant biochemical, biophysical and metabolic diversity in circulating human cord blood reticulocytes, *PLoS One* 8 (2013). <https://doi.org/10.1371/journal.pone.0076062>.
- [133] X. An, L. Chen, Flow cytometry (FCM) analysis and fluorescence-activated cell sorting (FACS) of erythroid cells, in: *Methods Mol. Biol.*, Humana Press, 2018, pp. 153–174. https://doi.org/10.1007/978-1-4939-7428-3_9.
- [134] A. Stewart, S. Urbaniak, M. Turner, H. Bessos, The application of a new quantitative assay for the monitoring of integrin-associated protein CD47 on red blood cells during storage and comparison with the expression of CD47 and phosphatidylserine with flow cytometry, *Transfusion* 45 (2005) 1496–1503. <https://doi.org/10.1111/j.1537-2995.2005.00564.x>.
- [135] P.A. Oldenborg, A. Zheleznyak, Y.F. Fang, C.F. Lagenaur, H.D. Gresham, F.P. Lindberg, Role of CD47 as a marker of self on red blood cells, *Science* (80-) 288 (2000) 2051–2054. <https://doi.org/10.1126/science.288.5473.2051>.
- [136] A. Giovannetti, L. Gambardella, D. Pietraforte, E. Rosato, A.M. Giammaroli, F. Salsano, W. Malorni, E. Straface, Red blood cell alterations in systemic sclerosis: a pilot study, *Cell. Physiol. Biochem.* 30 (2012) 418–427. <https://doi.org/10.1159/000339035>.
- [137] J. Kamhieh-Milz, B. Bartl, V. Sterzer, S. Kamhieh-Milz, A. Salama, Storage of RBCs results in an increased susceptibility for complement-mediated degradation, *Transfus. Med.* 24 (2014) 392–399. <https://doi.org/10.1111/tme.12166>.
- [138] K. Segawa, S. Nagata, An apoptotic “eat me” signal: phosphatidylserine exposure, *Trends Cell Biol.* 25 (2015) 639–650. <https://doi.org/10.1016/j.tcb.2015.08.003>.
- [139] M.C. Wesseling, L. Wagner-Britz, H. Huppert, B. Hanf, L. Hertz, D.B. Nguyen, I. Bernhardt, Phosphatidylserine exposure in human red blood cells depending on cell age, *Cell. Physiol. Biochem.* 38 (2016) 1376–1390. <https://doi.org/10.1159/000443081>.
- [140] A. Al Mamun Bhuyan, R. Bissinger, H. Cao, F. Lang, Triggering of suicidal erythrocyte death by exemestane, *Cell. Physiol. Biochem.* 42 (2017) 1–12. <https://doi.org/10.1159/000477224>.
- [141] E. Noulisri, S. Ardsiri, S. Lerdwana, K. Pattanapanyasat, Comparison of phosphatidylserine-exposing red blood cells, fragmented red blood cells and red blood cell-derived microparticles in β -thalassemia/HBE patients, *Lab. Med.* 50 (2019) 47–53. <https://doi.org/10.1093/labmed/lmy039>.
- [142] M. Zahedpanah, A. Azarkeivan, M. Aghaiepour, M. Nikogoftar, M. Ahmadi-nagad, B. Hajibeigi, M.R. Tabatabaiee, M. Maghsudlu, Erythrocytic phosphatidylserine exposure and hemostatic alterations in β -thalassemia intermediate patients, *Hematology* 19 (2014) 472–476. <https://doi.org/10.1179/1607845413Y.0000000148>.
- [143] N. Amabile, I. Bagdadi, S. Armero, S. Elhadad, F. Sebag, Q. Landolf, L. Saby, A. Mechulan, C.M. Boulanger, C. Caussin, Impact of left atrial appendage closure on circulating microvesicles levels: the MICROPLUG study, *Int. J. Cardiol.* (2019). <https://doi.org/10.1016/j.ijcard.2019.10.026>.
- [144] E. Gkaliagkousi, B. Nikolaidou, E. Gavrilaki, A. Lazaridis, E. Yiannaki, P. Anyfanti, I. Zografou, D. Markala, S. Douma, Increased erythrocyte- and platelet-derived microvesicles in newly diagnosed type 2 diabetes mellitus, *Diabetes Vasc. Dis. Res.* 16 (2019) 458–465. <https://doi.org/10.1177/1479164119844691>.
- [145] M.H. Nielsen, H. Irvine, S. Vedel, B. Raungaard, H. Beck-Nielsen, A. Handberg, The impact of lipoprotein-associated oxidative stress on cell-specific microvesicle release in patients with familial hypercholesterolemia, *Oxid. Med. Cell. Longev.* 2016 (2016) 2492858. <https://doi.org/10.1155/2016/2492858>.
- [146] I. Arvidsson, A. Ståhl, M. Manea Hedström, A.-C. Kristofferson, C. Rylander, J.S. Westman, J.R. Storry, M.L. Olsson, D. Karpman, Shiga toxin-induced complement-mediated hemolysis and release of complement-coated red

- blood cell—derived microvesicles in hemolytic uremic syndrome, *J. Immunol.* 194 (2015) 2309–2318. <https://doi.org/10.4049/jimmunol.1402470>.
- [147] A. Hashemi Tayer, N. Amirizadeh, M. Ahmadijeh, M. Nikougoftar, M.R. Deyhim, S. Zolfaghari, Procoagulant activity of red blood cell-derived microvesicles during red cell storage, *Transfus. Med. Hemotherapy* 46 (2019) 224–230. <https://doi.org/10.1159/000494367>.
- [148] G. Grisendi, E. Finetti, D. Mangano, N. Cordova, G. Montagnani, C. Spano, M. Prapa, V. Guarneri, S. Otsuru, E.M. Horwitz, G. Mari, M. Dominici, Detection of microparticles from human red blood cells by multiparametric flow cytometry, *Blood Transfus* 13 (2015) 274–280. <https://doi.org/10.2450/2014.0136-14>.
- [149] R. Almiraz, J.D.R. Tchir, J.L. Holovati, J.P. Acker, Storage of red blood cells affects membrane composition, microvesiculation, and in vitro quality, *Transfusion* 53 (2013) 2258–2267. <https://doi.org/10.1111/trf.12080>.
- [150] L. Wisgrill, C. Lamm, J. Hartmann, F. Preisling, K. Dragosits, A. Bee, L. Hell, J. Thaler, C. Ay, I. Pabinger, A. Berger, A. Spittler, Peripheral blood microvesicles secretion is influenced by storage time, temperature, and anticoagulants, *Cytometry* 89 (2016) 663–672. <https://doi.org/10.1002/cyto.a.22892>.
- [151] J. Kim, H. Lee, S. Shin, Advances in the measurement of red blood cell deformability: a brief review, *J. Cell. Biotechnol.* 1 (2015) 63–79. <https://doi.org/10.3233/JCB-15007>.
- [152] M.R. Hardeman, J.G. Dobbe, C. Ince, The laser-assisted optical rotational cell analyzer (LORCA) as red blood cell aggregometer, *Clin. Hemorheol. Microcirc.* 25 (2001) 1–11. <http://www.ncbi.nlm.nih.gov/pubmed/11790865>.
- [153] M.V. Kulkarni, R.R. Puniyani, Study of hemorheological parameters in maturity onset diabetic cases, *Clin. Hemorheol. Microcirc.* 14 (1994) 271–278. <https://doi.org/10.3233/CH-1994-14214>.
- [154] A.M. Banas, K. Banas, T.T.T. Chu, R. Naidu, P.E. Hutchinson, R. Agrawal, M.K.F. Lo, M. Kansiz, A. Roy, R. Chandramohanadas, M.B.H. Breese, Comparing infrared spectroscopic methods for the characterization of Plasmodium falciparum-infected human erythrocytes, *Commun. Chem.* 4 (2021) 129. <https://doi.org/10.1038/s42004-021-00567-2>.
- [155] R.R. Puniyani, R. Ajmani, P.A. Kale, Risk factors evaluation in some cardiovascular diseases, *J. Biomed. Eng.* 13 (1991) 441–443. [https://doi.org/10.1016/0141-5425\(91\)90029-7](https://doi.org/10.1016/0141-5425(91)90029-7).
- [156] A. Vayá, M. Martínez, J. García, J. Aznar, Hemorheological alterations in mild essential hypertension, *Thromb. Res.* 66 (1992) 223–229. [https://doi.org/10.1016/0049-3848\(92\)90192-D](https://doi.org/10.1016/0049-3848(92)90192-D).
- [157] H. Lee, W. Na, S.B. Lee, C.W. Ahn, J.S. Moon, K.C. Won, S. Shin, Potential diagnostic hemorheological indexes for chronic kidney disease in patients with type 2 diabetes, *Front. Physiol.* 10 (2019). <https://doi.org/10.3389/fphys.2019.01062>.
- [158] T. Mohaissen, B. Proniewski, M. Targosz-Korecka, A. Bar, A. Kij, K. Bulat, A. Wajda, A. Blat, K. Matyjaszczyk-Gwarda, M. Grosicki, A. Tworzydło, M. Sternak, R. Rodrigues-Diez, K. Wojnar-Lason, A. Kubisiak, A. Briones, K.M. Marzec, S. Chlopicki, Temporal relationship between systemic endothelial dysfunction and alterations in erythrocyte function in a murine model of chronic heart failure, *Cardiovasc. Res.* cvab306 (2021). <https://doi.org/10.1093/cvr/cvab306>.
- [159] M. Garnier, J.R. Attali, P. Valensi, E. Delatour-Haniss, F. Gaudy, D. Koutsouris, Erythrocyte deformability in diabetes and erythrocyte membrane lipid composition, *Metabolism* 39 (1990) 794–798. [https://doi.org/10.1016/0026-0495\(90\)90121-R](https://doi.org/10.1016/0026-0495(90)90121-R).
- [160] J.R. Attali, P. Valensi, Diabetes and hemorheology, *Diabetes Metab* 16 (1990) 1–6. <http://www.ncbi.nlm.nih.gov/pubmed/2185052>.
- [161] Z. Huang, L. Hearne, C.E. Irby, S.B. King, S.K. Ballas, D.B. Kim-Shapiro, Kinetics of increased deformability of deoxygenated sickle cells upon oxygenation, *Biophys. J.* 85 (2003) 2374–2383. [https://doi.org/10.1016/S0006-3495\(03\)74661-X](https://doi.org/10.1016/S0006-3495(03)74661-X).
- [162] S. Usami, S. Chien, J.F. Bertles, Deformability of sickle cells as studied by microsieving, *J. Lab. Clin. Med.* 86 (1975) 274–279. <http://www.ncbi.nlm.nih.gov/pubmed/1151150>.
- [163] J.G.G. Dobbe, M.R. Hardeman, G.J. Streekstra, C.A. Grimbergen, Validation and application of an automated rheoscope for measuring red blood cell deformability distributions in different species, *Biorheology* 41 (2004) 65–77. <http://www.ncbi.nlm.nih.gov/pubmed/15090677>.
- [164] J.G.G. Dobbe, M.R. Hardeman, G.J. Streekstra, J. Strackee, C. Ince, C.A. Grimbergen, Analyzing red blood cell-deformability distributions, blood cells, *Mol. Dis.* 28 (2002) 373–384. <https://doi.org/10.1006/bcmd.2002.0528>.
- [165] O.K. Başkurt, F. Mat, Importance of measurement temperature in detecting the alterations of red blood cell aggregation and deformability studied by ektacytometry: a study on experimental sepsis in rats, *Clin. Hemorheol. Microcirc.* 23 (2000) 43–49. <http://www.ncbi.nlm.nih.gov/pubmed/11214712>.
- [166] J.M. Sosa, N.D. Nielsen, S.M. Vignes, T.G. Chen, S.S. Shevkopyas, The relationship between red blood cell deformability metrics and perfusion of an artificial microvascular network, *Clin. Hemorheol. Microcirc.* 57 (2014) 275–289. <https://doi.org/10.3233/CH-131719>.
- [167] M.J. Simmonds, N. Atac, O.K. Başkurt, H.J. Meiselman, O. Yalcin, Erythrocyte deformability responses to intermittent and continuous subhemolytic shear stress, *Biorheology* 51 (2014) 171–185. <https://doi.org/10.3233/BIR-140665>.
- [168] O.K. Başkurt, M.R. Hardeman, M. Uyuklu, P. Ulker, M. Cengiz, N. Nemeth, S. Shin, T. Alexy, H.J. Meiselman, Comparison of three commercially available ektacytometers with different shearing geometries, *Biorheology* 46 (2009) 251–264. <https://doi.org/10.3233/BIR-2009-0536>.
- [169] S. Shin, Y. Ku, M.-S. Park, J.-S. Suh, Measurement of red cell deformability and whole blood viscosity using laser-diffraction slit rheometer, *Korea Aust. Rheol. J.* 16 (2004) 85–90.
- [170] M.R. Dayer, A.A. Moosavi-Movahedi, M.S. Dayer, Band assignment in hemoglobin porphyrin ring spectrum: using four-orbital model of Gouterman, *Protein Pept. Lett.* 17 (2010) 473–479. <https://doi.org/10.2174/092986610790963645>.
- [171] K.M. Marzec, D. Perez-Guaita, M. De Veij, D. McNaughton, M. Baranska, M.W.A. Dixon, L. Tilley, B.R. Wood, Red blood cells polarize green laser light revealing hemoglobin's enhanced non-fundamental Raman modes, *Chem-PhysChem* 15 (2014) 3963–3968. <https://doi.org/10.1002/cphc.201402598>.
- [172] F. Paulat, Quantum Chemical Investigation of Ferric Heme Model Complexes and Their Reaction with NO Dissertation Florian Paulat, 2007.
- [173] L.R. Milgrom, The Colours of Life, Oxford University Press, Oxford, 1997.
- [174] P. Sood, G. Paul, S. Puri, Interpretation of arterial blood gas, *Indian J. Crit. Care Med.* 14 (2010) 57–64. <https://doi.org/10.4103/0972-5229.68215>.
- [175] N.B. Hampson, C.A. Piantadosi, S.R. Thom, L.K. Weaver, Practice recommendations in the diagnosis, management, and prevention of carbon monoxide poisoning, *Am. J. Respir. Crit. Care Med.* 186 (2012) 1095–1101. <https://doi.org/10.1164/rccm.201207-1284CI>.
- [176] A. Zimna, M. Kaczmarek, E. Szczesny-malysiak, A. Wajda, K. Bulat, F.C. Alciçek, M. Zygmunt, T. Sacha, K.M. Marzec, An insight into the stages of ion leakage during red blood cell storage, *Int. J. Mol. Sci.* 22 (2021).
- [177] M. Baranska, Optical Spectroscopy and Computational Methods in Biology and Medicine, Springer Netherlands, Dordrecht, 2014. <https://doi.org/10.1007/978-94-007-7832-0>.
- [178] C.V. Raman, A new radiation, *Indian J. Phys.* 2 (1928) 387–398.
- [179] R.S. Czernuszewicz, M.B. Zaczek, Resonance Raman spectroscopy, in: *Encycl. Inorg. Bioinorg. Chem.*, John Wiley & Sons, Chichester, UK, 2011. <https://doi.org/10.1002/9781119951438.eibc0303>.
- [180] H.J. Butler, L. Ashton, B. Bird, G. Cinque, K. Curtis, J. Dorney, K. Esmonde-White, N.J. Fullwood, B. Gardner, P.L. Martin-Hirsch, M.J. Walsh, M.R. McAnish, N. Stone, F.L. Martin, Using Raman spectroscopy to characterize biological materials, *Nat. Protoc.* 11 (2016) 664–687. <https://doi.org/10.1038/nprot.2016.036>.
- [181] K. Kong, C. Kendall, N. Stone, I. Notingher, Raman spectroscopy for medical diagnostics - from in-vitro biofluid assays to in-vivo cancer detection, *Adv. Drug Deliv. Rev.* 89 (2015) 121–134. <https://doi.org/10.1016/j.addr.2015.03.009>.
- [182] J. Dybas, K.M. Marzec, M.Z. Pacia, K. Kochan, K. Czamara, K. Chrabaszcz, E. Staniszevska-Slezak, K. Malek, M. Baranska, A. Kaczor, Raman spectroscopy as a sensitive probe of soft tissue composition – imaging of cross-sections of various organs vs. single spectra of tissue homogenates, *TRAC Trends Anal. Chem.* (Reference Ed.) 85 (2016) 117–127. <https://doi.org/10.1016/j.trac.2016.08.014>.
- [183] C. Kraft, I.W. Schie, T. Meyer, M. Schmitt, J. Popp, Developments in spontaneous and coherent Raman scattering microscopic imaging for biomedical applications, *Chem. Soc. Rev.* 45 (2016) 1819–1849. <https://doi.org/10.1039/c5cs00564g>.
- [184] D.M. Jameson, Introduction to Fluorescence, CRC Press, 2014. <https://doi.org/10.1201/b16502>.
- [185] N.M. Htun, Y.C. Chen, B. Lim, T. Schiller, G.J. Maghzal, A.L. Huang, K.D. Elgass, J. Rivera, H.G. Schneider, B.R. Wood, R. Stocker, K. Peter, Near-infrared autofluorescence induced by intraplaque hemorrhage and heme degradation as marker for high-risk atherosclerotic plaques, *Nat. Commun.* 8 (2017) 75. <https://doi.org/10.1038/s41467-017-00138-x>.
- [186] K.C. Doty, G. McLaughlin, I.K. Lednev, A Raman “spectroscopic clock” for bloodstain age determination: the first week after deposition, *Anal. Bioanal. Chem.* 408 (2016) 3993–4001. <https://doi.org/10.1007/s00216-016-9486-z>.
- [187] A. Menzyk, A. Damin, A. Martyna, E. Alladio, M. Vincenti, G. Martra, G. Zadora, Toward a novel framework for bloodstains dating by Raman spectroscopy: how to avoid sample photodamage and subsampling errors, *Talanta* 209 (2020) 120565. <https://doi.org/10.1016/j.talanta.2019.120565>.
- [188] K.M. Marzec, K. Kochan, a. Fedorowicz, a. Jasztal, K. Chruszcz-Lipska, J.C. Dobrowolski, S. Chlopicki, M. Baranska, Raman microimaging of murine lungs: insight into the vitamin A content, *Analyst* 140 (2015) 2171–2177. <https://doi.org/10.1039/C4AN01881H>.
- [189] B.R. Wood, L. Hammer, L. Davis, D. McNaughton, Raman microspectroscopy and imaging provides insights into heme aggregation and denaturation within human erythrocytes, *J. Biomed. Opt.* 10 (2005) 14005. <https://doi.org/10.1117/1.1854678>.
- [190] R. Dasgupta, S. Ahlawat, R.S. Verma, A. Uppal, P.K. Gupta, Hemoglobin degradation in human erythrocytes with long-duration near-infrared laser exposure in Raman optical tweezers, *J. Biomed. Opt.* 15 (2010), 055009. <https://doi.org/10.1117/1.3497048>.
- [191] J.L. Lippert, L.E. Gorczyca, G. Meiklejohn, A laser Raman spectroscopic investigation of phospholipid and protein configurations in hemoglobin-free erythrocyte ghosts, *Biochim. Biophys. Acta Biomembr.* 382 (1975) 51–57. [https://doi.org/10.1016/0005-2736\(75\)90371-5](https://doi.org/10.1016/0005-2736(75)90371-5).
- [192] A. Chowdhury, Y. Singh, U. Das, D. Waghmare, R. Dasgupta, S.K. Majumder, Effects of mobile phone emissions on human red blood cells, *J. Biophot.* 14 (2021). <https://doi.org/10.1002/jbio.202100047>.

- [193] A. Blat, T. Stepanenko, K. Bulat, A. Wajda, T. Mohaissen, F.C. Alciček, J. Dybas, E. Szczesny-Malysiak, A. Fedorowicz, K.M. Marzec, Spectroscopic signature of red blood cells in the D-galactose-induced accelerated aging model, *Int. J. Mol. Sci.* 22 (2021) 1–15. <https://doi.org/10.3390/ijms22052660>.
- [194] E. Lenzi, S. Dinarelli, G. Longo, M. Giasole, V. Mussi, Multivariate analysis of mean Raman spectra of erythrocytes for a fast analysis of the biochemical signature of ageing, *Talanta* 221 (2021) 121442. <https://doi.org/10.1016/j.talanta.2020.121442>.
- [195] C. Ghanashyam, S. Shetty, S. Bharati, S. Chidangil, A. Bankapur, Optical trapping and micro-Raman spectroscopy of functional red blood cells using vortex beam for cell membrane studies, *Anal. Chem.* 93 (2021) 5484–5493. <https://doi.org/10.1021/acs.analchem.0c05204>.
- [196] D.Z. de Back, E.B. Kostova, M. van Kraaij, T.K. van den Berg, R. van Bruggen, Of macrophages and red blood cells; A complex love story, *Front. Physiol.* 5 (2014) 1–9. <https://doi.org/10.3389/fphys.2014.00009>.
- [197] B.R. Wood, D. McNaughton, Resonance Raman spectroscopy of erythrocytes, in: M. Diem (Editor), *Handb. Vib. Spectrosc.*, John Wiley & Sons, Chichester, UK, 2008. <https://doi.org/10.1002/0470027320.s8929>.
- [198] A.C. Albrecht, On the theory of Raman intensities, *J. Chem. Phys.* 34 (1961) 1476–1484. <https://doi.org/10.1063/1.1701032>.
- [199] S.A. Asher, UV resonance Raman studies of molecular structure and dynamics: applications in physical and biophysical chemistry, *Annu. Rev. Phys. Chem.* 39 (1988) 537–588. <https://doi.org/10.1146/annurev.pc.39.100188.002541>.
- [200] T.G. Spiro, T.C. Strekas, Resonance Raman spectra of heme proteins. Effects of oxidation and spin state, *J. Am. Chem. Soc.* 96 (1974) 338–345. <https://doi.org/10.1021/ja00809a004>.
- [201] E.R. Henry, D.L. Rousseau, J.J. Hopfield, R.W. Noble, S.R. Simon, Spectroscopic studies of protein-heme interactions accompanying the allosteric transition in methemoglobins, *Biochemistry* 24 (1985) 5907–5918. <https://doi.org/10.1021/bi00342a033>.
- [202] T. Kitagawa, T. Iizuka, M. Saito, Y. Kyogoku, Resonance Raman scattering from hemoproteins: the nature of the bond between the sixth ligand and the heme iron in ferrous low spin derivatives of hemoglobin, *Chem. Lett.* 4 (1975) 849–852. <https://doi.org/10.1246/cl.1975.849>.
- [203] M. Abe, T. Kitagawa, Y. Kyogoku, Resonance Raman spectra of octaethylporphyrinatonicel(II) and meso-deuterated and nitrogen-15 substituted derivatives. II. A normal coordinate analysis, *J. Chem. Phys.* 69 (1978) 4526–4534. <https://doi.org/10.1063/1.436450>.
- [204] D. Morikis, P.M. Champion, B.A. Springer, K.D. Egeby, S.G. Sligar, Resonance Raman studies of iron spin and axial coordination in distal pocket mutants of ferric myoglobin, *J. Biol. Chem.* 265 (1990) 12143–12145. [https://doi.org/10.1016/S0021-9258\(19\)38322-X](https://doi.org/10.1016/S0021-9258(19)38322-X).
- [205] B. Benko, N.T. Yu, Resonance Raman studies of nitric oxide binding to ferric and ferrous hemoproteins: detection of Fe(III)–NO stretching, Fe(III)–N–O bending, and Fe(II)–N–O bending vibrations, *Proc. Natl. Acad. Sci. Unit. States Am.* 80 (1983) 7042–7046. <https://doi.org/10.1073/pnas.80.22.7042>.
- [206] T.C. Strekas, A.J. Packer, T.G. Spiro, Resonance Raman spectra of ferri-hemoglobin fluoride: three scattering regimes, *J. Raman Spectrosc.* 1 (1973) 197–206. <https://doi.org/10.1002/jrs.1250010207>.
- [207] S. Hirota, T. Ogura, K. Shinzawa-Itoh, S. Yoshikawa, T. Kitagawa, Observation of multiple CN-Isotope-Sensitive Raman bands for CN - adducts of hemoglobin, myoglobin, and cytochrome c oxidase: evidence for vibrational coupling between the Fe–C–N bending and porphyrin in-plane modes, *J. Phys. Chem.* 100 (1996) 15274–15279. <https://doi.org/10.1021/jp953190m>.
- [208] B.R. Wood, D. McNaughton, Micro-Raman characterization of high- and low-spin heme moieties within single living erythrocytes, *Biopolymers* 67 (2002) 259–262. <https://doi.org/10.1002/bip.10120>.
- [209] B.R. Wood, L. Hammer, D. McNaughton, Resonance Raman spectroscopy provides evidence of heme ordering within the functional erythrocyte, *Vib. Spectrosc.* 38 (2005) 71–78. <https://doi.org/10.1016/j.vibspec.2005.02.016>.
- [210] I.P. Torres Filho, J. Turner, R.N. Pittman, E. Proffitt, K.R. Ward, Measurement of hemoglobin oxygen saturation using Raman microspectroscopy and 532-nm excitation, *J. Appl. Physiol.* 104 (2008) 1809–1817. <https://doi.org/10.1152/japplphysiol.00025.2008>.
- [211] M.F. Zhu, X.P. Ye, Y.Y. Huang, Z.Y. Guo, Z.F. Zhuang, S.H. Liu, Detection of methemoglobin in whole blood based on confocal micro-Raman spectroscopy and multivariate statistical techniques, *Scanning* 36 (2014) 471–478. <https://doi.org/10.1002/sca.21143>.
- [212] N.M. Ralbovsky, I.K. Lednev, Analysis of individual red blood cells for Celiac disease diagnosis, *Talanta* 221 (2021) 121642. <https://doi.org/10.1016/j.talanta.2020.121642>.
- [213] D. Perez-Guaita, M. de Veij, K.M. Marzec, A.R.D. Almohammadi, D. McNaughton, A.J. Hudson, B.R. Wood, Resonance Raman and UV-visible microscopy reveals that conditioning red blood cells with repeated doses of sodium dithionite increases haemoglobin oxygen uptake, *Chemistry* 2 (2017) 3342–3346. <https://doi.org/10.1002/slct.201700190>.
- [214] A. Khoshmanesh, M.W.A. Dixon, S. Kenny, L. Tilley, D. McNaughton, B.R. Wood, Detection and quantification of early-stage malaria parasites in laboratory infected erythrocytes by attenuated total reflectance infrared spectroscopy and multivariate analysis, *Anal. Chem.* 86 (2014) 4379–4386. <https://doi.org/10.1021/ac500199x>.
- [215] A.J. Hobro, A. Konishi, C. Coban, N.I. Smith, Raman spectroscopic analysis of malaria disease progression via blood and plasma samples, *Analyst* 138 (2013) 3927–3933. <https://doi.org/10.1039/c3an00255a>.
- [216] A.C.B. Filho, L. Silveira, A.L.S. Yanai, A.B. Fernandes, Raman spectroscopy for a rapid diagnosis of sickle cell disease in human blood samples: a preliminary study, *Laser Med. Sci.* 30 (2014) 247–253. <https://doi.org/10.1007/s10103-014-1635-z>.
- [217] A. Cao, R. Galanello, Beta-thalassemia, *Genet. Med.* 12 (2010) 61–76. <https://doi.org/10.1097/GIM.0b013e3181cd68ed>.
- [218] G. Rusciano, A.C. De Luca, G. Pesce, A. Sasso, Raman tweezers as a diagnostic tool of hemoglobin-related blood disorders, *Sensors* 8 (2008) 7818–7832. <https://doi.org/10.3390/s8127818>.
- [219] A.C. De Luca, G. Rusciano, R. Ciancia, V. Martinelli, G. Pesce, B. Rotoli, L. Selvaggi, A. Sasso, Spectroscopic and mechanical characterization of normal and thalassemic red blood cells by Raman Tweezers, *Opt Express* 16 (2008) 7943. <https://doi.org/10.1364/oe.16.007943>.
- [220] A. Blat, J. Dybas, K. Chrabaszcz, K. Bulat, A. Jasztal, M. Kaczmarek, R. Pulyk, T. Popiela, A. Slowik, K. Malek, M.G. Adamski, K.M. Marzec, FTIR, Raman and AFM characterization of the clinically valid biochemical parameters of the thrombi in acute ischemic stroke, *Sci. Rep.* 9 (2019) 1–25. <https://doi.org/10.1038/s41598-019-51932-0>.
- [221] H.-L. Wang, E.-M. You, R. Panneerselvam, S.-Y. Ding, Z.-Q. Tian, Advances of surface-enhanced Raman and IR spectroscopies: from nano/microstructures to macro-optical design, *Light Sci. Appl.* 10 (2021) 161. <https://doi.org/10.1038/s41377-021-00599-2>.
- [222] H. Xu, E.J. Bjerneld, M. Käll, L. Börjesson, Spectroscopy of single hemoglobin molecules by surface enhanced Raman scattering, *Phys. Rev. Lett.* 83 (1999) 4357–4360. <https://doi.org/10.1103/PhysRevLett.83.4357>.
- [223] M.S. Kiran, T. Itoh, K.I. Yoshida, N. Kawashima, V. Biju, M. Ishikawa, Selective detection of hba1c using surface enhanced resonance Raman spectroscopy, *Anal. Chem.* 82 (2010) 1342–1348. <https://doi.org/10.1021/ac902364h>.
- [224] M. Casella, A. Lucotti, M. Tommasini, M. Bedoni, E. Forvi, F. Gramatica, G. Zerbi, Raman and SERS recognition of β -carotene and haemoglobin fingerprints in human whole blood, *Spectrochim. Acta Part A Mol. Biomol. Spectrosc.* 79 (2011) 915–919. <https://doi.org/10.1016/j.saa.2011.03.048>.
- [225] D. Drescher, T. Büchner, D. McNaughton, J. Kneipp, SERS reveals the specific interaction of silver and gold nanoparticles with hemoglobin and red blood cell components, *Phys. Chem. Chem. Phys.* 15 (2013) 5364–5373. <https://doi.org/10.1039/c3cp43883j>.
- [226] R. Agoston, E.L. Izake, A. Sivanesan, W.B. Lott, M. Silience, R. Steel, Rapid isolation and detection of erythropoietin in blood plasma by magnetic core gold nanoparticles and portable Raman spectroscopy, *Nanomed. Nanotechnol. Biol. Med.* 12 (2016) 633–641. <https://doi.org/10.1016/j.nano.2015.11.003>.
- [227] N.A. Brazhe, S. Abdali, A.R. Brazhe, O.G. Luneva, N.Y. Bryzgalova, E.Y. Parshina, O.V. Sosnovtseva, G.V. Maksimov, New insight into erythrocyte through in vivo surface-enhanced Raman spectroscopy, *Biophys. J.* 97 (2009) 3206–3214. <https://doi.org/10.1016/j.bpj.2009.09.029>.
- [228] N. Fleitas-Salazar, S. Pedrosa-Santana, E. Silva-Campa, A. Angulo-Molina, J.R. Toledo, R. Riera, M. Pedrosa-Montero, Raman spectroscopy and silver nanoparticles for efficient detection of membrane proteins in living cells, *Nanotechnology* 32 (2021) 495101. <https://doi.org/10.1088/1361-6528/ac21ee>.
- [229] X.S. Zheng, I.J. Jahn, K. Weber, D. Cialla-May, J. Popp, Label-free SERS in biological and biomedical applications: recent progress, current challenges and opportunities, *Spectrochim. Acta Part A Mol. Biomol. Spectrosc.* 197 (2018) 56–77. <https://doi.org/10.1016/j.saa.2018.01.063>.
- [230] Z. Cai, Y. Hu, Y. Sun, Q. Gu, P. Wu, C. Cai, Z. Yan, Plasmonic SERS biosensor based on multibranched gold nanoparticles embedded in polydimethylsiloxane for quantification of hematin in human erythrocytes, *Anal. Chem.* 93 (2021) 1025–1032. <https://doi.org/10.1021/acs.analchem.0c03921>.
- [231] B.R. Wood, E. Bailo, M.A. Khiavi, L. Tilley, S. Deed, T. Deckert-Gaudig, D. McNaughton, V. Deckert, Tip-enhanced Raman scattering (TERS) from hemozoin crystals within a sectioned erythrocyte, *Nano Lett.* 11 (2011) 1868–1873. <https://doi.org/10.1021/nl103004n>.
- [232] A. Dogariu, A. Goltsov, M.O. Scully, Real-time monitoring of blood using coherent anti-Stokes Raman spectroscopy, *J. Biomed. Opt.* 13 (2008) 054004. <https://doi.org/10.1117/1.2978064>.
- [233] H.A. Rinia, M. Bonn, E.M. Vartiainen, C.B. Schaffer, M. Müller, Spectroscopic analysis of the oxygenation state of hemoglobin using coherent anti-Stokes Raman scattering, *J. Biomed. Opt.* 11 (2006), 050502. <https://doi.org/10.1117/1.2355671>.
- [234] E.O. Potma, X.S. Xie, Detection of single lipid bilayers with coherent anti-Stokes Raman scattering (CARS) microscopy, *J. Raman Spectrosc.* 34 (2003) 642–650. <https://doi.org/10.1002/jrs.1045>.
- [235] M.A. Toderi, G.E. Galizzi, B.D. Riquelme, D. Dumas, Study of the red blood cell aggregation by coherent anti-Stokes Raman spectroscopy, in: N.T. Shaked, O. Hayden (Editors), *Label-Free Biomed. Imaging Sens.* 2020, SPIE, 2020, p. 77. <https://doi.org/10.1117/12.2543073>.
- [236] F.K. Lu, D. Calligaris, O.I. Olubiye, I. Norton, W. Yang, S. Santagata, X.S. Xie, A.J. Golby, N.Y.R. Agar, Label-free neurosurgical pathology with stimulated Raman imaging, *Cancer Res.* 76 (2016) 3451–3462. <https://doi.org/10.1158/0008-5472.CAN-16-0270>.

- [237] Y. Suzuki, K. Kobayashi, Y. Wakisaka, D. Deng, S. Tanaka, C.J. Huang, C. Lei, C.W. Sun, H. Liu, Y. Fujiwaki, S. Lee, A. Isozaki, Y. Kasai, T. Hayakawa, S. Sakuma, F. Arai, K. Koizumi, H. Tezuka, M. Inaba, K. Hiraki, T. Ito, M. Hase, S. Matsusaka, K. Shiba, K. Suga, M. Nishikawa, M. Jona, Y. Yatom, Y. Yalikun, Y. Tanaka, T. Sugimura, N. Nitta, K. Goda, Y. Ozeki, Label-free chemical imaging flow cytometry by high-speed multicolor stimulated Raman scattering, *Proc. Natl. Acad. Sci. U.S.A.* 116 (2019) 15842–15848. <https://doi.org/10.1073/pnas.1902322116>.
- [238] W. Yang, *Biomedical Applications of Stimulated Raman Scattering Microscopy A Dissertation Presented*, 2017.
- [239] *SRS Microscopy Captures Blood Cells at Video Rate*, Wiley Analytical Science, 2010 (n.d.).
- [240] T.P. Wrobel, K.M. Marzec, K. Majzner, K. Kochan, M. Bartus, S. Chlopicki, M. Baranska, Attenuated total reflection Fourier transform infrared (ATR-FTIR) spectroscopy of a single endothelial cell, *Analyst* 137 (2012) 4135–4139. <https://doi.org/10.1039/c2an35331h>.
- [241] S.G. Kazarian, K.L.A. Chan, ATR-FTIR spectroscopic imaging: recent advances and applications to biological systems, *Analyst* 138 (2013) 1940. <https://doi.org/10.1039/c3an36865c>.
- [242] C. Koch, M. Brandstetter, P. Wechselberger, B. Loranffy, M.R. Plata, S. Radel, C. Herwig, B. Lendl, Ultrasound-enhanced attenuated total reflection mid-infrared spectroscopy in-line probe: acquisition of cell spectra in a bioreactor, *Anal. Chem.* 87 (2015) 2314–2320. <https://doi.org/10.1021/ac504126v>.
- [243] K. Kochan, D.E. Bedolla, D. Perez-Guaita, J.A. Adegoke, T. Chakkumpulakkal Puthan Veetil, M. Martin, S. Roy, S. Pebotuwa, P. Heraud, B.R. Wood, Infrared spectroscopy of blood, *Appl. Spectrosc.* (2021), 000370282098585. <https://doi.org/10.1177/0003702820985856>.
- [244] S. Roy, D. Perez-Guaita, D.W. Andrew, J.S. Richards, D. McNaughton, P. Heraud, B.R. Wood, Simultaneous ATR-FTIR based determination of malaria parasitemia, glucose and urea in whole blood dried onto a glass slide, *Anal. Chem.* 89 (2017) 5238–5245. <https://doi.org/10.1021/acs.analchem.6b04578>.
- [245] S.F. Ruggeri, C. Marcott, S. Dinarelli, G. Longo, M. Girasole, G. Dietler, P.T. Knowles, Identification of oxidative stress in red blood cells with nanoscale chemical resolution by infrared nanospectroscopy, *Int. J. Mol. Sci.* 19 (2018). <https://doi.org/10.3390/ijms19092582>.
- [246] R.H. Sills, D.J. Moore, R. Mendelsohn, Erythrocyte peroxidation: quantitation by fourier transform infrared spectroscopy, *Anal. Biochem.* 218 (1994) 118–123. <https://doi.org/10.1006/abio.1994.1149>.
- [247] C. Petibois, G. Deléris, Evidence that erythrocytes are highly susceptible to exercise oxidative stress: FT-IR spectrometric studies at the molecular level, *Cell Biol. Int.* 29 (2005) 709–716. <https://doi.org/10.1016/j.cellbi.2005.04.007>.
- [248] C. Petibois, A.M. Melin, A. Perromat, G. Cazorla, G. Deléris, Glucose and lactate concentration determination on single microsamples by Fourier-transform infrared spectroscopy, *J. Lab. Clin. Med.* 135 (2000) 210–215. <https://doi.org/10.1067/mlc.2000.104460>.
- [249] M. Mahato, P. Pal, T. Kamilya, R. Sarkar, A. Chaudhuri, G.B. Talapatra, Hemoglobin-silver interaction and bioconjugate formation: a spectroscopic study, *J. Phys. Chem. B* 114 (2010) 7062–7070. <https://doi.org/10.1021/jp100188s>.
- [250] A.M.A. Pistorius, M. Luten, G.J.C.G.M. Bosman, W.J. Degrip, A single assay for multiple storage-sensitive red blood cell characteristics by means of infrared spectroscopy, *Transfusion* 50 (2010) 366–375. <https://doi.org/10.1111/j.1537-2995.2009.02400.x>.
- [251] H. Liu, Q. Su, D. Sheng, W. Zheng, X. Wang, Comparison of red blood cells from gastric cancer patients and healthy persons using FTIR spectroscopy, *J. Mol. Struct.* 1130 (2017) 33–37. <https://doi.org/10.1016/j.molstruc.2016.10.019>.
- [252] M. Martin, D. Perez-Guaita, D.W. Andrew, J.S. Richards, B.R. Wood, P. Heraud, The effect of common anticoagulants in detection and quantification of malaria parasitemia in human red blood cells by ATR-FTIR spectroscopy, *Analyst* 142 (2017) 1192–1199. <https://doi.org/10.1039/c6an02075e>.
- [253] D. Perez-Guaita, D. Andrew, P. Heraud, J. Beeson, D. Anderson, J. Richards, B.R. Wood, High resolution FTIR imaging provides automated discrimination and detection of single malaria parasite infected erythrocytes on glass, *Faraday Discuss* 187 (2016) 341–352. <https://doi.org/10.1039/C5FD00181A>.
- [254] D. Perez-Guaita, K. Kochan, M. Batty, C. Doerig, J. Garcia-Bustos, S. Espinoza, D. McNaughton, P. Heraud, B.R. Wood, Multispectral atomic force microscopy-infrared nano-imaging of malaria infected red blood cells, *Anal. Chem.* 90 (2018) 3140–3148. <https://doi.org/10.1021/acs.analchem.7b04318>.
- [255] J. Espada, Current methods to unravel ROS biology, *Methods* 109 (2016) 1–2. <https://doi.org/10.1016/j.ymeth.2016.10.006>.
- [256] S. Suzen, H. Gurer-Orhan, L. Saso, Detection of reactive oxygen and nitrogen species by electron paramagnetic resonance (EPR) technique, *Molecules* 22 (2017). <https://doi.org/10.3390/molecules22010181>.
- [257] T. Kubiak, R. Krzymiński, B. Dobosz, EPR study of paramagnetic centers in human blood, *Curr. Top. Biophys.* 36 (2013) 7–13. <https://doi.org/10.2478/ctb-2013-0006>.
- [258] R. Krzymiński, Z. Kruczyński, B. Dobosz, A. Zając, A. Mackiewicz, E. Leporowska, S. Folwaczna, EPR study of iron ion complexes in human blood, *Appl. Magn. Reson.* 40 (2011) 321–330. <https://doi.org/10.1007/s00723-011-0219-3>.
- [259] M.J. Davies, Detection and characterisation of radicals using electron paramagnetic resonance (EPR) spin trapping and related methods, *Methods* 109 (2016) 21–30. <https://doi.org/10.1016/j.ymeth.2016.05.013>.
- [260] J.A. Reisz, N. Bansal, J. Qian, W. Zhao, C.M. Furdul, Effects of ionizing radiation on biological molecules - mechanisms of damage and emerging methods of detection, *Antioxidants Redox Signal.* 21 (2014) 260–292. <https://doi.org/10.1089/ars.2013.5489>.
- [261] S.A. Mendanha, J.L.V. Anjos, A.H.M. Silva, A. Alonso, Electron paramagnetic resonance study of lipid and protein membrane components of erythrocytes oxidized with hydrogen peroxide, *Braz. J. Med. Biol. Res.* 45 (2012) 473–481. <https://doi.org/10.1590/S0100-879X2012007500050>.
- [262] C.L. Bianco, A. Savitsky, M. Feilich, M.M. Cortese-Krott, Investigations on the role of hemoglobin in sulfide metabolism by intact human red blood cells, *Biochem. Pharmacol.* 149 (2018) 163–173. <https://doi.org/10.1016/j.bcp.2018.01.045>.
- [263] P.M. Rodi, V.M. Trucco, A.M. Gennaro, Factors determining detergent resistance of erythrocyte membranes, *Biophys. Chem.* 135 (2008) 14–18. <https://doi.org/10.1016/j.bpc.2008.02.015>.
- [264] A. Ciana, C. Achilli, G. Minetti, Membrane rafts of the human red blood cell, *Mol. Membr. Biol.* 31 (2014) 47–57. <https://doi.org/10.3109/09687688.2014.896485>.
- [265] R. Morabito, O. Romano, G. La Spada, A. Marino, H2O2-induced oxidative stress affects SO4 = Transport in human erythrocytes, *PLoS One* 11 (2016). <https://doi.org/10.1371/journal.pone.0146485>.
- [266] K. Tsuda, Association of resistin with impaired membrane fluidity of red blood cells in hypertensive and normotensive men: an electron paramagnetic resonance study, *Heart Ves.* 31 (2016) 1724–1730. <https://doi.org/10.1007/s00380-015-0755-0>.
- [267] M.G. Makletsova, T.N. Fedorova, V.V. Poleschuk, G.T. Rikhireva, The effect of dopamine on in vitro methemoglobin formation in erythrocytes of patients with Parkinson's disease under oxidative stress, *Biophys. (Russian Fed)* 62 (2017) 247–251. <https://doi.org/10.1134/S0006350917020154>.
- [268] H. Hou, J.H. Baek, H. Zhang, F. Wood, Y. Gao, A.B. Flood, H.M. Swartz, P.W. Buehler, Electron paramagnetic resonance oximetry as a novel approach to monitor the effectiveness and quality of red blood cell transfusions, *Blood Transfus* 17 (2019) 296–306. <https://doi.org/10.2450/2019.0037-19>.
- [269] M. Baryn, J.D. Tissot, M. Prudent, Oxidative stress and antioxidant defenses during blood processing and storage of erythrocyte concentrates, *Transfus. Clin. Biol.* 25 (2018) 96–100. <https://doi.org/10.1016/j.tracbi.2017.08.001>.
- [270] J.M. Rifkind, J.G. Mohanty, E. Nagababu, M.T. Salgado, Z. Cao, Potential modulation of vascular function by nitric oxide and reactive oxygen species released from erythrocytes, *Front. Physiol.* 9 (2018). <https://doi.org/10.3389/fphys.2018.00690>.
- [271] C. Liu, N. Wajih, X. Liu, S. Basu, J. Janes, M. Marvel, C. Keggi, C.C. Helms, A.N. Lee, A.M. Belanger, D.I. Diz, P.J. Laurienti, D.L. Caudell, J. Wang, M.T. Gladwin, D.B. Kim-Shapiro, Mechanisms of human erythrocytic bioactivation of nitrite, *J. Biol. Chem.* 290 (2015) 1281–1294. <https://doi.org/10.1074/jbc.M114.609222>.
- [272] S.D. Dumitrescu, A.T. Meszaros, S. Puchner, A. Weidinger, M. Boros, H. Redl, A.V. Kozlov, EPR analysis of extra- and intracellular nitric oxide in liver biopsies, *Magn. Reson. Med.* 77 (2017) 2372–2380. <https://doi.org/10.1002/mrm.26291>.
- [273] V. Schünemann, H. Winkler, Structure and dynamics of biomolecules studied by Mössbauer spectroscopy, *Rep. Prog. Phys.* 63 (2000) 263. <https://doi.org/10.1088/0034-4885/63/3/202>.
- [274] M.I. Oshtrakh, Applications of mössbauer spectroscopy in biomedical research, *Cell Biochem. Biophys.* 77 (2019) 15–32. <https://doi.org/10.1007/s12013-018-0843-8>.
- [275] G. Lang, W. Marshali, Mössbauer effect in some haemoglobin compounds, *Proc. Phys. Soc.* 87 (1966) 3–34. <https://doi.org/10.1088/0370-1328/87/1/302>.
- [276] G. Lang, Mössbauer spectroscopy of haem proteins, *Q. Rev. Biophys.* 3 (1970) 1. <https://doi.org/10.1017/S0033583500004406>.
- [277] A.A. Novakova, T.Y. Kiseleva, S.M. Khvastunov, Mossbauer study of different factors influence on donated blood quality, *Hyperfine Interact.* 239 (2018) 1–10. <https://doi.org/10.1007/s10751-017-1482-y>.
- [278] G.R. Hoy, D.C. Cook, R.L. Berger, F.K. Friedman, Mössbauer spectroscopic studies of hemoglobin and its isolated subunits, *Biophys. J.* 49 (1986) 1009–1015. [https://doi.org/10.1016/S0006-3495\(86\)83729-8](https://doi.org/10.1016/S0006-3495(86)83729-8).
- [279] M. Kaczmarek, D. Żydek, J. Wilkiacz-Potoczny, M. Fornal, T. Grodzicki, E. Kochowska, K. Kozak, Ł. Gocal, W. Pohorecki, K. Matlak, J. Korecki, K. Burda, The influence of very small doses of alpha radiation on the stability of erythrocytes, *Microsc. Res. Tech.* 80 (2017). <https://doi.org/10.1002/jemt.22803>.
- [280] M. Kaczmarek, Z. Kopyścińska, M. Fornal, T. Grodzicki, K. Matlak, J. Korecki, K. Burda, Effects of low doses of gamma rays on the stability of normal and diabetic erythrocytes, *Acta Biochim. Pol.* 58 (2011). <https://doi.org/10.18388/abp.2011.2215>.
- [281] K. Niemiec, M. Kaczmarek, M. Buczkowski, M. Fornal, W. Pohorecki, K. Matlak, J. Korecki, T. Grodzicki, K. Burda, Mössbauer studies of hemoglobin in erythrocytes exposed to neutron radiation, *Hyperfine Interact.* 206 (2012) 95–100. <https://doi.org/10.1007/s10751-011-0491-5>.
- [282] M. Kaczmarek, M. Fornal, F.H. Messerli, J. Korecki, T. Grodzicki, K. Burda, Erythrocyte membrane properties in patients with essential hypertension, *Cell Biochem. Biophys.* 67 (2013). <https://doi.org/10.1007/s12013-013-9613-9>.

- [283] M. Kaczmarek, I. Habina, A. Orzechowska, K. Niemiec-Murzyn, M. Fornal, W. Pohorecki, K. Matlak, J. Korecki, T. Grodzicki, K. Burda, Influence of neutron radiation on the stability of the erythrocyte membrane and an oxyhemoglobin formation - Petkau effect studies, *Acta Phys. Pol. B* 47 (2016). <https://doi.org/10.5506/APhysPolB.47.425>.
- [284] R. Mukherjee, M. Saha, A. Routray, C. Chakraborty, Nanoscale surface characterization of human erythrocytes by atomic force microscopy: a critical review, *IEEE Trans. NanoBioscience* 14 (2015) 625–633. <https://doi.org/10.1109/TNB.2015.2424674>.
- [285] N. Yeow, R.F. Tabor, G. Garnier, Atomic force microscopy: from red blood cells to immunohaematology, *Adv. Colloid Interface Sci.* 249 (2017) 149–162. <https://doi.org/10.1016/j.cis.2017.05.011>.
- [286] M. Baranska, M. Roman, K. Majzner, General overview on vibrational spectroscopy applied in biology and medicine, in: *Opt. Spectrosc. Comput. Methods Biol. Med.*, Springer Netherlands, Dordrecht, 2014, pp. 3–14. https://doi.org/10.1007/978-94-007-7832-0_1.
- [287] N. Vogt, Atomic force microscopy in super-resolution, *Nat. Methods* 18 (2021) 859. <https://doi.org/10.1038/s41592-021-01246-9>.
- [288] T. Smijs, F. Galli, A. van Asten, Forensic potential of atomic force microscopy, *Forensic Chem* 2 (2016) 93–104. <https://doi.org/10.1016/j.forc.2016.10.005>.
- [289] M. Depond, B. Henry, P. Buffet, P.A. Ndour, Methods to investigate the deformability of RBC during malaria, *Front. Physiol.* 10 (2020). <https://doi.org/10.3389/fphys.2019.01613>.
- [290] G. Tomauiolo, Biomechanical properties of red blood cells in health and disease towards microfluidics, *Biomicrofluidics* 8 (2014). <https://doi.org/10.1063/1.4895755>.
- [291] E. Kozlova, A. Chernysh, V. Moroz, V. Sergunova, O. Gudkova, E. Manchenko, Morphology, membrane nanostructure and stiffness for quality assessment of packed red blood cells, *Sci. Rep.* 7 (2017) 7846. <https://doi.org/10.1038/s41598-017-08255-9>.
- [292] M. Kaczmarek, M. Grosicki, K. Bulat, M. Mardyla, E. Szczesny-Malysiak, A. Blat, J. Dybas, T. Sacha, K.M. Marzec, Temporal sequence of the human RBCs' vesiculation observed in nano-scale with application of AFM and complementary techniques, *Nanomed. Nanotechnol. Biol. Med.* 28 (2020) 102221. <https://doi.org/10.1016/j.nano.2020.102221>.
- [293] S. Tjalu, S. Stach, M. Kaczmarek, M. Fornal, T. Grodzicki, W. Pohorecki, K. Burda, Multifractal characterization of morphology of human red blood cells membrane skeleton, *J. Microsc.* 262 (2016). <https://doi.org/10.1111/jmi.12342>.
- [294] A. Bitler, R.S. Dover, Y. Shai, Fractal properties of cell surface structures: a view from AFM, *Semin. Cell Dev. Biol.* 73 (2018) 64–70. <https://doi.org/10.1016/j.semcdb.2017.07.034>.
- [295] E. Szczesny-Malysiak, T. Mohaissen, K. Bulat, M. Kaczmarek, A. Wajda, K.M. Marzec, Sex-dependent membranopathy in stored human red blood cells, *Haematologica* 106 (2021) xxx. <https://doi.org/10.3324/haematol.2021.278895>.
- [296] K. Preißinger, P. Molnar, B. Vertessy, I. Kezsmarki, M. Kellermayr, Stage-dependent topographical and optical properties of Plasmodium falciparum-infected red blood cells, *J. Biotechnol. Biomed.* 4 (2021). <https://doi.org/10.26502/jbb.2642-91280040>.
- [297] M. Saito, T. Watanabe-Nakayama, S. Machida, T. Osada, R. Afrin, A. Ikai, Spectrin-ankyrin interaction mechanics: a key force balance factor in the red blood cell membrane skeleton, *Biophys. Chem.* 200–201 (2015) 1–8. <https://doi.org/10.1016/j.bpc.2015.03.007>.
- [298] P.N. Nirmalraj, T. Schneider, A. Felbecker, Spatial organization of protein aggregates on red blood cells as physical biomarkers of Alzheimer's disease pathology, *Sci. Adv.* 7 (2021). <https://doi.org/10.1126/sciadv.abj2137>.
- [299] E. Kozlova, A. Chernysh, V. Sergunova, O. Gudkova, E. Manchenko, A. Kozlov, Atomic force microscopy study of red blood cell membrane nanostructure during oxidation-reduction processes, *J. Mol. Recogn.* 31 (2018). <https://doi.org/10.1002/jmr.2724>.
- [300] E. Kozlova, A. Chernysh, E. Manchenko, V. Sergunova, V. Moroz, Nonlinear Biomechanical Characteristics of Deep Deformation of Native RBC Membranes in Normal State and under Modifier Action, 2018. <https://doi.org/10.1155/2018/1810585>.
- [301] G. Ciasca, M. Papi, S. Di Claudio, M. Chiarpotto, V. Palmieri, G. Maulucci, G. Nocca, C. Rossi, M. De Spirito, Mapping viscoelastic properties of healthy and pathological red blood cells at the nanoscale level, *Nanoscale* 7 (2015) 17030–17037. <https://doi.org/10.1039/c5nr03145a>.
- [302] S. Dinarelli, G. Longo, S. Krumova, S. Todinova, A. Danailova, S.G. Taneva, E. Lenzi, V. Mussi, M. Girasole, Insights into the morphological pattern of erythrocytes' aging: coupling quantitative AFM data to microcalorimetry and Raman spectroscopy, *J. Mol. Recogn.* 31 (2018). <https://doi.org/10.1002/jmr.2732>.
- [303] G. Longo, M. Girasole, G. Pompeo, R. Generosi, M. Luce, A. Cricenti, An inverted/scanning near-field optical microscope for applications in materials science and biology, *Phys. Status Solidi* 247 (2010) 2051–2055. <https://doi.org/10.1002/pssb.200983935>.
- [304] A. Cricenti, G. Longo, A. Ustione, V. Mussi, R. Generosi, M. Luce, M. Rinaldi, P. Perfetti, D. Vobornik, G. Margaritondo, J.S. Sanghera, P. Thielen, I.D. Aggarwal, B. Ivanov, J.K. Miller, R. Haglund, N.H. Tolk, A. Congiu-Castellano, M.A. Rizzo, D.W. Piston, F. Somma, G. Baldacchini, F. Bonfigli, T. Marolo, F. Flora, R.M. Monteleale, A. Faenov, T. Pikuz, Optical nanospectroscopy applications in material science, in: *Appl. Surf. Sci.*, Elsevier, 2004, pp. 374–386. <https://doi.org/10.1016/j.apsusc.2004.05.023>.
- [305] S. Prauzner-Bechcicki, J. Wiltowska-Zuber, A. Budkowski, M. Lekka, J. Rysz, Implementation of NSOM to biological samples, in: *Acta Phys. Pol. A*, Polish Academy of Sciences, 2012, pp. 533–538. <https://doi.org/10.12693/APhysPolA.121.533>.
- [306] A. Rasmussen, V. Deckert, New dimension in nano-imaging: breaking through the diffraction limit with scanning near-field optical microscopy, *Anal. Bioanal. Chem.* 381 (2005) 165–172. <https://doi.org/10.1007/s00216-004-2896-3>.
- [307] G. Longo, M. Girasole, A. Cricenti, Implementation of a bimorph-based aperture tapping-SNOM with an incubator to study the evolution of cultured living cells, *J. Microsc.* 229 (2008) 433–439. <https://doi.org/10.1111/j.1365-2818.2008.01924.x>.
- [308] S. Pilevar, W.A. Atia, C.C. Davis, Reflection near-field scanning optical microscopy: an interferometric approach, *Ultramicroscopy* 61 (1995) 233–236. [https://doi.org/10.1016/0304-3991\(95\)00115-8](https://doi.org/10.1016/0304-3991(95)00115-8).
- [309] T. Enderle, T. Ha, D.S. Chemla, S. Weiss, Near-field fluorescence microscopy of cells, *Ultramicroscopy* 71 (1998) 303–309. [https://doi.org/10.1016/S0304-3991\(97\)00075-2](https://doi.org/10.1016/S0304-3991(97)00075-2).
- [310] M.F. García-Parajó, B.I. De Bakker, M. Koopman, A. Cambi, F. De Lange, C.G. Figdor, N.F. Van Hulst, Near-field fluorescence microscopy: an optical nanotool to study protein organization at the cell membrane, *Nano-Biotechnology* 1 (2005) 113–120. <https://doi.org/10.1385/NBT:1:1:113>.
- [311] K.A.D. Walker, S.H. Doak, P.R. Dunstan, Mechanisms of cell-cell adhesion identified by immunofluorescent labelling with quantum dots: a scanning near-field optical microscopy approach, *Ultramicroscopy* 111 (2011) 1200–1205. <https://doi.org/10.1016/j.ultramic.2011.01.008>.
- [312] R.C. Dunn, Near-field scanning optical microscopy, *Chem. Rev.* 99 (1999) 2891–2927. <https://doi.org/10.1021/cr980130e>.
- [313] K. Bulat, A. Rygula, E. Szafraniec, Y. Ozaki, M. Baranska, Live endothelial cells imaged by Scanning Near-field Optical Microscopy (SNOM): capabilities and challenges, *J. Biophot.* 10 (2017) 928–938. <https://doi.org/10.1002/jbio.201600081>.
- [314] J.J. Wang, J. Kirkham, J. Donegan, D.A. Smith, High resolution imaging of actin filaments in living cells under physiologically relevant conditions using apertureless near-field microscopy, *J. Nanosci. Nanotechnol.* 10 (2010) 7489–7493. <https://doi.org/10.1166/jnn.2010.2908>.
- [315] D. Vobornik, G. Margaritondo, J.S. Sanghera, P. Thielen, I.D. Aggarwal, B. Ivanov, J.K. Miller, R. Haglund, N.H. Tolk, A. Congiu-Castellano, M.A. Rizzo, D.W. Piston, F. Somma, G. Baldacchini, F. Bonfigli, T. Marolo, F. Flora, R.M. Monteleale, A. Faenov, T. Pikuz, G. Longo, V. Mussi, R. Generosi, M. Luce, P. Perfetti, A. Cricenti, Infrared near-field microscopy with the Vanderbilt free electron laser: overview and perspectives, *Infrared Phys. Technol.* (2004) 409–416. <https://doi.org/10.1016/j.infrared.2004.01.007>.
- [316] D. Vobornik, G. Margaritondo, J.S. Sanghera, P. Thielen, I.D. Aggarwal, B. Ivanov, N.H. Tolk, V. Manni, S. Grimaldi, A. Lisi, S. Rieti, D.W. Piston, R. Generosi, M. Luce, P. Perfetti, A. Cricenti, Spectroscopic infrared scanning near-field optical microscopy (IR-SNOM), *J. Alloys Compd.* 401 (2005) 80–85. <https://doi.org/10.1016/j.jallcom.2005.02.057>.
- [317] J. Laverdant, S. Buil, X. Quélin, Local field enhancements on gold and silver nanostructures for aperture near field spectroscopy, *J. Lumin.* 127 (2007) 176–180. <https://doi.org/10.1016/j.jlumin.2007.02.050>.
- [318] T. Enderle, T. Ha, D.F. Ogletree, D.S. Chemla, C. Magowan, S. Weiss, Membrane specific mapping and colocalization of malarial and host skeletal proteins in the Plasmodium falciparum infected erythrocyte by dual-color near-field scanning optical microscopy, *Proc. Natl. Acad. Sci. U.S.A.* 94 (1997) 520–525. <https://doi.org/10.1073/pnas.94.2.520>.
- [319] Z.J. Lapin, C. Höppener, H.A. Gelbard, L. Novotny, Near-field quantification of complement receptor 1 (CR1/CD35) protein clustering in human erythrocytes, *J. Neuroimmune Pharmacol.* 7 (2012) 539–543. <https://doi.org/10.1007/s11481-012-9346-3>.
- [320] D.E. Tranca, S.G. Stanciu, R. Hristu, B.M. Witgen, G.A. Stanciu, Nanoscale mapping of refractive index by using scattering-type scanning near-field optical microscopy, *Nanomed. Nanotechnol. Biol. Med.* 14 (2018) 47–50. <https://doi.org/10.1016/j.nano.2017.08.016>.
- [321] E. Szczesny-Malysiak, J. Dybas, A. Blat, K. Bulat, K. Kus, M. Kaczmarek, A. Wajda, K. Malek, S. Chlopicki, K.M. Marzec, Irreversible alterations in the hemoglobin structure affect oxygen binding in human packed red blood cells, *Biochim. Biophys. Acta Mol. Cell Res.* 1867 (2020) 118803. <https://doi.org/10.1016/j.bbamcr.2020.118803>.
- [322] K. Buckley, C.G. Atkins, D. Chen, H.G. Schulze, D.V. Devine, M.W. Blades, R.F.B. Turner, Non-invasive spectroscopy of transfusable red blood cells stored inside sealed plastic blood-bags, *Analyst* 141 (2016) 1678–1685. <https://doi.org/10.1039/C5AN02461G>.
- [323] C.G. Atkins, K. Buckley, D. Chen, H.G. Schulze, D.V. Devine, M.W. Blades, R.F.B. Turner, Raman spectroscopy as a novel tool for monitoring biochemical changes and inter-donor variability in stored red blood cell units, *Analyst* 141 (2016) 3319–3327. <https://doi.org/10.1039/C6AN00373G>.
- [324] M.M. Cortese-Krott, M. Kelm, Endothelial nitric oxide synthase in red blood cells: key to a new erythrocrine function? *Redox Biol* 2 (2014) 251–258. <https://doi.org/10.1016/j.redox.2013.12.027>.
- [325] C.G. Tocchetti, B.A. Stanley, C.I. Murray, V. Sivakumaran, S. Donzelli, D. Mancardi, P. Pagliaro, W.D. Gao, J. Van Eyk, D.A. Kass, D.A. Wink,

- N. Paolocci, Playing with cardiac redox switches: the HNO way to modulate cardiac function, *Antioxid. Redox Signal* 14 (2011) 1687–1698. <https://doi.org/10.1089/ars.2010.3859>.
- [326] F. Doctorovich, D.E. Bikiel, J. Pellegrino, S.A. Suárez, M.A. Martí, Reactions of HNO with metal porphyrins: underscoring the biological relevance of HNO, *Acc. Chem. Res.* 47 (2014) 2907–2916. <https://doi.org/10.1021/ar500153c>.
- [327] A.J. Gow, B.P. Luchsinger, J.R. Pawloski, D.J. Singel, J.S. Stamler, The oxyhemoglobin reaction of nitric oxide, *Proc. Natl. Acad. Sci. U.S.A.* 96 (1999) 9027–9032. <https://doi.org/10.1073/pnas.96.16.9027>.
- [328] B.R. Wood, D. McNaughton, Resonance Raman spectroscopy in malaria research, *Expert Rev. Proteomics* 3 (2006) 525–544. <https://doi.org/10.1586/14789450.3.5.525>.